



JIMMA UNIVERSITY

SCHOOL OF GRADUATE STUDIES

JIMMA INSTITUTE OF TECHNOLOGY

FACULTY OF CIVIL AND ENVIRONMENTAL ENGINEERING

STRUCTURAL ENGINEERING STREAM

Comparative Study on Steel and Reinforced Concrete Beam on the Basis of Modular Ratio for Flexural Capacity and Fire Resistance Using Finite Element Analysis

A Thesis Submitted to School Of Graduate Studies of Jimma University in Partial Fulfillment of the Requirements for the Degree of Master of Science in Structural Engineering

BY:

SOLOMON GETACHEW MEKONEN

December, 2019

JIMMA, ETHIOPIA



JIMMA UNIVERSITY

SCHOOL OF GRADUATE STUDIES

JIMMA INSTITUTE OF TECHNOLOGY

FACULTY OF CIVIL AND ENVIRONMENTAL ENGINEERING

STRUCTURAL ENGINEERING STREAM

Comparative Study on Steel and Reinforced Concrete Beam on the Basis of Modular Ratio for Flexural Capacity and Fire Resistance Using Finite Element Analysis

A Thesis Submitted to School Of Graduate Studies of Jimma University in Partial Fulfillment of the Requirements for the Degree of Master of Science in Structural Engineering

BY:

SOLOMON GETACHEW MEKONEN

ADVISOR: - Engr. Elmer C. Agon (Asso. Prof)

CO-ADVISOR:-Engr. Solomon Biratu, Msc.

December, 2019

JIMMA, ETHIOPIA

DECLARATION

I, SOLOMON GETACHEW, declare that all the work done in this study originates from my own work and that all secondary sources referred to in this work have been duly acknowledged.

Name: SOLOMON GETACHEW

Signature: _____

Place: Jimma University, Institute of Technology

Date of Submission: November, 2019

Engr. Elmer C. Agon (Asso. Prof) _____

AdvisorSignature Date

Engr. SolomonBiratu _____

Co-Advisor SignatureDate

ACKNOWLEDGMENT

Most importantly I might want to submit greatness to omnipotent God for unending gift. Next I would to thank my advisor **Engr. Elmer C. Agon and Engr. Solomon Biratu** for their willingness to advise me. And furthermore I have to thank all people and companions for their consolation and giving me extra data's related to my profession. At long last, my exceptional much gratitude goes to Jimma institute of technology for encouraging this program which causes me for upgrading my profession.

ABSTRACT

Any structural element has to be design for economy and safely. Beam is one of the main structural elements and it has to be design appropriately. To guide structural designers selecting material it is good to carry out comparative study on materials of steel and concrete with respect to their flexural and fire resistance on the basis of modular ratio.

Modular ratio is the ratio of YoungsModulii of Elasticity of two different materials in construction of steel and concrete materials. In relation to this gross area cross section of RC beam changed to the equivalent area of steel and then comparative analysis was done for effect of flexure and fire on RC and steel beam.

Fire starts when flammable materials light. At that point, it spreads horizontally and vertically relying upon the compartment limits. A temperature slope is produced through uncovered RC components. These raised temperatures cause the component's solidness to corrupt and deliver warm distortions. Basic fire wellbeing of reinforced concrete structures is presently assessed dependent on the flame evaluations of single components, i.e. columns, beams, walls, and slabs. However, the overall behavior of the structure during a fire should be assessed to ensure the safety of the occupants and the fire fighters during evacuation.

Flexural strength is a material property, defined as the stress in a material just before it yields in a flexure test. The flexural strength represents the highest stress experienced within the material at its moment yield. It is measured in terms of stress.

The general goal of this paper is to make comparative study on steel and concrete beam with respect to flexural and fire resistance on the basis of modular ratio and to propose economical and structurally safe type of beam for construction industry. In order to compare steel and concrete beam Finite Element Software was used.

The attention of this study would be simply supported rectangular reinforced concrete and I section steel beam under fire and uniformly distributed load were considered.

Accordingly, from study bending resistance of reinforced concrete beam is higher than I section steel beam under fire. As well as when I section steel beam increase the size of the cross section with the same length the bending resistance decrease.

Up on the study it has been recommended that use of reinforced concrete members should have to increase in Ethiopia for better bending and fire resistance and in Ethiopia there is nothing done at this field of study so it should have to be a progress from now on as the construction industry is rapidly growing. Moreover, Ethiopian building code has limitation on fire design methods, but fire analysis is most important analysis like strength and stability analysis.

TABLE OF CONTENTS

DECLARATION	I
ACKNOWLEDGMENT	II
ABSTRACT	III
LIST OF TABLES	VII
LIST OF FIGURES	VIII
LIST OF NOTATIONS	XI
ACRONYMS	XIII
CHAPTER ONE	1
INTRODUCTION	1
1.1 Background of the Study	1
1.2 Statement of the Problem.....	2
1.3 Research Question	3
1.4 Objectives of the Study.....	3
1.4.1 General objective	3
1.4.2 Specific objective.....	3
1.5 Significance of the Study.....	3
1.6 Scope and Limitation of the Study.....	4
CHAPTER TWO	5
REVIEW OF RELATED LITERATURE	5

2.1 Background.....	5
2.1.1 Beam	5
2.1.2 Reinforced Concrete Structure.....	6
2.1.3 Steel Structure.....	6
2.2 Material Properties at Normal Temperature	6
2.3 Historical background of flexural (bending) resistance.....	9
2.4 Fire resistance according to Euro-Code.....	16
2.5 Relation between flexure and fire resistance	40
2.6 Modular Ratio	41
CHAPTER THREE	42
RESEARCH METHODS AND MATERIALS	42
3.1 Research Design.....	42
3.2 Study Variables.....	42
3.3 Study Population.....	42
3.4 Sample size.....	43
3.5 Span Length and Support Condition.....	43
3.6 Materials.....	44
3.7 Solver Used.....	45
3.8 Model Background.....	46
3.9 Analysis Fire Models	47

3.10 Major Assumptions.....	48
3.11 Material Properties.....	49
3.12 Boundary Conditions	49
3.13 Ambient Loading	49
3.14 Thermal Loading.....	50
CHAPTER FOUR	51
RESULTS AND DISCUSSIONS	51
4.1 Conversion of Reinforced Concrete Beam to I section Steel Beam By Modular Ratio	51
4.2 Checking of Steel Beam Cross Section	52
4.3 Deformation of Reinforced Concrete Beam due to fire and flexure.....	54
4.4 Deformation of I – Section Steel Beam due to fire and flexure.....	63
4.5 Validation of the finite element model	72
4.5.1 Validation of reinforced concrete beam.....	72
4.5.2 Validation of I section steel beam.....	75
CHAPTER FIVE	77
CONCLUSIONS AND RECOMMENDATIONS	77
5.1 Conclusions	77
5.2 Recommendations.....	77
REFERENCE	79
Appendix A: Design calculations	82
Appendix B: Input Material Properties	85

LIST OF TABLES

Table 2.1: Values for the main parameters of the stress-strain relationships concrete18

Table 2.2: Class N values for the parameters of the stress-strain relationship of steel21

Table 2.3: Reduction for stress-strain relationship of carbon steel at elevated temperature.....28

Table 4.1: Conversion reinforced beam to I section Steel beam by using modular ratio51

Table 4.2: The converted I - section steel beam52

Table 4.3: Check for Cross Section as per Euro Code.....52

Table 4.4: Check for Cross Section Modulus as per Euro Code.....53

Table 4.5: Deflection of Reinforced Concrete Beam due to fire and flexure.....54

Table 4.6: Deflection of I – Section Steel Beam due to fire and flexure.....63

LIST OF FIGURES

Figure 2.1:Simply supported beam with loading.....5

Figure 2.2: Stress – Strain relation for concrete under compression.....7

Figure 2.3: Stress-strain diagrams of typical reinforcing steel.....8

Figure 2.4: Shear Force Bending Moment Diagram.....10

Figure 2.5: Pure Bending.....11

Figure 2.6: Stress Diagram.....12

Figure 2.7:Cross-section of a beam15

Figure 2.8: Coefficient allowing for decrease of tensile strength of concrete19

Figure 2.9: Mathematical model for stress-strain relationships of reinforcing steel20

Figure 2.10: Total thermal elongation of concrete.....22

Figure 2.11: Specific heat, $c_p(\theta)$, as function of temperature.....23

Figure 2.12: Design values for reduction of modulus of elasticity with temperature.....24

Figure 2.13: Thermal elongation of concrete at elevated temperatures.....25

Figure 2.14: Collapsed textile factory in Alexandria, Egypt.....26

Figure 2.15: Stress-strain relationships for steel at elevated temperatures.....29

Figure 2.16: Relative thermal elongation of carbon steel as a function of the temperature.....31

Figure 2.17: Specific heat of carbon steel as a function of the temperature.....32

Figure 2.18: Thermal conductivity of carbon steel as a function of the temperature.....33

Figure 2.19: Thermal strain of steel at elevated temperatures.....34

Figure 2.20: Relative mechanical properties at elevated temperatures in comparison35

Figure 2.21: Temperature-time curves.....	37
Figure 2.22: Nominal fire curves compared with a parametric fire.....	39
Figure 2.23: Development of cracks in a flexural member.....	41
Figure 3.1: Type of beams.....	42
Figure 3.2: Equivalent area conversion diagram.....	43
Figure 3.3: Sample of detail modeling.....	46
Figure 3.4: The Generalized Exponential Curve Suggested by Usmani.....	48
Figure 3.5: The side of steel and reinforced concrete by affected by fire.....	50
Figure 4.1: Mid span deflection of RC-B1-C20 beam.....	55
Figure 4.2: Mid span deflection of RC-B1-C25 beam.....	55
Figure 4.3: Mid span deflection of RC-B1-C30 beam.....	56
Figure 4.4: Mid span deflection of RC-B1-C35 beam.....	56
Figure 4.5: Mid span deflection of RC-B2-C20 beam.....	57
Figure 4.6: Mid span deflection of RC-B2-C25 beam.....	57
Figure 4.7: Mid span deflection of RC-B2-C30 beam.....	58
Figure 4.8: Mid span deflection of RC-B2-C35 beam.....	58
Figure 4.9: Mid span deflection of RC-B3-C20 beam.....	59
Figure 4.10: Mid span deflection of RC-B3-C25 beam.....	59
Figure 4.11: Mid span deflection of RC-B3-C30 beam.....	60
Figure 4.12: Mid span deflection of RC-B3-C35 beam.....	60
Figure 4.13: Mid span deflection of RC-B4-C20 beam.....	61

Figure 4.14: Mid span deflection of RC-B4-C25 beam.....	61
Figure 4.15: Mid span deflection of RC-B4-C30 beam.....	62
Figure 4.16: Mid span deflection of RC-B4-C35 beam.....	62
Figure 4.17: Mid span deflection of IS-B1-C20 beam.....	64
Figure 4.18: Mid span deflection of IS-B1-C25 beam.....	64
Figure 4.19: Mid span deflection of IS-B1-C30 beam.....	65
Figure 4.20: Mid span deflection of IS-B1-C35 beam.....	65
Figure 4.21: Mid span deflection of IS-B2-C20 beam.....	66
Figure 4.22: Mid span deflection of IS-B2-C25 beam.....	66
Figure 4.23: Mid span deflection of IS-B2-C30 beam.....	67
Figure 4.24: Mid span deflection of IS-B2-C35 beam.....	67
Figure 4.25: Mid span deflection of IS-B3-C20 beam.....	68
Figure 4.26: Mid span deflection of IS-B3-C25 beam.....	68
Figure 4.27: Mid span deflection of IS-B3-C30 beam.....	69
Figure 4.28: Mid span deflection of IS-B3-C35 beam.....	69
Figure 4.29: Mid span deflection of IS-B4-C20 beam.....	70
Figure 4.30: Mid span deflection of IS-B4-C25 beam.....	70
Figure 4.31: Mid span deflection of IS-B4-C30 beam.....	71
Figure 4.32: Mid span deflection of IS-B4-C35 beam.....	71
Figure 4.33: Details of specimens.....	72
Figure 4.34: Comparisons of the RC beams tested.....	73

LIST OF NOTATIONS

$\theta_{a,t}$	steel temperature at time
λ_p	thermal conductivity [W/mK]
ρ_p	specific mass [J/kgK] of the fire protection system
ϕ	diameter of a reinforcing bar
ρ_a	specific mass of steel [kg/m ³]
γ	partial safety factor
A	Cross sectional area
A _c	Cross sectional area of concrete
C _p	Temperature independent specific heat of the fire protection material [J/kgK]
E _a	Modulus of elasticity of structural steel
E _{cm}	Secant modulus of elasticity of concrete
E _s	Design value of modulus of elasticity of reinforcing steel
I	Second moment of area of concrete section
L	Length
R120	Fire resistance class for the load-bearing criterion for 120 minutes in standard fire
T	Temperature
b	overall width of a cross-section
d	diameter ;
d _p	thickness of the fire protection material [m]

f_c	compressive strength of concrete
f_{cd}	design value of concrete compressive strength
f_{ck}	characteristic compressive cylinder strength of concrete at 28 days
f_{ctd}	tensile strength of concrete
f_y	yield strength of reinforcement
f_{yd}	design yield strength of reinforcement
h	overall depth of a cross-section
k	coefficient ; Factor
t	time being considered
P_d	design load
M_d	design moment
D	depth of the beam
A_{st}	area of steel reinforcement
S	spacing of stirrup
V_{Rd}	diagonal compression failure in the concrete the shear resistance
V_s	the applied shear force at d distance from face of support

ACRONYMS

ACI	American Concrete Institute
AISC	American Institute of Steel Construction
ASTM	American Society for Testing Materials
EBCS	Ethiopian Building Code Standard
ECCS	European Convention for Constructional Steelwork
EN	European Standard
NIST	National Institute of Standards and Technology

CHAPTER ONE

INTRODUCTION

1.1 Background of the Study

Bending member is a general term for individuals subjected to bending. Beams can be constructed from various materials like, basic steel, strengthened cement and steel-solid composite materials and other. The decision of sort of bar relies upon various criteria resembles quality, accessibility, imperviousness to fire and cost.

Structural fire safety is one of the primary considerations in the design of high-rise buildings where steel is often the material of choice for structural members. At present, structural fire safety resistance of steel members is generally achieved through prescriptive approaches which are based on either standard fire resistance tests or empirical calculation methods. These prescriptive based approaches have major drawbacks and do not provide a rational or realistic fire resistance assessment. The recent move toward performance-based fire design has increased the focus on the use of computer simulations for evaluating fire resistance of structural members. Knowledge of high-temperature properties of steel is critical for evaluating fire resistance using numerical models [1].

Beams can be constructed from various materials like, basic steel, strengthened cement and steel-solid composite materials and other. Bending causes the bottoms of simple beams to become stretched in tension and the tops of beams to be pushed together in compression. Continuous beams and cantilever beams have tension forces at the top and a compression at the bottom near their supports. At mid span, the forces are in the same locations as for simple beams and slabs. Vertical cracks develop near the mid span of concrete, since the tension force causes the concrete to crack. The reinforcing steel provided in the tension zones is assumed to resist the entire tension force. This tension cracking can be observed in damaged structures and may be used to monitor and determine the potential for collapse. Stable, hairline cracks are normal, but widening cracks indicate impending failure.

In the elastic theory, structures having different materials are made equivalent to one common material. To convert cross section area of concrete to steel the use modular ratio is applied.

The flexural and fire resistance analysis is according to Euro Code. Euro code norms provide basic guidelines for the analysis of reinforced concrete and steel structures subjected to fire. To determine the behavior of structure, an advanced calculation method must be applied, to comprehend nonlinear material properties and effects that occur during the course of fire. These include thermal and mechanical properties of concrete and steel and transient thermal and structural analysis. The paper presented comparative study on different type of beam for flexure and fire resistance based on modular ratio by using Finite Element Software (Abaqus 6.14-1). The purpose of the work presented here is to compare different beams based on their flexural and fire resistance and to recommend the best type of beam.

1.2 Statement of the Problem

Now a days cost of construction material is increasing and availability of a material is decreasing. As well as factors that affect resistance capacity of beam is increasing through the time, from those flexural and fire is critical.

Various numerical, experimental and finite element method studies have been carried out to evaluate different type of beam with respect to fire resistance and some with respect to bending. Nonetheless, still now there is limited experience about which material is economically and structurally safe to fit flexural and fire resistance.

A comparative study was carried out on steel and reinforced concrete beam their capacity to resist flexure and fire on the basis of modular ratio to select the economical beam on the basis of safety.

1.3 Research Question

1. To what extent is that reinforced concrete beam affected by fire and bending?
2. To what extent is that steel beam affected by fire and bending?
3. What is the combined effect of fire and flexure on steel and RC beam on the basis of modular ratio?
4. Which type of beam is economical and safe with respect to fire and bending resistance on the basis of modular ratio?

1.4 Objectives of the Study

1.4.1 General objective

The general objective of the study was to make a comparative study on steel and concrete beam with respect to flexural and fire resistance on the basis of modular ratio and to propose economical and structurally safe type of beam for construction industry using finite element analysis.

1.4.2 Specific objective

- 1 To evaluate the effect of fire on RC and steel beam on the basis of modular ratio.
- 2 To determine the resistance of RC and steel beam to flexure on the basis of modular ratio.
- 3 To find out economical and structurally safe beam type with respect to fire and bending resistance on the basis of modular ratio.

1.5 Significance of the Study

In Ethiopia, there is an interest to construct high rise building to use the land effectively for different purpose. As well as that there is shortage of construction material and cost is increasing rapidly day by day. To simplify these problems, it is necessary to make comparative study on steel and reinforced concrete beam to propose the economical and structurally safe type of beam regarding to resistance of fire and flexure on the basis of modular ratio. Additionally to create awareness about the effect of flexure and fire on reinforced concrete and steel beam.

Moreover, that fire cause heavy damage on building than other cause. Hence fire resistance is main issue for structural element. Ethiopian building code has constraint on presenting fire design processes; accordingly this study described methods of fire design of beam to fill this gap by referring different codes. This study leads to show the advantage and disadvantages of different of reinforced concrete and I section steel beam on the basis of modular ratio.

1.6 Scope and Limitation of the Study

The scope of study was to analyze and model simply supported short span beams. Symmetrical I section steel beam and rectangular reinforced concrete beam based on their modular ratio subjected to uniform loading and fire using ABAQUS software.

The research is limited to other resistivity capacity such as torsional capacity for RC and steel beam and lateral buckling for steel beam.

CHAPTER TWO

REVIEW OF RELATED LITERATURE

2.1 Background

2.1.1 Beam

A beam is a structural member that supports applied loads and its own weight primarily by internal moments and shears [2].

The loads applied to the beam result in reaction forces at the beam's support points. The total effect of all the forces acting on the beam is to produce shear forces and bending moments within the beam, that in turn induce internal stresses, strains and deflections of the beam. Beams are characterized by their manner of support, profile (shape of cross-section), length, and their material.

Beams are traditionally descriptions of building or civil engineering structural elements, but any structures such as automotive automobile frames, aircraft components, machine frames, and other mechanical or structural systems contain beam structures that are designed to carry lateral loads are analyzed in a similar fashion.

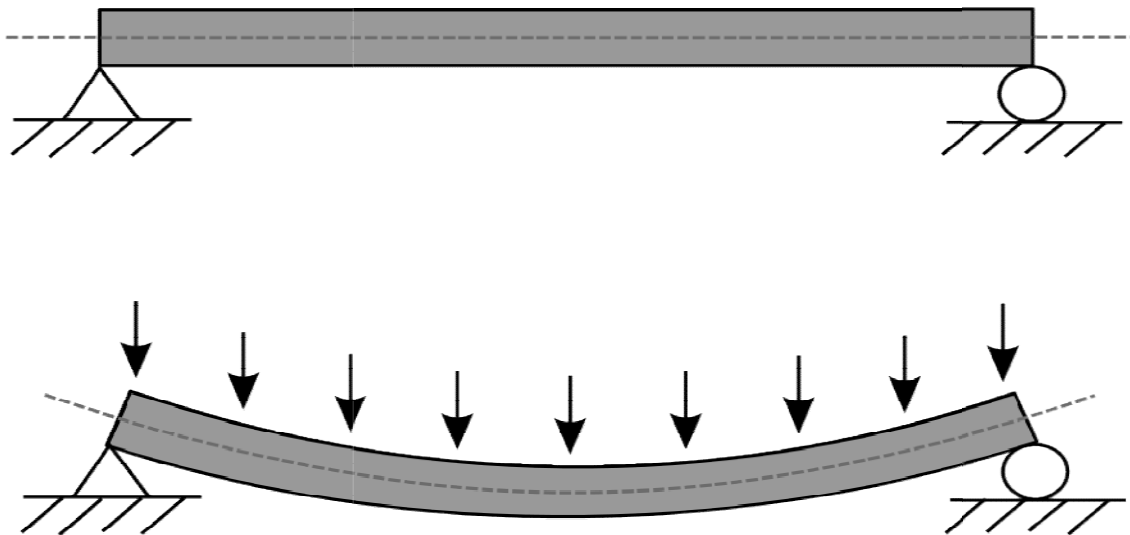


Figure 2.1: simply supported Beam with loading

2.1.2 Reinforced Concrete Structure

W. B. Wilkinson of Newcastle-upon-Tyne obtained a patent in 1854 for a reinforced concrete floor system that used hollow plaster domes as forms. The ribs between the forms were filled with concrete and were reinforced with discarded steel mine-hoist ropes in the center of the ribs. In France, Lambot built a rowboat of concrete reinforced with wire in 1848 and patented it in 1855. His patent included drawings of a reinforced concrete beam and a column reinforced with four round iron bars. In 1861, another Frenchman, Coignet, published a book illustrating uses of reinforced concrete [2].

2.1.3 Steel Structure

The exact date at which people discovered the technique of smelting iron ore to produce usable metal is not known. But metal as a structural material began with cast iron, used in England in 1777. Then wrought iron began replacing cast iron soon after 1840. The process of rolling various shapes was developing as cast iron and wrought iron received wider usage. Bars were rolled on an industrial scale beginning about 1780. The rolling of rails began about 1820 and extended to I shapes by the 1870s. Since 1890 steel has replaced wrought iron as the principal metallic building material [3].

Steel is a structural material which consists mostly of iron and carbon. Steel has the same strength in tension as it has in compression, unlike concrete. Its great strength, uniformity, light weight, ease of use, and many other desirable properties makes it the material of choice for numerous structures such as steel bridges, high rise buildings, towers, and other structure.

2.2 Material Properties at Normal Temperature

Concrete

Plain concrete is formed from a hardened mixture of cement, water, fine aggregate, and coarse aggregate, air and often other admixtures. The plastic mix is placed and consolidated in the form work and, then cured to facilitate the acceleration of the chemical hydration reaction of the cement-water mix. The result is hardened concrete. The finished product has high compressive

strength and low resistance to tensile. so tensile and shear reinforcement in the tensile region is provided.

The characteristic compressive strength of concrete is f_{ck} is given in EN1992-1-1 Table 3.1.

Typical properties of normal strength Portland cement concrete

- Density : 2240 – 2400 kg/m³
- Coefficient of thermal expansion: $\alpha = 10 \cdot 10^{-6} \text{ K}^{-1}$
- Poisson's ratio : 0.2 for un cracked concrete

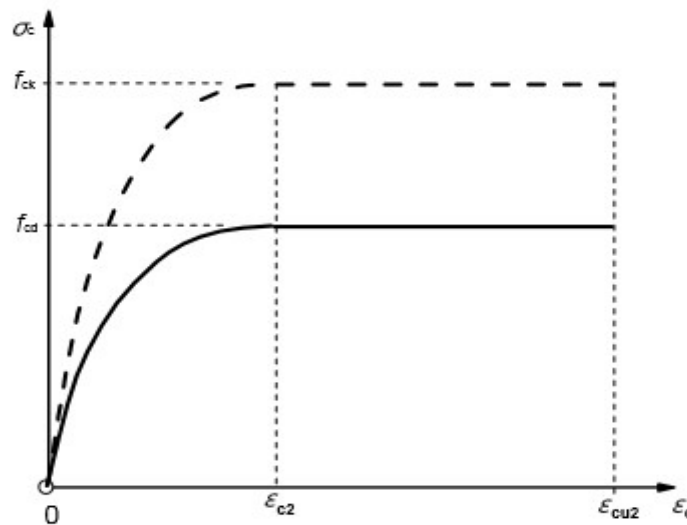


Figure 2.2: Stress – Strain relation for concrete under compression (Euro Code, 1992-1-2)

Steel

The most important structural properties of steel are yield strength, ultimate strength and modulus of elasticity.

Material properties for hot rolled steel

Modulus of elasticity $E = 210 \text{ GPa}$

Poisson's ratio $\nu = 0.3$

Coefficient of linear thermal expansion $\alpha = 12 \cdot 10^{-6}$ per K

Unit mass $\rho = 7850 \text{ kg/m}^3$

Stress – strain Behavior of Steel

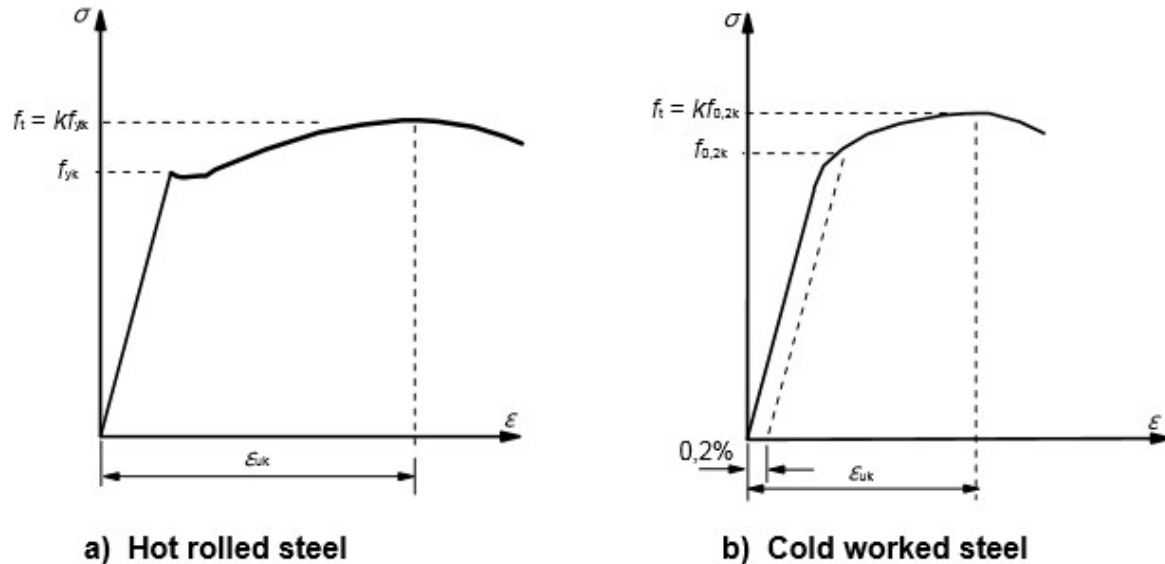


Figure 2.3: Stress-strain diagrams of typical reinforcing steel (Euro Code, 1992-1-1)

- Elastic Region

In this region the stress is proportional to the strain, and hook's law applies. The constant of proportionality is the modulus of elasticity or young's modulus, E . the modulus of elasticity of steel has values ranging from **195 – 210 GPa**.

- Inelastic Region

In this section the steel section deforms plastically under a constant stress, f_y . Generally, the ability of a material to undergo plastic deformation prior to fracture decreases with increasing steel strength.

- Strain-Hardening

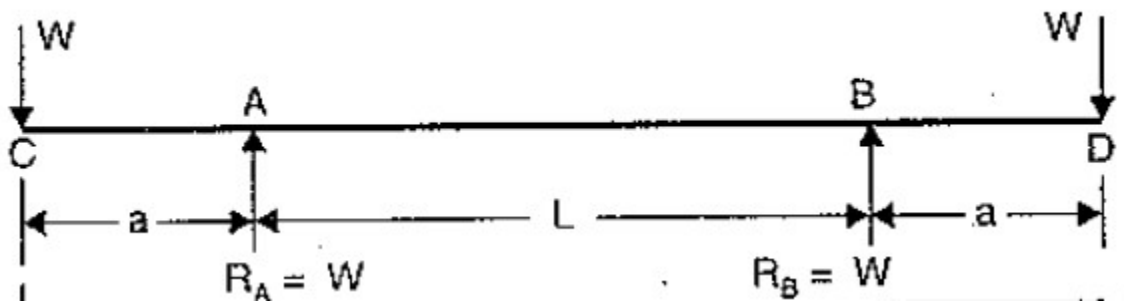
Region In this region deformation is accompanied by an increase in stress. The peak point of the ideal stress-strain curve is the ultimate stress, **fu**. This is the largest stress the material can attain under uni-axial condition.

2.3 Historical background of flexural (bending) resistance

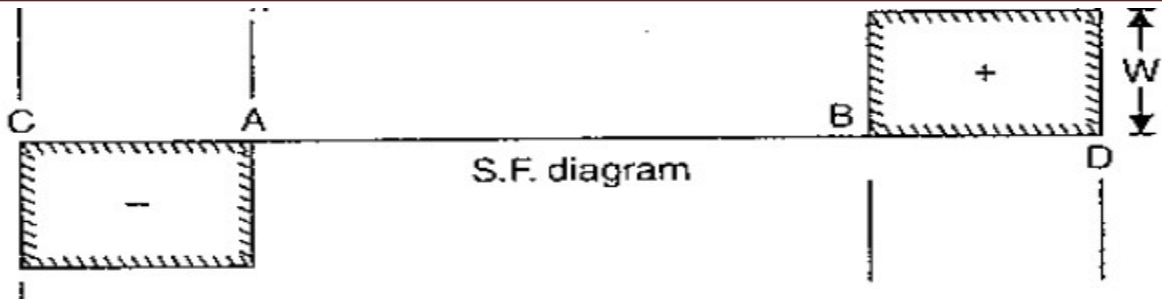
When some external load acts on a beam, the shear force and bending moments are set up at all sections of the beam, Due to the shear force and bending moment, the beam under goes certain deformation. The material of the beam will offer resistance or stresses against these certain deformation. The material of the beam will offer resistance or stresses against these deformations. These stresses with certain assumptions can be calculated. The stresses introduced by bending moment are known as bending stresses [4].

2.3.1 Pure Bending

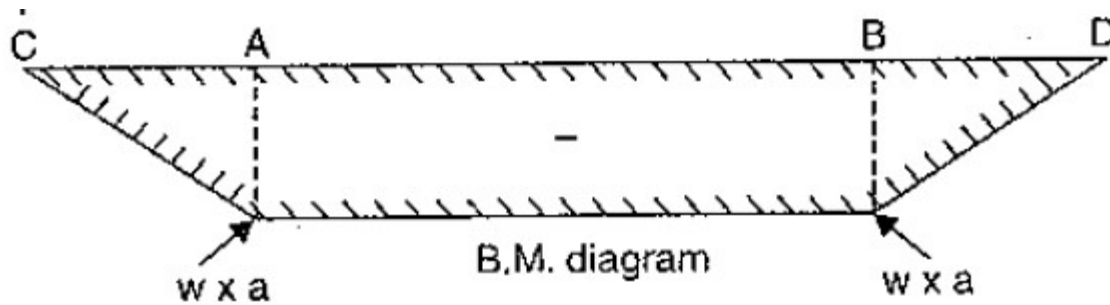
If a length of a beam is subjected to a constant bending moment and no shear force (i.e., zero shear force), then the stresses will be set up in that length of the beam due to B.M. only and that length of the beam is said to be in pure bending or simple bending. The stresses set up in that length of beam are known as bending stresses[4].



(a)



(b)



(c)

Figure 2.4: Shear Force Bending Moment Diagram

A beam simply supported at A and B and overhanging by same length at each support is shown in Fig.2.4 . A point load W is applied at each end of the overhanging portion. The S.F and B.M. for the beam are drawn as shown in Fig. 2.4 (b) and Fig. 2.4 (c) respectively. From these diagrams, it is clear that there is no shear force between A and B but the B.M. between A and B are constant.

This means that between A and B, the beam is subjected to a constant bending moment only. This condition of the beam between A and B is known as pure bending or simple bending.

2.3.2 Theory of pure bending with assumptions made

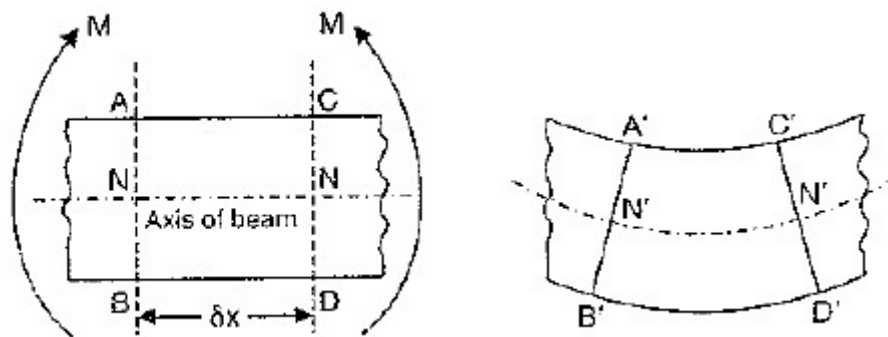
Before discussing the theory of simple bending, let us see the assumptions made in the theory of pure bending. The following are the important assumption [4]:

1. The material of the beam is homogenous and isotropic.
2. The value of Young's modulus of elasticity is the same in tension and compression.

3. The transverse section which were plane before bending, remain plane after bending also.
4. The beam is initially straight and all longitudinal filaments bend into circular arcs with a common center of curvature.
5. The radius of curvature is large compared with the dimensions of the cross-section.
6. Each layer of the beam is free to expand or contract, independently of the layer, above or below it.

Fig. 2.5(a) shows a part of a beam subjected to pure bending. Consider a small length or of this part of beam. Consider two section AB and CD which are normal to the axis of the beam N-N. Due to the action of the bending moment, the part of length or will be deformed as shown in Fig 2.5 (b). From the figure, it is clear that all the layers of the beam, which were originally of the same length, do not remain of the same length any more.

The top layer such as AC has deformed to the shape A'C'. This layer has been shortened in its length. The bottom layer BD has deformed to the shape B'D'. This layer has been elongated. From the Fig. 2.5(b), it is clear that some of the layers have been shortened while some of them are elongated. At a level between the top and bottom of the beam, there will be a layer which is neither shortened nor elongated. This is known as neutral layer or neutral surface. This layer Fig. 2.5(b) is shown by N'-N' and in Fig. 2.5 (a) by N-N. The line of intersection of the neutral layer on cross-section of a beam is known as neutral axis[4].



(a) Before Bending (b) Before Bending

Figure 2.5: Pure Bending

2.3.3 Expression for Bending Stress

Fig. 2.6(a) shows a small length δx of a beam subjected to a simple bending. Due to the action of bending, the part of length δx will be deformed as shown in Fig. 2.6 (b) Let A'B' and C'D' meet at O.

Let R = Radius of neutral layer N'N'

Θ = Angle subtended at O by A'B' and C'D' produced.

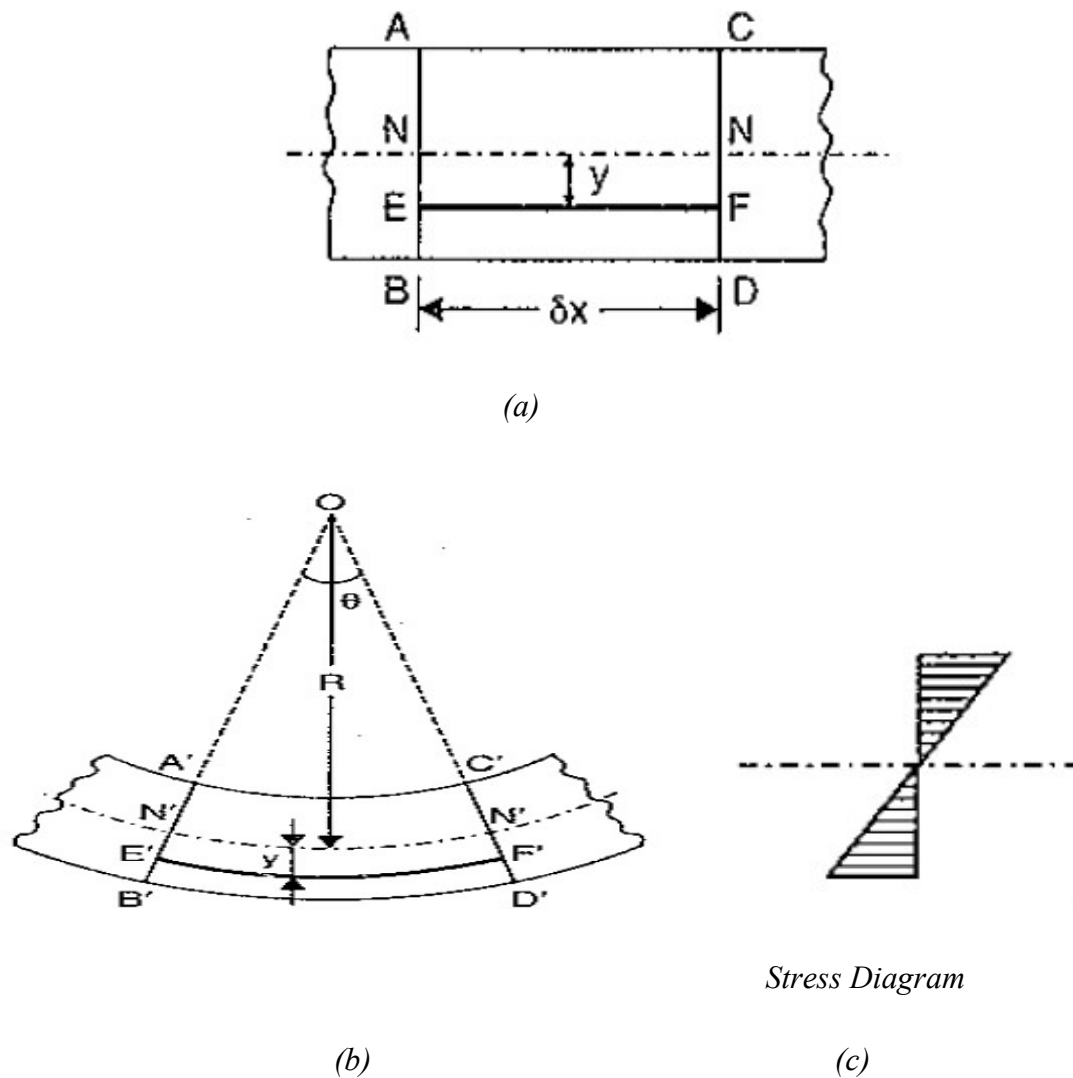


Figure 2.6:Stress Diagram

2.3.3.1 Strain Variation along the Depth of Beam

Consider a layer EF at a distance y below the neutral layer NN. After Bending this layer will be elongated to E'F' [4].

Original length of layer EF = δx

Also length of neutral layer NN = δx

After bending, the length of neutral layer N'N' will remain unchanged. But length of layer E'F' will increase. Hence

$$N'N' = NN = \delta x$$

Now from Fig. 7.3(b),

$$N'N' = R\theta \quad \text{and} \quad E'F' = R(\theta + \theta)$$

Radius of E'F' = $R + y$

$$\text{Hence} \quad \delta x = R\theta$$

Increase in the length of the layer EF

$$= E'F' - EF = (R + y)\theta - R\theta \quad (EF = \delta x = R\theta)$$

Strain in the layer EF

$$= \frac{\text{Increase in Length}}{\text{Original Length}}$$

$$= \frac{(yx\theta)}{(EF)} = \frac{(yx\theta)}{(R\theta)}$$

$$= y/R$$

2.3.3.2 Stress Variation

Let σ = Stress in the layer EF

E = Young's modulus of the beam

Then $E = \frac{\text{Stress in the layer EF}}{\text{Strain in the layer EF}}$

$E = \sigma / (y/R)$ (Strain in EF = y/R)

$$\sigma = E \times \frac{y}{R} = y \times \frac{E}{R}$$

Since E and R are constant, therefore stress in any layer is directly proportional to the distance of the layer from the neutral layer.

2.3.4 Neutral Axis and Moment of Resistance

The neutral axis of any transverse section of a beam is defined as the line of intersection of the neutral layer with the transverse section. It is written as N.A.

In Fig. 2.7, we have seen that if a section of a beam is subjected to pure sagging moment, then the stresses will be compressive at any point above the neutral axis and tensile below the neutral axis. There is no stress at the neutral axis. The stress at a distance y from the neutral axis is given by equation as;

$$\sigma = \frac{E}{R} \times y$$

Fig. 2.7 shows the cross-section of a beam. Let N.A. be the neutral axis of the section. Consider a small layer at a distance y from the neutral axis. Let dA = Area of the layer.

Now the force on the layer

= Stress on layer x Area of the layer

$$= \sigma \times dA$$

$$= \frac{E}{R} \times y \times dA$$

Total force on the beam section is obtained by integrating the above equation.

$$\text{Total force on the beam section} = \int \frac{E}{R} \times y \times dA$$

$$= \frac{E}{R} \int y \times dA \quad (\text{E and R is constant})$$

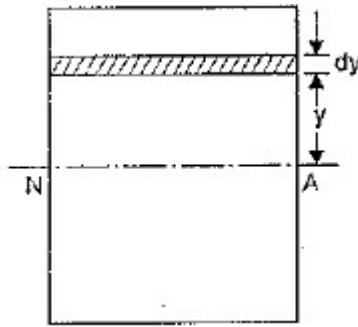


Figure 2.7: Cross-section of a beam

But for pure bending, there is no force on the section of the beam

$$\frac{E}{R} \int y \times dA = 0$$

Or
$$\int y \times dA = 0$$

2.3.4.1 Moment of Resistance

Due to pure bending, the layer above the N.A. are subjected to compressive stresses whereas the layers below the N.A. are subjected to tensile stresses. Due to these stresses, the forces will be acting on the layers. These forces will have moment about the N.A. The total moment of these forces about the N.A. for a section is known as moment of resistance of that section [4].

Force on layer
$$= \frac{E}{R} \times y \times dA$$

Moment of this force about N.A.

$$= \text{Force on layer} \times y^2$$

$$= \frac{E}{R} \times y \times dA \times y$$

$$= \frac{E}{R} \times y^2 \times dA$$

Total moment of the forces on the section of the beam (or moment of resistance)

$$= \int \frac{E}{R} \times y^2 \times dA = \frac{E}{R} \int y^2 \times dA$$

Let M=External moment applied on the beam section. For the equilibrium the moment of resistance offered by the section by the section should be equal to the external bending moment.

$$M = \frac{E}{R} \int y^2 \times dA$$

But the expression $\int y^2 \times dA$ represents the moment of inertia of the area of the section about the neutral axis. Let this moment of inertia be I.

$$M = \frac{E}{R} I \quad \text{or} \quad \frac{M}{I} = \frac{E}{R}$$

$$\frac{\sigma}{y} = \frac{E}{R}$$

Bending Equation;

$$\frac{M}{I} = \frac{\sigma}{y} = \frac{E}{R}$$

2.4 Fire resistance according to Euro-Code

Structural fire safety is one of the primary considerations in the design of high-rise buildings where steel is often the material of choice for structural members. At present, structural fire safety (fire resistance) of steel members is generally achieved through prescriptive approaches which are based on either standard fire resistance tests or empirical calculation methods. These prescriptive based approaches have major drawbacks and do not provide a rational or realistic fire resistance assessment. The recent move toward performance-based fire design has increased the focus on the use of computer simulations for evaluating fire resistance of structural members. Knowledge of high-temperature properties of steel is critical for evaluating fire resistance using numerical models [5].

Exposure of an RC beam to elevated temperatures during a fire leads to significant losses in the strength and stiffness of the concrete and the reinforcing steel as well as the bond between them. However, in all existing numerical models, except the model presented in a recent publication by Huang [6].

2.4.1 Material properties of concrete at elevated temperatures

2.4.1.1 Mechanical properties (strength and deformation properties)

Concrete under compression:

The strength and deformation properties of uniaxial stressed concrete at elevated temperatures shall be obtained from the stress-strain relationships as presented in the next table.

The stress-strain relationships are defined by two parameters:

- The compressive strength $f_{c,\theta}$
- The strain $\epsilon_{1,\theta}$ corresponding to $f_{c,\theta}$

Table 2.1: Values for the main parameters of the stress-strain relationships of normal weight concrete with siliceous or calcareous aggregates concrete at elevated temperatures. (Euro Code, 1992-1-2)

Concrete temp. θ [°C]	Siliceous aggregates			Calcareous aggregates		
	$f_{c,\theta} / f_{ck}$ [-]	$\varepsilon_{c1,\theta}$ [-]	$\varepsilon_{cu1,\theta}$ [-]	$f_{c,\theta} / f_{ck}$ [-]	$\varepsilon_{c1,\theta}$ [-]	$\varepsilon_{cu1,\theta}$ [-]
1	2	3	4	5	6	7
20	1,00	0,0025	0,0200	1,00	0,0025	0,0200
100	1,00	0,0040	0,0225	1,00	0,0040	0,0225
200	0,95	0,0055	0,0250	0,97	0,0055	0,0250
300	0,85	0,0070	0,0275	0,91	0,0070	0,0275
400	0,75	0,0100	0,0300	0,85	0,0100	0,0300
500	0,60	0,0150	0,0325	0,74	0,0150	0,0325
600	0,45	0,0250	0,0350	0,60	0,0250	0,0350
700	0,30	0,0250	0,0375	0,43	0,0250	0,0375
800	0,15	0,0250	0,0400	0,27	0,0250	0,0400
900	0,08	0,0250	0,0425	0,15	0,0250	0,0425
1000	0,04	0,0250	0,0450	0,06	0,0250	0,0450
1100	0,01	0,0250	0,0475	0,02	0,0250	0,0475
1200	0,00	-	-	0,00	-	-

Concrete Tensile strength:

The tensile strength of concrete should normally be ignored (conservative). If it is necessary to take account of the tensile strength, when using the simplified or advanced calculation method, this clause may be used.

The reduction of the characteristic tensile strength of concrete is allowed for by the coefficient $k_{c,t}(\theta)$ as given,

$$f_{ck,t}(\theta) = k_{c,t}(\theta) f_{ck,t}$$

In absence of more accurate information the following $k_{c,t}(\theta)$ values should be used,

$$k_{c,t}(\theta) = 1,0 \quad \text{for } 20\text{ }^{\circ}\text{C} \leq \theta \leq 100\text{ }^{\circ}\text{C}$$

$$k_{c,t}(\theta) = 1,0 - 1,0 (\theta - 100)/500 \quad \text{for } 100\text{ }^{\circ}\text{C} < \theta \leq 600\text{ }^{\circ}\text{C}$$

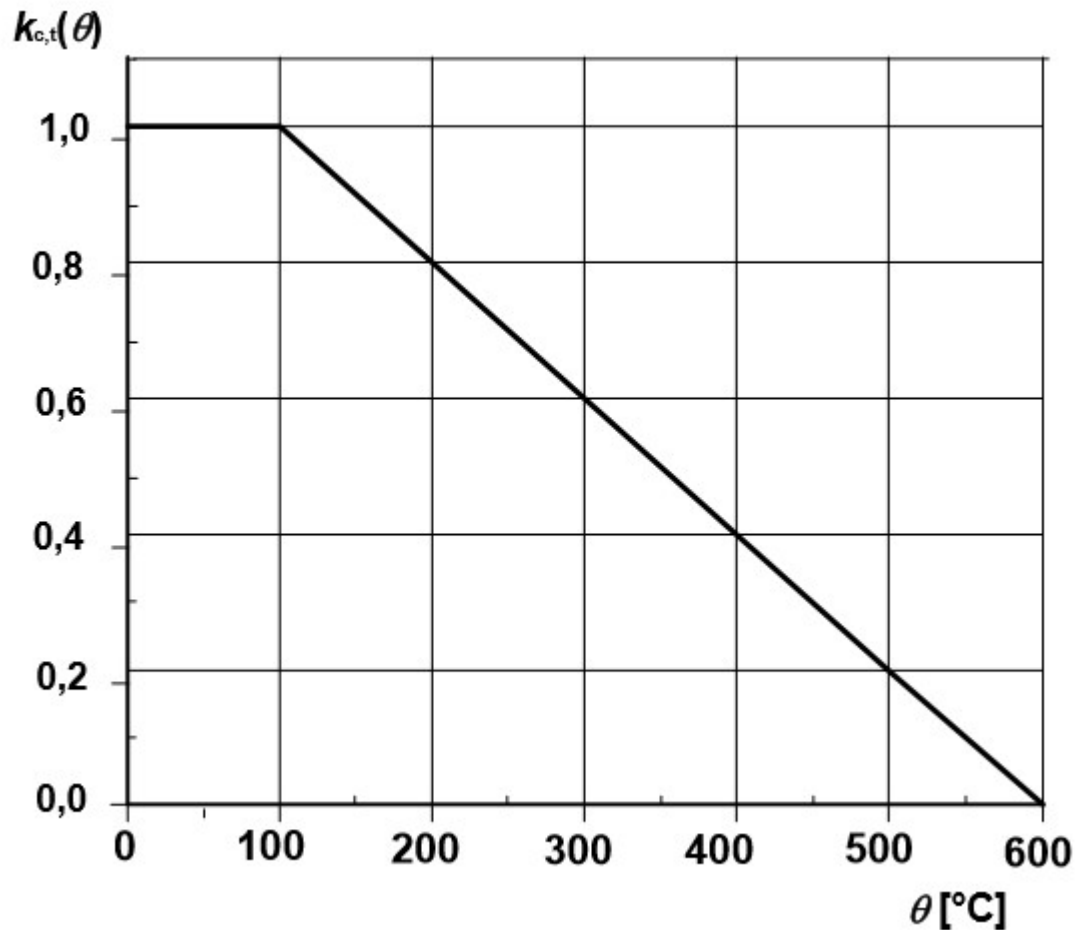


Figure 2.8: Coefficient $k_{c,t}(\theta)$ allowing for decrease of tensile strength ($f_{ck,t}$) of concrete at elevated temperatures. (Euro Code, 1992-1-2)

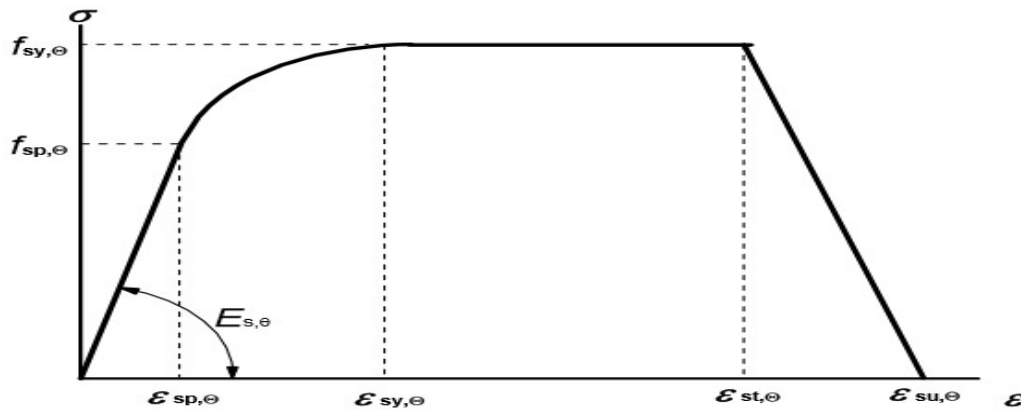
Reinforcing steel:

The stress-strain relationships given in Figure 2.9 are defined by three parameters:

- the slope of the linear elastic range $E_{s,\theta}$

- the proportional limit $f_{sp,\theta}$
- the maximum stress level f_{sy} ,

Values for the parameters in (2) for hot rolled and cold worked reinforcing steel at elevated temperatures are given in Table 2.2 . For intermediate values of the temperature, linear interpolation may be used.



Range	Stress $\sigma(\theta)$	Tangent modulus
$\varepsilon_{sp,\theta}$	$\varepsilon E_{s,\theta}$	$E_{s,\theta}$
$\varepsilon_{sp,\theta} \leq \varepsilon \leq \varepsilon_{sy,\theta}$	$f_{sp,\theta} - c + (b/a)[a^2 - (\varepsilon_{sy,\theta} - \varepsilon)^2]^{0,5}$	$\frac{b(\varepsilon_{sy,\theta} - \varepsilon)}{a[a^2 - (\varepsilon - \varepsilon_{sy,\theta})^2]^{0,5}}$
$\varepsilon_{sy,\theta} \leq \varepsilon \leq \varepsilon_{st,\theta}$	$f_{sy,\theta}$	0
$\varepsilon_{st,\theta} \leq \varepsilon \leq \varepsilon_{su,\theta}$	$f_{sy,\theta} [1 - (\varepsilon - \varepsilon_{st,\theta}) / (\varepsilon_{su,\theta} - \varepsilon_{st,\theta})]$	-
$\varepsilon = \varepsilon_{su,\theta}$	0,00	-
Parameter ^{*)}	$\varepsilon_{sp,\theta} = f_{sp,\theta} / E_{s,\theta}$ $\varepsilon_{sy,\theta} = 0,02$ $\varepsilon_{st,\theta} = 0,15$ $\varepsilon_{su,\theta} = 0,20$	
	Class A reinforcement: $\varepsilon_{st,\theta} = 0,05$ $\varepsilon_{su,\theta} = 0,10$	
Functions	$a^2 = (\varepsilon_{sy,\theta} - \varepsilon_{sp,\theta})(\varepsilon_{sy,\theta} - \varepsilon_{sp,\theta} + c/E_{s,\theta})$ $b^2 = c (\varepsilon_{sy,\theta} - \varepsilon_{sp,\theta}) E_{s,\theta} + c^2$ $c = \frac{(f_{sy,\theta} - f_{sp,\theta})^2}{(\varepsilon_{sy,\theta} - \varepsilon_{sp,\theta})E_{s,\theta} - 2(f_{sy,\theta} - f_{sp,\theta})}$	

^{*)} Values for the parameters $\varepsilon_{pt,\theta}$ and $\varepsilon_{pu,\theta}$ for prestressing steel may be taken from Table 3.3. Class A reinforcement is defined in Annex C of EN 1992-1-1.

Figure 2.9:Mathematical model for stress-strain relationships of reinforcing and prestressing steel at elevated temperatures (notations for prestressing steel “p” instead of “s”).(Euro Code, 1992-1-2)

Table 2.2: Class N values for the parameters of the stress-strain relationship of hot rolled and cold worked reinforcing steel at elevated temperatures.(Euro Code, 1992-1-2)

Steel Temperature θ [°C]	$f_{sy,\theta} / f_{yk}$		$f_{sp,\theta} / f_{yk}$		$E_{s,\theta} / E_s$	
	hot rolled	cold worked	hot rolled	cold worked	hot rolled	cold worked
1	2	3	4	5	6	7
20	1,00	1,00	1,00	1,00	1,00	1,00
100	1,00	1,00	1,00	0,96	1,00	1,00
200	1,00	1,00	0,81	0,92	0,90	0,87
300	1,00	1,00	0,61	0,81	0,80	0,72
400	1,00	0,94	0,42	0,63	0,70	0,56
500	0,78	0,67	0,36	0,44	0,60	0,40
600	0,47	0,40	0,18	0,26	0,31	0,24
700	0,23	0,12	0,07	0,08	0,13	0,08
800	0,11	0,11	0,05	0,06	0,09	0,06
900	0,06	0,08	0,04	0,05	0,07	0,05
1000	0,04	0,05	0,02	0,03	0,04	0,03
1100	0,02	0,03	0,01	0,02	0,02	0,02
1200	0,00	0,00	0,00	0,00	0,00	0,00

2.4.1.2 Thermal and physical properties of concrete

1. Thermal elongation

The variation of the thermal elongation with temperatures

Siliceous aggregates:

$$\epsilon_c(\theta) = -1.8 \times 10^{-4} + 9 \times 10^{-6}\theta + 2.3 \times 10^{-11}\theta^3 \quad \text{for } 20^\circ\text{C} \leq \theta \leq 700^\circ\text{C}$$

$$\epsilon_c(\theta) = 14 \times 10^{-3} \quad \text{for } 700^\circ\text{C} < \theta \leq 1200^\circ$$

The variation of the thermal elongation with temperatures is illustrated in Figure 2.10.

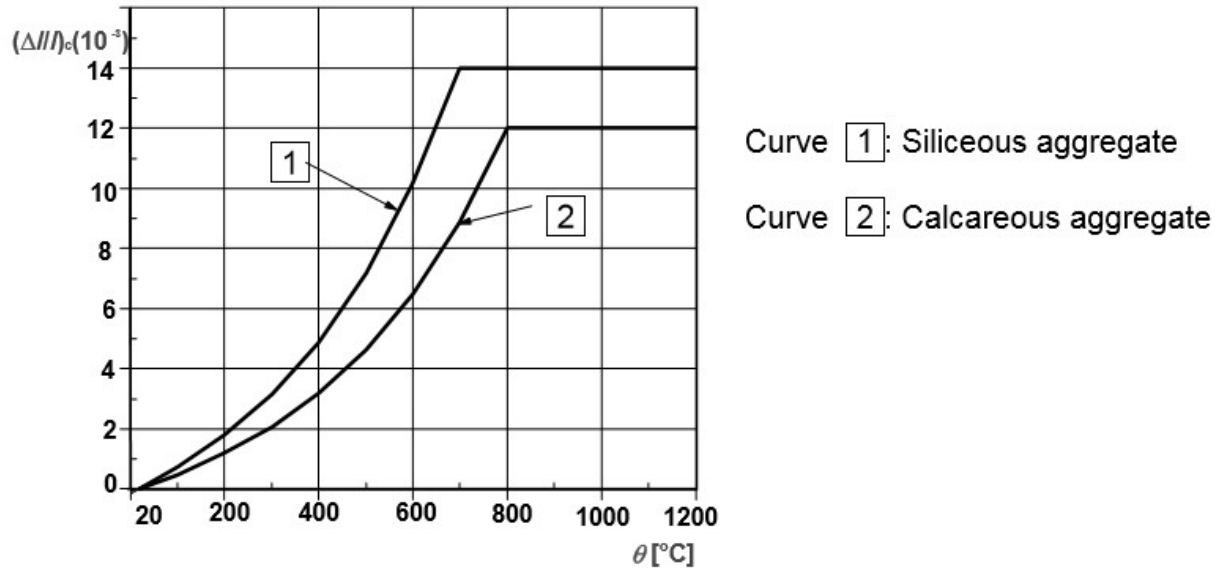


Figure 2.10: Total thermal elongation of concrete. (Euro Code, 1992-1-2)

2. Specific heat

The specific heat $C_p(\theta)$ of dry concrete ($u = 0\%$) may be determined from the following:

$$C_p(\theta) = 900 \text{ (J/kg K)} \quad \text{for } 20^\circ\text{C} \leq \theta \leq 100^\circ\text{C}$$

$$C_p(\theta) = 900 + (\theta - 100) \text{ (J/kg K)} \quad \text{for } 100^\circ\text{C} < \theta \leq 200^\circ\text{C}$$

$$C_p(\theta) = 1000 + (\theta - 200)/2 \text{ (J/kg K)} \quad \text{for } 200^\circ\text{C} < \theta \leq 400^\circ\text{C}$$

$$C_p(\theta) = 1100 \text{ (J/kg K)} \quad \text{for } 400^\circ\text{C} < \theta \leq 1200^\circ\text{C}$$

When there is moisture content different from zero C_p has different values.

And linear relationship between $(115^\circ\text{C}, c_{p,\text{peak}})$ and $(200^\circ\text{C}, 1000 \text{ J/kg K})$. For other moisture contents a linear interpolation is acceptable. The peaks of specific heat are illustrated in Figure 2.11.

The variation of density with temperature is influenced by water loss and is defined as follows

$$\rho(\theta) = \rho(20^\circ\text{C}) \quad \text{for } 20^\circ\text{C} \leq \theta \leq 115^\circ\text{C}$$

$$\rho(\theta) = \rho(20^\circ\text{C}) \cdot (1 - 0,02(\theta - 115)/85) \quad \text{for } 115^\circ\text{C} < \theta \leq 200^\circ\text{C}$$

$$\rho(\theta) = \rho(20^\circ\text{C}) \cdot (0,98 - 0,03(\theta - 200)/200) \quad \text{for } 200^\circ\text{C} < \theta \leq 400^\circ\text{C}$$

$$\rho(\theta) = \rho(20^\circ\text{C}) \cdot (0,95 - 0,07(\theta - 400)/800) \quad \text{for } 400^\circ\text{C} < \theta \leq 1200^\circ\text{C}$$

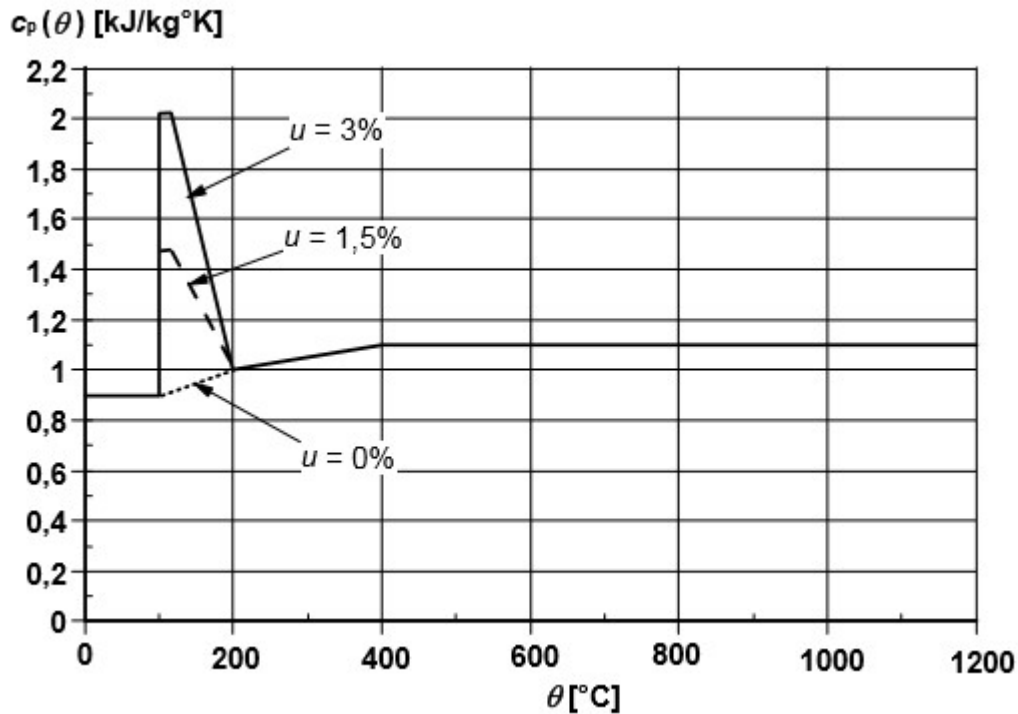


Figure 2.11: Specific heat, $c_p(\theta)$, as function of temperature at 3 different moisture contents, u , of 0, 1,5 and 3 % by weight for siliceous concrete. (Euro Code, 1992-1-2)

3. Thermal conductivity (λ_c)

The thermal conductivity λ_c of concrete may be determined between lower and upper limit

Values,

Upper limit

$$\lambda_c = 2 - 0.2451(\theta / 100) + 0.0107 (\theta / 100)^2 \text{ W/m K} \quad \text{for } 20^\circ\text{C} \leq \theta \leq 1200^\circ\text{C}$$

Lower limit

$$\lambda_c = 1.36 - 0.136 (\theta / 100) + 0.0057 (\theta / 100) \text{ W/m K} \quad \text{for } 20^\circ\text{C} \leq \theta \leq 1200^\circ\text{C}$$

4. Modulus of Elasticity

The modulus of elasticity is decreases with increasing temperature. The following equations from BS 8110 (1985), provides a simplification of the modulus of elasticity at elevated temperatures:

$$\frac{E(T)}{E(20^\circ\text{C})} = 1.0 \text{ for } T \leq 150^\circ\text{C}$$

$$\frac{E(T)}{E(20^\circ\text{C})} = (700 - T)/550 \text{ for } T > 150^\circ\text{C}$$

This simplification can be applied to lightweight, normal weight, and high strength concretes. More complex expressions are available in Euro code 2, 2005. As seen Figure 2.13 from Buchanan [7], the modulus of elasticity reaches zero before the strength of concrete reaches zero. Due to this disconnect, Inwood (1999) has proposed an extension (which appears in the dotted line)[8].

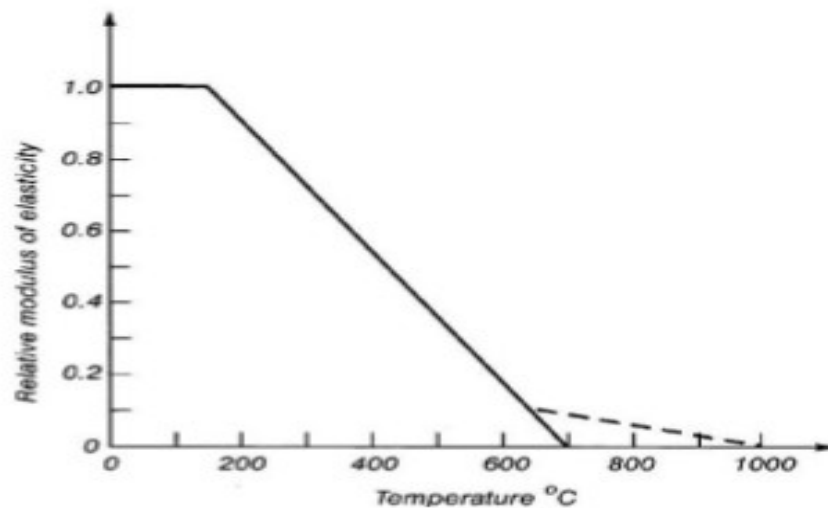


Figure 2.12: -Design values for reduction of modulus of elasticity with temperature. (Reproduced from Buchanan)

5. Thermal Strain

The thermal strain of concrete varies with temperature. Figure 2.13 from Euro code 2 illustrates the variation of the thermal elongation with temperatures. Expressions for these strains (ϵ_c) are as follows for siliceous and calcareous aggregates:

Siliceous aggregates:

$$\begin{aligned}\epsilon_c(\theta) &= -1,8 \times 10^{-4} + 9 \times 10^{-6}\theta + 2,3 \times 10^{-11}\theta^3 && \text{for } 20^\circ\text{C} \leq \theta \leq 700^\circ\text{C} \\ \epsilon_c(\theta) &= 14 \times 10^{-3} && \text{for } 700^\circ\text{C} < \theta \leq 1200^\circ\text{C}\end{aligned}$$

Calcareous aggregates:

$$\begin{aligned}\epsilon_c(\theta) &= -1,2 \times 10^{-4} + 6 \times 10^{-6}\theta + 1,4 \times 10^{-11}\theta^3 && \text{for } 20^\circ\text{C} \leq \theta \leq 805^\circ\text{C} \\ \epsilon_c(\theta) &= 12 \times 10^{-3} && \text{for } 805^\circ\text{C} < \theta \leq 1200^\circ\text{C}\end{aligned}$$

Where θ is the concrete temperature ($^\circ\text{C}$).

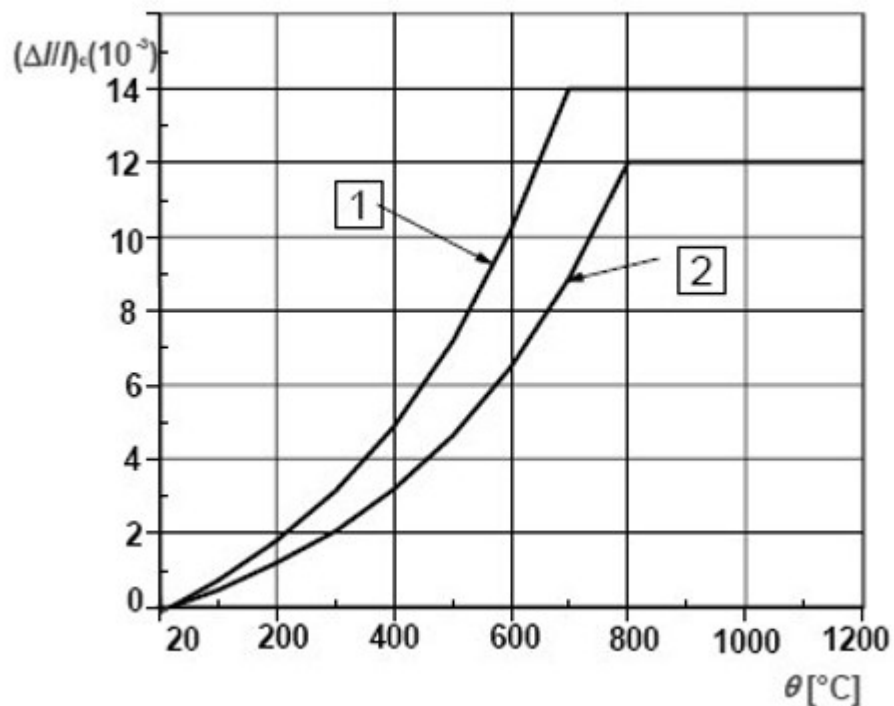


Figure 2.13: - Thermal elongation for siliceous and calcareous concrete at elevated temperatures (Euro Code, 1992-1-2)

6. Spalling

The loss of cover in fire conditions is one of the more difficult phenomena to characterize and predict in concrete structures. This event plays a critical role in a concrete structure's ability to withstand a thermal assault. In some cases, the spalling of the cover concrete is related to type of aggregate or to thermal stresses near corners; however, according to Buchanan it is more often connected to the response of the cement paste[9].

In general, most spalling occurs when water vapor within the concrete microstructure is driven off from the cement paste during heating. The changing of phase of the embedded water creates high pore pressures in the concrete matrix and produces tensile stresses in excess of the tensile strength of the concrete. Experiments from Malhotra (1984) and Phan (1996) have shown that concrete is more susceptible to spalling as a result of high moisture content, rapid rates of heating, slender members, and high concrete stresses. In addition, high strength concrete tends to be more vulnerable to spalling than normal strength concrete due to the reduced porosity, which inhibits the diffusion of the water vapor through the concrete[10, 11].



Figure 2.14: Collapsed textile factory in Alexandria, Egypt (BBC News, 2000)

Generally Concrete shows these mechanical properties at high temperatures

- Concrete loses strength and stiffness for temperature higher than 100°C.

- It does not recover during cooling.
- Properties at elevated temperature depend on the coarse aggregate (calcareous better than siliceous).

2.4.2 Material properties of structural steel

2.4.2.1 Mechanical properties of carbon steels

Strength and deformation properties

Reduction factors for the stress-strain relationship for steel at elevated temperatures given in table. These reduction factors are defined as follows:

- Effective yield strength, relative to yield strength at 20 °C: $k_{y,\theta} = f_{y,\theta} / f_y$
- Proportional limit, relative to yield strength at 20 °C: $k_{p,\theta} = f_{p,\theta} / f_y$
- Slope of linear elastic range, relative to slope at 20 °C: $k_{E,\theta} = E_{a,\theta} / E_a$

Unit mass:

The unit mass of steel ρ_a may be considered to be independent of the steel temperature. The following value may be taken:

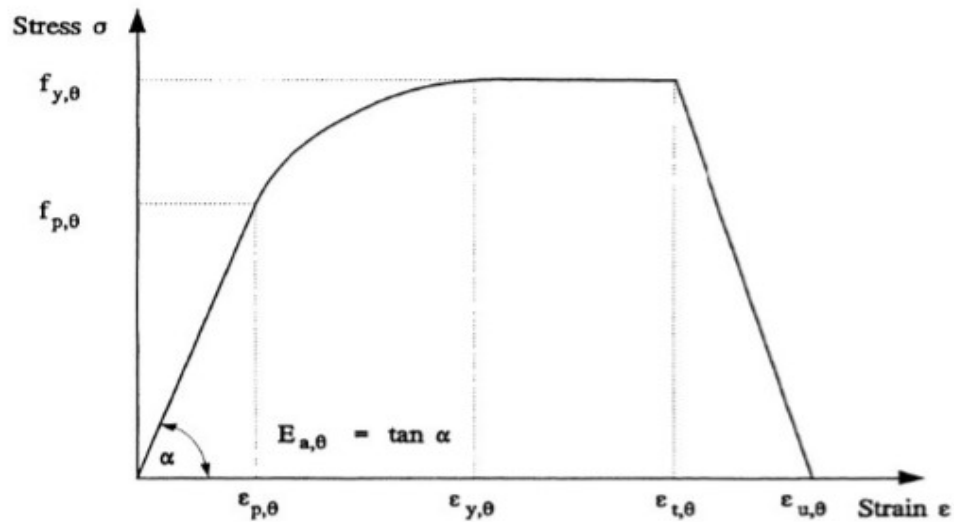
$$\rho_a = 7850 \text{ kg/m}^3$$

Table 2.3: Reduction for stress-strain relationship of carbon steel at elevated temperature (Euro code, 1993-1-2)

Steel Temperature θ_c	Reduction factors at temperature θ_c relative to the value of f_y or E_s at 20°C		
	Reduction factor (relative to f_y) for effective yield strength $k_{y,\theta} = f_{y,\theta}/f_y$	Reduction factor (relative to f_y) for proportional limit $k_{p,\theta} = f_{p,\theta}/f_y$	Reduction factor (relative to E_s) for the slope of the linear elastic range $k_{E,\theta} = E_{s,\theta}/E_s$
20°C	1,000	1,000	1,000
100°C	1,000	1,000	1,000
200°C	1,000	0,807	0,900
300°C	1,000	0,613	0,800
400°C	1,000	0,420	0,700
500°C	0,780	0,360	0,600
600°C	0,470	0,180	0,310
700°C	0,230	0,075	0,130
800°C	0,110	0,050	0,090
900°C	0,060	0,0375	0,0675
1000°C	0,040	0,0250	0,0450
1100°C	0,020	0,0125	0,0225
1200°C	0,000	0,0000	0,0000

NOTE: For intermediate values of the steel temperature, linear interpolation may be used.

Strain range	Stress σ	Tangent modulus
$\varepsilon \leq \varepsilon_{p,\theta}$	$\varepsilon E_{a,\theta}$	$E_{a,\theta}$
$\varepsilon_{p,\theta} < \varepsilon < \varepsilon_{y,\theta}$	$f_{p,\theta} - c + (b/a) [a^2 - (\varepsilon_{y,\theta} - \varepsilon)^2]^{0,5}$	$\frac{b(\varepsilon_{y,\theta} - \varepsilon)}{a [a^2 - (\varepsilon_{y,\theta} - \varepsilon)^2]^{0,5}}$
$\varepsilon_{y,\theta} \leq \varepsilon \leq \varepsilon_{t,\theta}$	$f_{y,\theta}$	0
$\varepsilon_{t,\theta} < \varepsilon < \varepsilon_{u,\theta}$	$f_{y,\theta} [1 - (\varepsilon - \varepsilon_{t,\theta}) / (\varepsilon_{u,\theta} - \varepsilon_{t,\theta})]$	-
$\varepsilon = \varepsilon_{u,\theta}$	0,00	-
Parameters	$\varepsilon_{p,\theta} = f_{p,\theta} / E_{a,\theta}$ $\varepsilon_{y,\theta} = 0,02$	$\varepsilon_{t,\theta} = 0,15$ $\varepsilon_{u,\theta} = 0,20$
Functions	$a^2 = (\varepsilon_{y,\theta} - \varepsilon_{p,\theta})(\varepsilon_{y,\theta} - \varepsilon_{p,\theta} + c/E_{a,\theta})$ $b^2 = c(\varepsilon_{y,\theta} - \varepsilon_{p,\theta})E_{a,\theta} + c^2$ $c = \frac{(f_{y,\theta} - f_{p,\theta})^2}{(\varepsilon_{y,\theta} - \varepsilon_{p,\theta})E_{a,\theta} - 2(f_{y,\theta} - f_{p,\theta})}$	



- Key:**
- $f_{y,\theta}$ is the effective yield strength;
 - $f_{p,\theta}$ is the proportional limit;
 - $E_{a,\theta}$ is the slope of the linear elastic range;
 - $\varepsilon_{p,\theta}$ is the strain at the proportional limit;
 - $\varepsilon_{y,\theta}$ is the yield strain;
 - $\varepsilon_{t,\theta}$ is the limiting strain for yield strength;
 - $\varepsilon_{u,\theta}$ is the ultimate strain.

Figure 2.15: Stress-strain relationships for steel at elevated temperatures (EC3:1995)

2.4.2.2 Thermal properties of carbon steels

1, Thermal elongation

The relative thermal elongation of steel $\Delta l/l$ should be determined from the following:

- For $20^\circ \text{C} \leq \theta_a < 750^\circ \text{C}$:

$$\Delta l/l = 1.2 \times 10^{-5} \theta_a + 0.4 \times 10^{-8} \theta_a^2 - 2.416 \times 10^{-4}$$

- For $750^\circ \text{C} \leq \theta_a \leq 860^\circ \text{C}$:

$$\Delta l/l = 1.1 \times 10^{-2}$$

- For $860^\circ \text{C} < \theta_a \leq 1200^\circ \text{C}$:

$$\Delta l/l = 2 \times 10^{-5} \theta_a - 6.2 \times 10^{-3}$$

where:

l is the length at 20°C ;

Δl is the temperature induced elongation;

θ_a is the steel temperature [$^\circ \text{C}$].

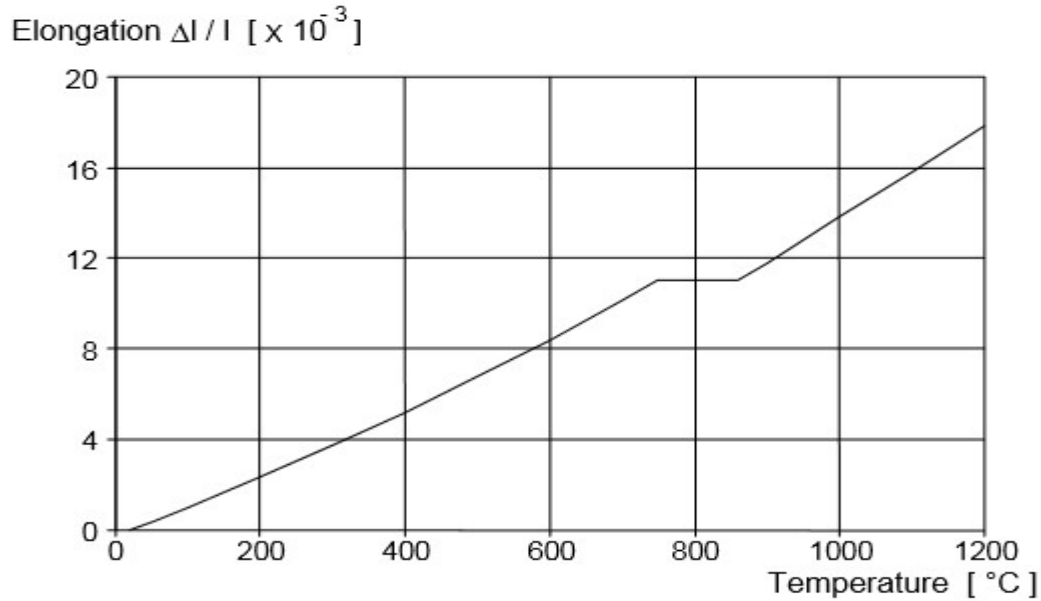


Figure 2.16: Relative thermal elongation of carbon steel as a function of the temperature. (Euro code, 1993-1-2)

2. Specific heat

The specific heat of steel C_a should be determined from the following

- For $20^\circ\text{C} \leq \theta_a < 600^\circ\text{C}$:

$$C_a = 425 + 7.73 \times 10^{-1}\theta_a - 1.69 \times 10^{-3} \theta_a^2 + 2.22 \times 10^{-6} \theta_a^3 \text{ J/kgK}$$

- For $600^\circ\text{C} \leq \theta_a < 735^\circ\text{C}$:

$$C_a = 666 + 13002/(738 - \theta_a) \text{ J/kgK}$$

- For $735^\circ\text{C} \leq \theta_a < 900^\circ\text{C}$:

$$C_a = 545 + 17820/(\theta_a - 731) \text{ J/kgK}$$

- For $900^\circ\text{C} \leq \theta_a \leq 1200^\circ\text{C}$:

$$C_a = 650 \text{ J/kgK}$$

where:

θ_a is the steel temperature [°C].

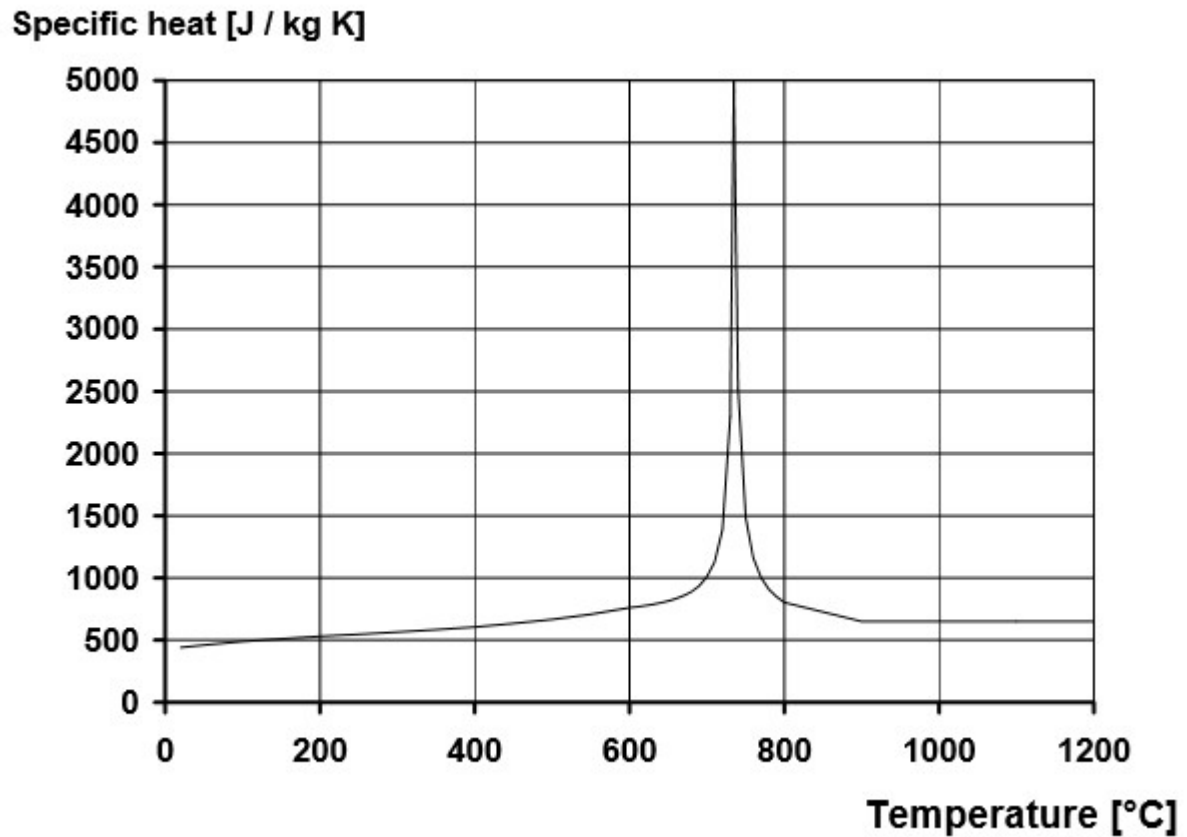


Figure 2.17: Specific heat of carbon steel as a function of the temperature.(Euro Code, 1993-1-2)

3, Thermal conductivity

The thermal conductivity of steel λ_a should be determined from the following:

- For $20^\circ\text{C} \leq \theta_a < 800^\circ\text{C}$:

$$\lambda_a = 54 - 3.33 \times 10^{-2}\theta_a \text{ W/mK}$$

- For $800^\circ\text{C} \leq \theta_a \leq 1200^\circ\text{C}$:

$$\lambda_a = 27.3 \text{ W/mK}$$

Thermal conductivity [W / mK]

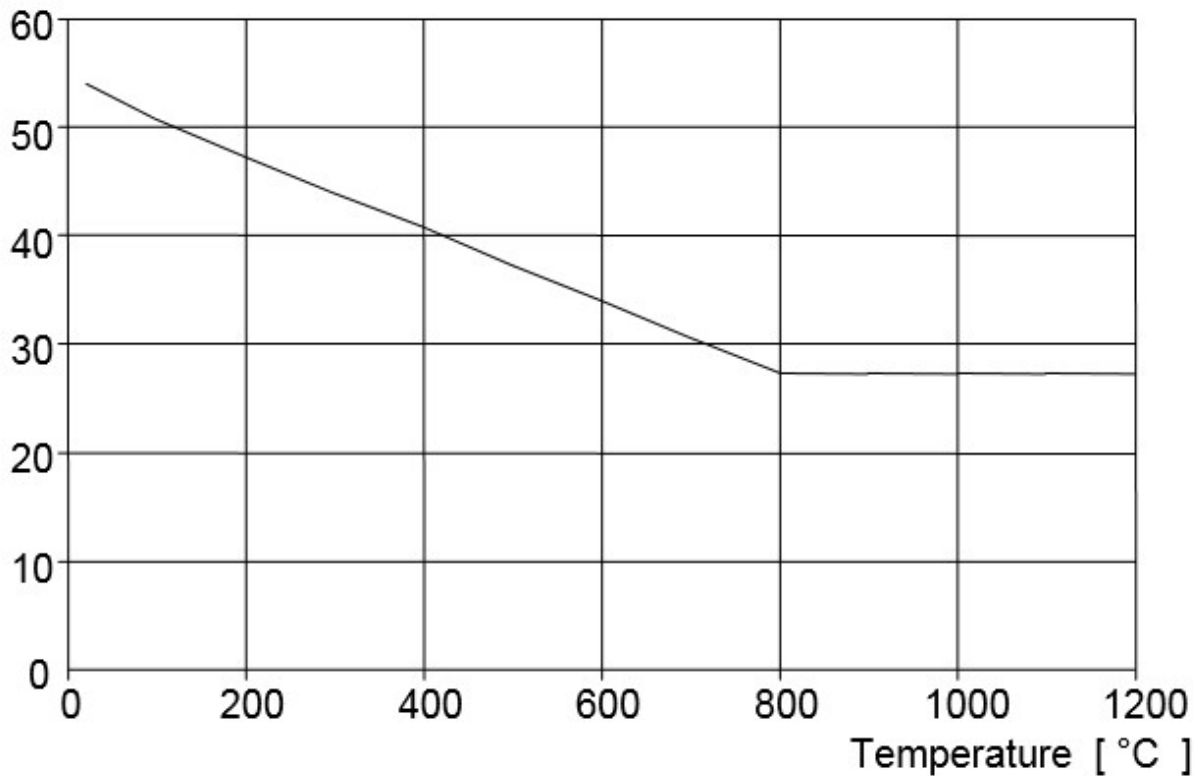


Figure 2.18: Thermal conductivity of carbon steel as a function of the temperature. (Euro Code, 1993-1-2)

4. Thermal strain

Thermal strain is the well-known phenomenon that occurs when most materials are heated. At room temperature, the coefficient of thermal expansion for steel can be taken as $14.0 \times 10^{-6} / ^\circ\text{C}$ from Euro Code, 1993-1-2. At higher temperatures, the coefficient increases, resulting in the thermal strain as seen in Figure 2.19, reproduced from the Euro codes (Euro Code, 1993-1-2).

$$\epsilon_T \theta_{a,t} = 1.2 \times 10^{-5} * \theta_{a,t} + 0.4 \times 10^{-8} * (\theta_{a,t})^2 + 2.416 \times 10^{-4} \quad \text{if } 20 \leq \theta_{a,t} \leq 750$$

$$\epsilon_T \theta_{a,t} = 1.1 \times 10^{-2} \quad \text{if } 750 \leq \theta_{a,t} \leq 860$$

$$\epsilon_T \theta_{a,t} = (2 \times 10^{-5})\theta_{a,t} - 6.2 \times 10^{-3} \quad \text{if } 860 \leq \theta_{a,t} \leq 1200$$

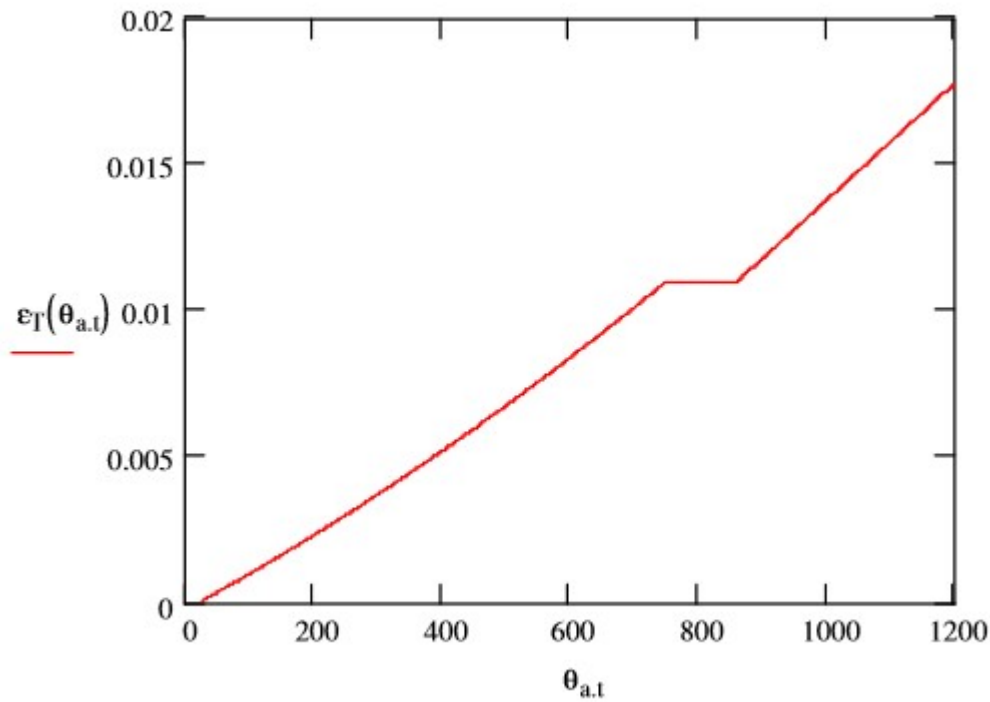


Figure 2.19: Thermal strain of steel at elevated temperatures (Euro Code, 1993-1-2)

5. Modulus of Elasticity

As described to in the above section, the modulus of elasticity decreases with increasing temperatures. The reduction in modulus shows the same trend as the reduction in yield strength; however, the modulus tends to reduce at a slightly more rapid rate (See Figure 2.20). Table 2.4 and Figure 15 from the Euro Code can be used for design purposes in determining the temperature history of the elastic modulus.

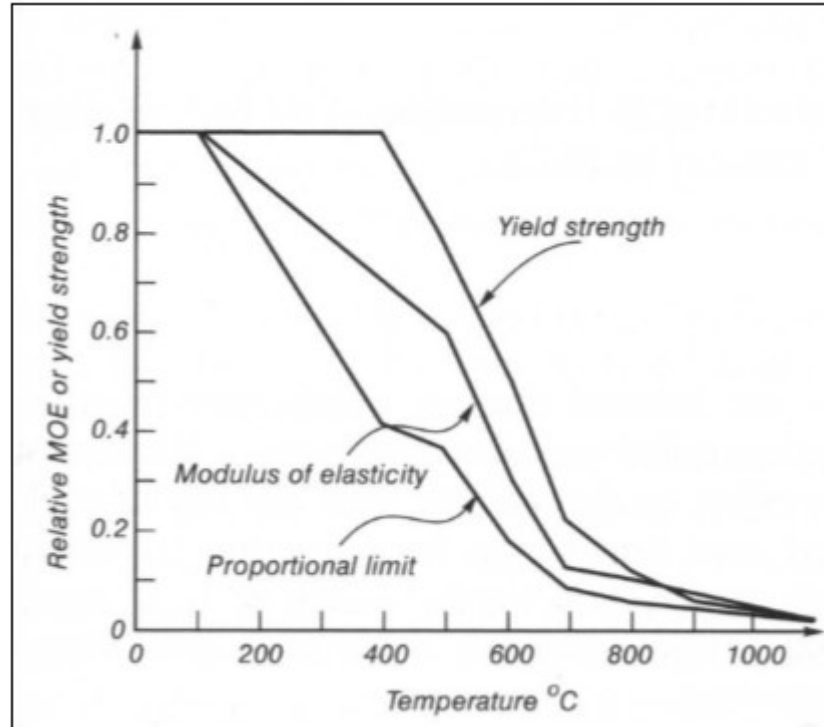


Figure 2.20:Relative mechanical properties at elevated temperatures in comparison to ambient conditions. (Buchanan)

2.4.3 Basics of fire resistance

In the structural fire analysis, as noted by Buchanan [12], the methods of assessment are essentially similar to the analysis techniques used during ambient condition design. That is, the methods to determine the deformations and internal forces induced by the applied loads are conceptually the same [12]. However, the main differences at the time of fire, as highlighted by Buchanan are as follows:

- Reduced applied loads
- Thermally induced internal forces
- Reduced strengths of materials
- Reduced cross-section areas by charring and spalling
- Deflections are less critical
- Different failure mechanisms dominate

These factors manifest themselves differently depending on the materials used in construction and the types of boundary conditions. Historically, it was believed that the thermal effects on material properties dominated the global behavior of the structure.

However, with the increase in research and understanding of thermo-mechanics, the role of boundary conditions appears to play a more significant role in structural response to fire. Much of this recent work on understanding the behavior of structures under fire conditions has been conducted by Usmani et al at the University of Edinburgh in Scotland, who participated in the “Cardington tests” [13] sponsored by British Steel PLC (now CORUS) following the 1990 Broadgate fire in London [14]. Their analysis of the Cardington tests provides new insights into the response of structures to fire, particularly with respect to elongation and thermal curvature.

The relevant design fire scenarios and the associated design fires should be determined on the basis of a fire risk assessment. For each design fire scenario, a design fire, in a fire compartment, should be estimated according to section 3 of Euro Code 1991-1-2.

2.4.3.1 Temperature Analysis

Depending on the design fire chosen by using a temperature-time curve, the temperature analysis of the structural members is made for a specified period of time.

Temperature-time curves

Temperature of gas in the environment of the member surfaces as a function of time.

They may be:

- Nominal time-temperature curve: conventional curves, adopted for classification or verification of fire resistance, e.g. the standard temperature-time curve, external fire curve, hydrocarbon fire curve;
- Parametric time-temperature curve: determined on the basis of fire models and the specific physical parameters defining the conditions in the fire compartment.

Nominal temperature-time

There are three types of temperature-time curves

1. Standard time-temperature curve: ISO standard temperature time curve;

$$\theta_g = 20 + 345 \log_{10}(8 \times t + 1) \text{ } ^\circ\text{C}$$

$$\alpha_c = 25 \text{ W/m}^2\text{K}$$

2. External fire temperature-time curve

$$\theta_g = 20 + 660(1 - 0.687 \times e^{-0.32t} - 0.31 \times e^{-3.8t}) \text{ } ^\circ\text{C}$$

$$\alpha_c = 25 \text{ W/m}^2\text{K}$$

3. Hydrocarbon temperature-time curve

$$\theta_g = 20 + 1080(1 - 0.325 \times e^{-0.167t} - 0.675 \times e^{-2.5t}) \text{ } ^\circ\text{C}$$

$$\alpha_c = 50 \text{ W/m}^2\text{K}$$

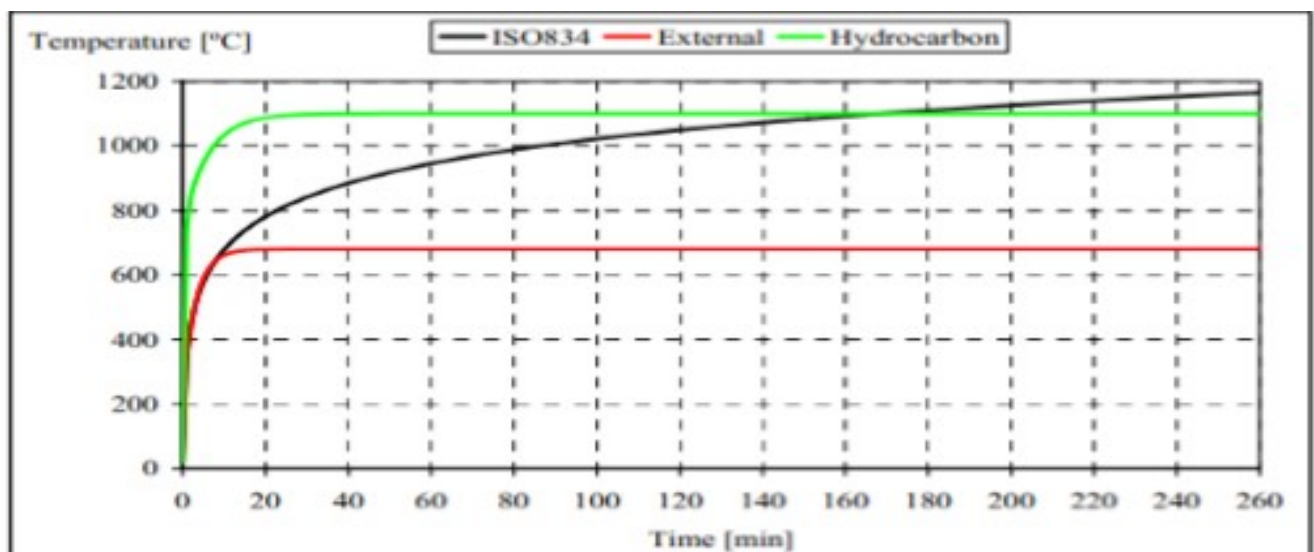


Figure 2.21: Temperature-time curves

Natural fire models

1, Simplified fire models:

Simple fire models are based on specific physical parameters with a limited field of application. Gas temperatures should be determined on the basis of physical parameters considering at least the fire load density and the ventilation conditions. For external members, the radiative heat flux component should be calculated as the sum of the contributions of the fire compartment and of the flames emerging from the openings.

2. Advanced fire models

Advanced fire models should take into account the following:

- gas properties,
- mass exchange,
- Energy exchange.

One of the following models should be used:

- One-zone models assuming a uniform, time dependent temperature distribution in the compartment.
- Two-zone models assuming an upper layer with time dependent thickness and with time dependent uniform temperature, as well as a lower layer with a time dependent uniform and lower temperature.
- Computational Fluid Dynamic models giving the temperature evolution in the compartment in a completely time dependent and space dependent manner.

The coefficient of heat transfer by convection should be taken as $\alpha_c = 35$ [W/m²K], unless more detailed information is available.

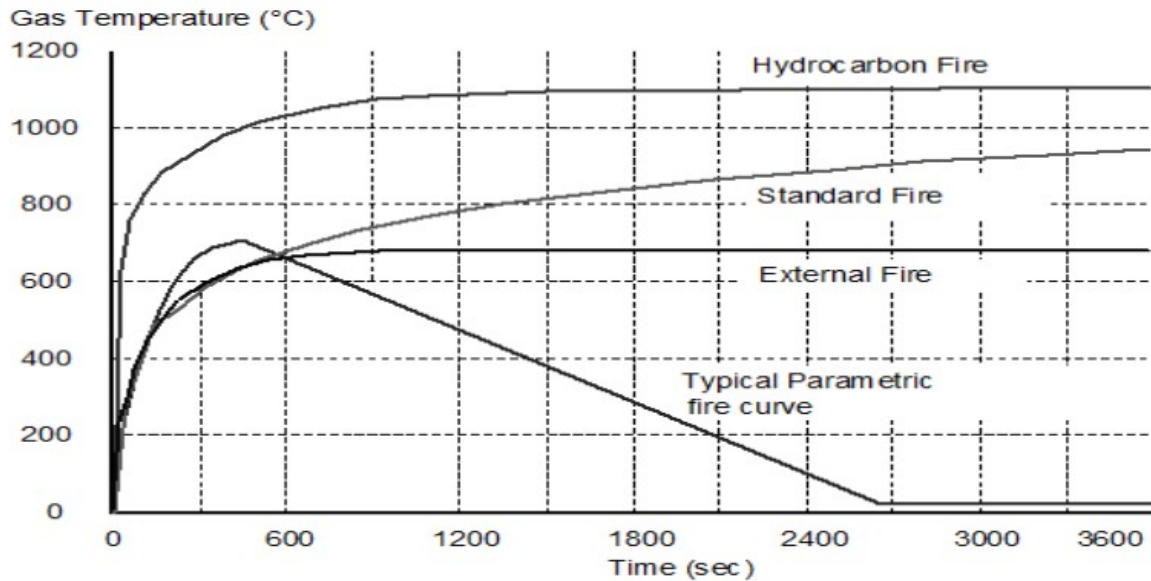


Figure 2.22: Nominal fire curves compared with a parametric fire (Euro-Code 1 part 1-2)

2.4.3.2 Mechanical Analysis

Imposed and constrained expansions and deformations caused by temperature changes due to fire exposure result in effects of actions, e.g. forces and moments, which shall be considered with the exception of those cases where they :

- may be recognized a priori to be either negligible or favorable;
- Are accounted for by conservatively chosen support models and boundary conditions, and/or implicitly considered by conservatively specified fire safety requirements.

The mechanical analysis shall be performed for the same duration as used in the temperature analysis.

Fire resistance can be expressed in three alternative ways:

- The fire resistance time should exceed the requirement for the building usage and type when loaded to the design load level and subjected to the fire temperature curve:

$$t_{fi,d} \geq t_{fi,requ}$$

- The load-bearing resistance of the element should exceed the design loading at any time during the fire and until when it has been heated for the required time in the fire:

$$R_{f_i,d,t} \geq E_{f_i,d,t}$$

- The critical temperature of an element loaded to the design level should exceed the design temperature at any time during the fire and until the required time (this approach is only possible when the behavior of the member is governed by one single representative temperature as is the case, for example, for steel members at uniform temperature):

$$\theta_{cr,d} \geq \theta_d$$

Where:

$t_{fi,d}$design fire resistance time

$t_{fi,requ}$...required fire resistance time

$R_{fi,d,t}$design value of the resistance of the member in the fire situation at time t

$E_{fi,d,t}$ design value of the relevant effects of actions in the fire situation at time t

θ_d the design value of material temperature

$\theta_{cr,d}$ the design value of the critical material temperature

2.5 Relation between flexure and fire resistance

Fire is one of the most severe conditions which may be encountered by a reinforced concrete (RC) building during its service life. Therefore, the fire resistance of RC members is an important issue that needs to be considered in the design of RC buildings. In current design codes, such as BS 8110-2, FIP/CEB, ACI 216.1 and AS 3600, the fire resistance period of an RC member is usually determined using a prescriptive approach, such as the tabulated method which specifies some deemed-to-satisfy requirements of the minimum member dimensions and the minimum concrete cover for the reinforcing steel. These requirements are usually derived from empirical approaches and rely heavily on the limited results from fire resistance tests of RC members in which an RC member is commonly pre-loaded and exposed to a prescribed temperature–time curve as defined by BS 476-20, ISO 834-1 or ASTM E119[15].

Bending forces occur mostly as a result of vertical loads applied to floor slabs and beams. Bending causes the bottoms of simple beams to become stretched in tension and the tops of beams to be pushed together in compression. Continuous beams and cantilever beams have tension forces at the top and a compression at the bottom near their supports. At midspan, the forces are in the same locations as for simple beams and slabs. Vertical cracks develop near the midspan of concrete, since the tension force causes the concrete to crack (see Figure 2.23). The reinforcing steel provided in the tension zones is assumed to resist the entire tension force. This tension cracking can be observed in damaged structures and may be used to monitor and determine the potential for collapse. Stable, hairline cracks are normal, but widening cracks indicate impending failure. As stated previously, beams in reinforced concrete moment-resistant frames may experience tension and compression stresses alternately due to stress reversals during earthquakes[16].

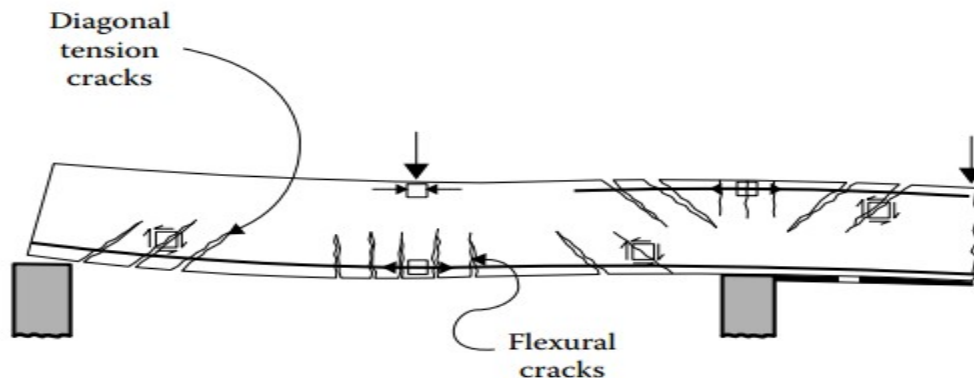


Figure 2.23:Development of cracks in a flexural member. Vertical cracks may develop near midspan

2.6 Modular Ratio

In the elastic theory, structures having different materials are made equivalent to one common material. To convert cross section area of concrete to steel beam we use modular ratio. This is done by converting using the modular ratio n which is the ratio of modulus of elasticity of steel and concrete. Thus, $n = E_a/E_c$. where E_a is the modulus of elasticity of steel which is 210,000 N/mm². However, concrete has different moduli, as it is not a perfectly elastic material. The short-term modulus of concrete $E_c = 5000\sqrt{f_{ck}}$ in N/mm², where f_{ck} is the characteristic strength of concrete [17].

CHAPTER THREE

RESEARCH METHODS AND MATERIALS

3.1 Research Design

So as to accomplish the above objectives of the study was done by utilizing different computer skills and to accompany great theoretical background and analysis done by different researchers related to resistance of different type of beam to fire and flexure.

3.2 Study Variables

Dependent variables

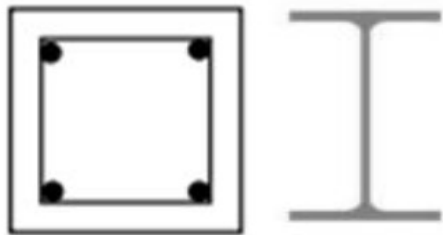
- Response of steel and RC beam

Independent variables

- Area of cross section.
- Amount of heat applied.
- Amount of load applied.
- Grade of Concrete
- Rebar Grade

3.3 Study population

This Study considered simply support beam, symmetrical I section steel beam and rectangular reinforced concrete beam of different cross section and span length under uniform load for the analysis of flexure and fire resistance.



(a) RC beam cross section

(b) I section steel beam cross section

Figure 3.1: Type of beams

3.4 Sample size

On this study two rectangular cross section of reinforced concrete beams were taken and for steel beam converting cross sectional area of reinforced concrete beam to cross section of steel by using modular ratio and to select universal steel beam of those equivalent area of the gross cross section of reinforced concrete beam. To select reinforced concrete beam ratio of height to width is 1.2 and it is listed down;

Sample 1: $B \times H = 200\text{mm} \times 240\text{mm}$

Sample 2: $B \times H = 250\text{mm} \times 300\text{mm}$

This research considered beam with two different lengths (3m and 4.5 m) for each cross section. Concrete with two different cross sections (200mm*240mm and 250mm*300mm), steel with sixteen different cross section totally 32 types of beams were analyzed for flexural and fire resistance using ABAQUS 6.14-2 software.

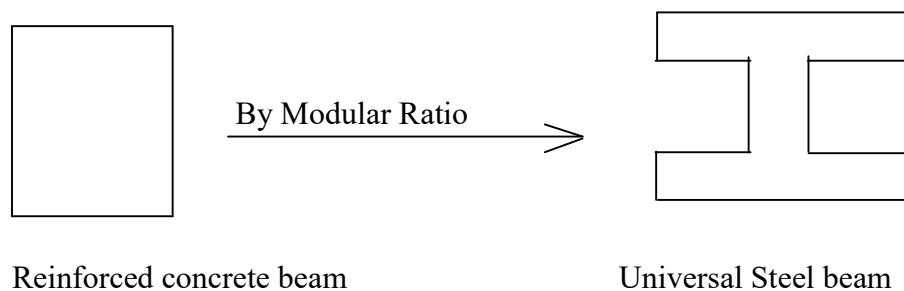


Figure 3.2:Equivalent area conversion diagram

3.5 Span Length and Support Condition

Analysis will be carried out on simply supported beam using two different span length those are; 3 m and 4.5 m center to center from support.

3.6 Materials

This research use this data for the analysis:

Concrete: Grade C-20 , $f_{ck} = 16 \text{ N/mm}^2$, $E_c = 30\text{GPa} = 30,000 \text{ N/mm}^2$

Grade C-25 , $f_{ck} = 20 \text{ N/mm}^2$, $E_c = 31\text{GPa} = 31,000 \text{ N/mm}^2$

Grade C-30 , $f_{ck} = 24 \text{ N/mm}^2$, $E_c = 32\text{GPa} = 32,000 \text{ N/mm}^2$

Grade C-35 , $f_{ck} = 28 \text{ N/mm}^2$, $E_c = 34\text{GPa} = 34,000 \text{ N/mm}^2$

$f_{ck} = 0.8 f_{cu}$

Rebar: S-300, $f_y = 300 \text{ N/mm}^2$, $E_s = 200\text{GPa} = 200,000 \text{ N/mm}^2$, diameter of 20mm and 12mm for longitudinal reinforcement and diameter of 8mm for stirrup

Structural steel: Grade Fe 430 I section, $f_y = 275 \text{ N/mm}^2$, $f_u = 430 \text{ N/mm}^2$, $E_a = 210\text{GPa} = 210,000 \text{ N/mm}^2$

Concrete cover for concrete reinforcement of beams = 30mm

Partial safety factor at normal temperature condition:

For structural steel $\gamma_a = 1.0$

For concrete $\gamma_c = 1.5$

For reinforcement steel $\gamma_s = 1.15$

Partial safety factor at elevated temperature condition:

For concrete $\gamma_c = 1$

For reinforcement steel $\gamma_s = 1$

For structural steel $\gamma_a = 1$

Fire design fire rating of assume fire rate R120 for all the beams.

3.7 Solver Used

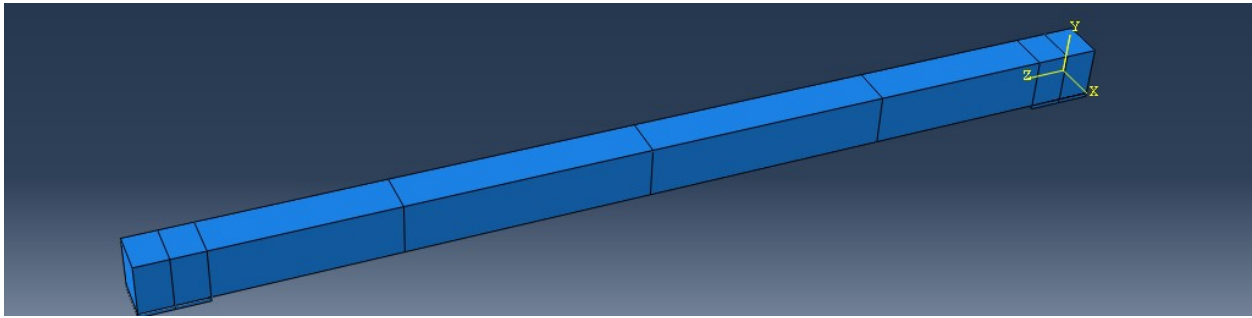
Abaqus is a suite of powerful engineering simulation programs, based on the finite element method that can solve problems ranging from relatively simple linear analyses to the most challenging nonlinear simulations. Abaqus contains an extensive library of elements that can model virtually any geometry. It has an equally extensive list of material models that can simulate the behavior of most typical engineering materials including metals, rubber, polymers, composites, reinforced concrete, crushable and resilient foams, and geotechnical materials such as soils and rock. Designed as a general-purpose simulation tool, Abaqus can be used to study more than just structural (stress/displacement) problems.

Abaqus can simulate problems in such diverse areas as heat transfer, mass diffusion, thermal management of electrical components (coupled thermal-electrical analyses), acoustics, soil mechanics (coupled pore fluid-stress analyses), and piezoelectric analysis. Abaqus offers a wide range of capabilities for simulation of linear and nonlinear applications. Problems with multiple components are modeled by associating the geometry defining each component with the appropriate material models and specifying component interactions. In a nonlinear analysis Abaqus automatically chooses appropriate load increments and convergence tolerances and continually adjusts them during the analysis to ensure that an accurate solution is obtained efficiently [18].

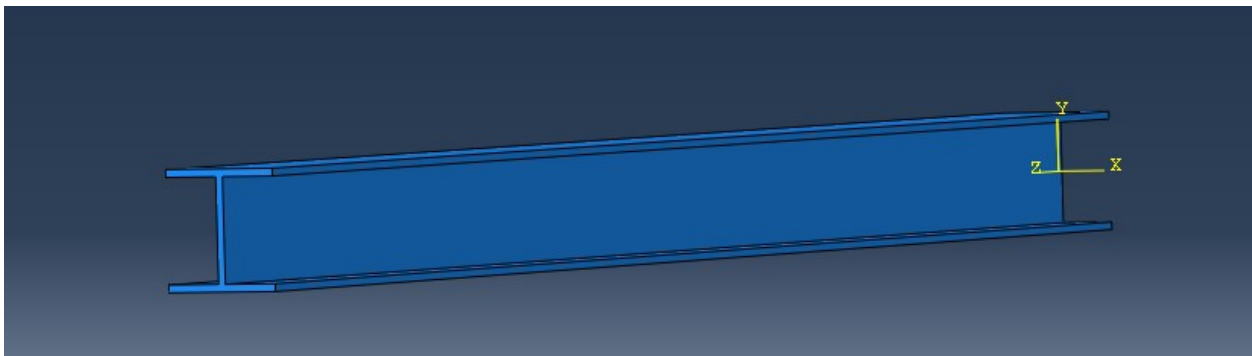
The results obtained from the implicit analysis matched the explicit analysis up until the point that the implicit model was stopped; therefore, the use of the explicit solver is proposed to be reasonable.

3.8 Model Background

The structural system modeled in this study consisted of 3 and 4.5 meter length simply supported beam with different cross section of reinforced concrete and I section steel beam (See Figure 3.3).



(a) Reinforced Concrete Beam Modeling Using Abaqus 6.14-2



(b) Section Steel Beam Modeling Using Abaqus 6.14-2

Figure 3.3: Sample of detail modeling

3.9 Analysis Fire Models

For a preliminary study, the heating phase of the fire was only considered. Given this constraint, several heating conditions were created for this analysis based on two general fire curves: the standard fire (ISO 834) [19] and a generalized exponential curve. The ISO 834 curve is represented as follows:

$$T(t) = 345 \log \left(8 \frac{t}{60} + 1 \right) + T_0$$

The generalized exponential curve suggested by Usmani is given by:

$$T(t) = T_0 + (T_{max} - T_0)(1 - e^{-\alpha t})$$

where, T_{max} is the maximum compartment temperature, T_0 is the initial or ambient temperature, α is an arbitrary ‘rate of heating’ parameter and t represents the time over which the model is analyzed. This curve provides a temperature-time relationship representing a post-flashover compartment fire, for input to the heat transfer analysis. In this form, the artificially generated “rate of heating” term coupled with the T_{max} term is used to provide a sensitivity analysis that can capture an envelope of different fires or different levels of insulation, as indicated by Usmani et al [20]. Figure 3.4 illustrates how the rate of heating term (α) can be varied to achieve a wide range of fire scenarios. Similarly, the T_{max} term can be varied to achieve hotter fires.

While heat-flux vs. time curves are a more appropriate measure for determining the energy input into the structure, the use of equation above is a justified approach for doing a parametric study for a significant range of heat fluxes and rates of change of heat flux. These temperature time curves should not be taken as representations of realistic fires, but just a mechanism to assign in a systematic manner different heating conditions. In this way, numerous fire scenarios can be analyzed without formally resolving the gas phase temperature and solid phase temperature disconnect [21].

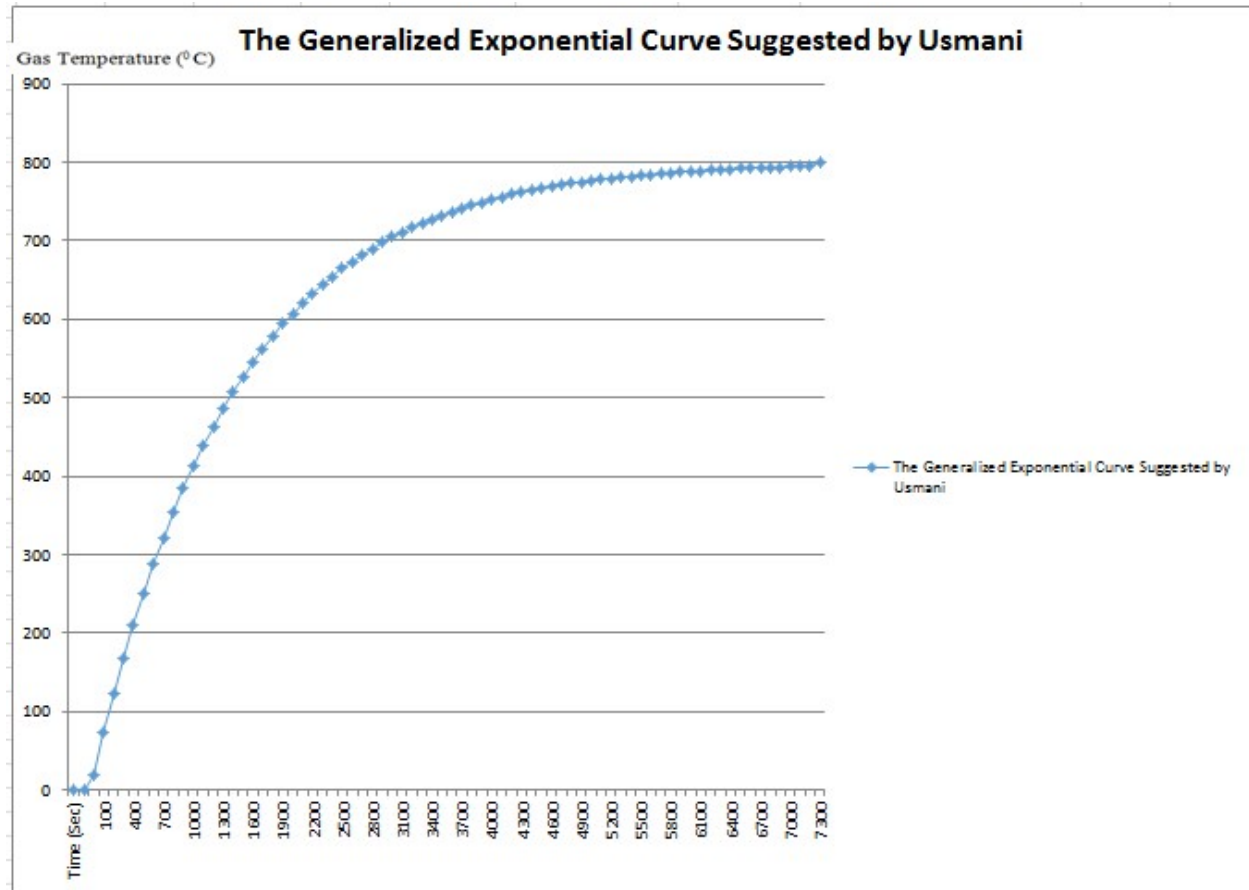


Figure 3.4: The Generalized Exponential Curve Suggested by Usmani

Figure 3.4 illustrates the gas compartment temperatures examined in this study. These compartment time-temperature curves provide a wide range of heating rates and maximum temperature fires. T_{max} (800°C) and a range of heating rate (0.0007) were used in this study.

3.10 Major Assumptions

In this study, a 2-hour fire exposure was assumed in a simply supported beam. Therefore, beam was assigned time-temperature curves based on the Euro code 3 (1995) heat transfer models for unprotected steelwork [22].

Initially, the standard fire and generalized time-temperature curves described earlier were going to be applied to the beam models directly.

The exposed reinforced concrete and I – section steel beam elements were assumed uniformly heated along the length and depth. This approach has generally been accepted in practice to simplify the analysis and is representative of a mean temperature rise in the structure. The thermal gradient that occurs in a real building fire is typically captured by modeling the slab with the actual thermal gradient.

3.11 Material Properties

In this study, the properties of both steel and concrete varied with temperature and were described in detail in Appendix B. The values input into ABAQUS were the design values stipulated in EuroCode 2: 1993 [21] and EuroCode 3:1995 [23] for concrete and steel structures, respectively.

3.12 Boundary Conditions

All the beams in the model were simply supported and it is modeled on left hand side by considering U2 and U3 and on right hand side for U2.

3.13 Ambient Loading

The dead and live loads were factored in accordance with the structural EuroCode (EuroCode 1:1994, EuroCode 2:1995, EuroCode 3:1995). For ambient conditions, the beams were designed using the follow load combination:

$$1.2 \text{ Dead Load} + 1.6 \text{ Live Load}$$

For fire conditions, the loads were factored in accordance with BS 5950 Part 8(2004) [21] for office buildings as follows:

$$1.0 \text{ Dead Load} + 1.0 \text{ Permanent Imposed Load} + 0.5 \text{ Non-Permanent Imposed Load}$$

Typical loads were applied to the structure, and are as follows:

$$\text{Dead Load (DL)} = 8.352 \text{ kN/m}$$

$$\text{Live Load (LL)} = 6 \text{ kN/m}$$

The uniformly distributed load applied on full span length in the fire limit state is:

$$(8.352 \times 1) + (6 \times 1) = 14.352 \text{ kN/m}$$

3.14 Thermal Loading

The methods for determining the solid phase time-temperature curves for the steel and reinforced concrete beam in the models were explained in detail in Section 3.6. This section illustrates the time-temperature curves that were input in the ABAQUS structural analysis models for each scenario. As mentioned in the thermal assumptions section, this study consisted of a 2hour fire exposure.

The standard fire curve (ISO 834) was used to calculate the solid phase temperatures of the unprotected steel members using Equation 4.22 of EuroCode 3 Part 1-2, respectively. These solid phase time temperature curves were applied uniformly across the length and depth of the members. Fire is applied on three sides by excluding top surface by considering slab.

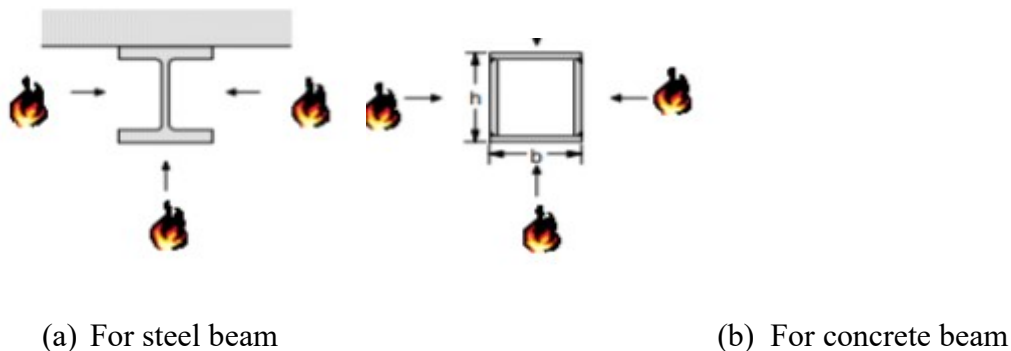


Figure 3.5: The side of steel and reinforced concrete by affected by fire

CHAPTER FOUR

RESULTS AND DISCUSSIONS

4.1 Conversion of Reinforced Concrete Beam to I section Steel Beam By Modular Ratio

Reinforced concrete beam is converted to I section steel beam by considering the gross cross section area of reinforced concrete beam for each concrete compressive strength and it is tabulated and shown on table 4.1.

Concrete: Grade C-20 , $f_{ck} = 16 \text{ N/mm}^2$, $E_c = 30\text{GPa} = 30,000 \text{ N/mm}^2$

Grade C-25 , $f_{ck} = 20 \text{ N/mm}^2$, $E_c = 31\text{GPa} = 31,000 \text{ N/mm}^2$

Grade C-30 , $f_{ck} = 24 \text{ N/mm}^2$, $E_c = 32\text{GPa} = 32,000 \text{ N/mm}^2$

Grade C-35 , $f_{ck} = 28 \text{ N/mm}^2$, $E_c = 34\text{GPa} = 34,000 \text{ N/mm}^2$

Concrete Sample 1: $B \cdot H = 200\text{mm} \cdot 240\text{mm} = 48000 \text{ mm}^2$

Sample 2: $B \cdot H = 250\text{mm} \cdot 300\text{mm} = 75000 \text{ mm}^2$

Modular Ratio, $n = E_s / E_c$

$A_s = A_c / n$

Where:

A_s - Cross sectional area of I - section steel beam

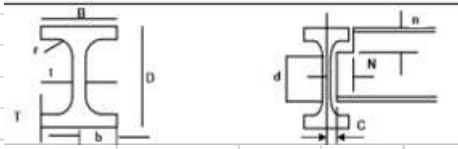
A_c – Cross sectional area of reinforced concrete beam

n - Modular ratio of concrete and steel

Table 4.1: Conversion reinforced beam to I section Steel beam by using modular ratio

Ea (N/mm ²)	Ec(N/mm ²)		Modular Ratio (n)	As (mm ²)	
				For Sample 1	For Sample 2
210,000.00	Grade C-20	30,000.00	7.0	6,857.14	10,714.29
	Grade C-25	31,000.00	6.8	7,085.71	11,071.43
	Grade C-30	32,000.00	6.6	7,314.29	11,428.57
	Grade C-35	34,000.00	6.2	7,771.43	12,142.86

Table 4.2:The converted I - section steel beam

		SAMPLE 1										
		Section Type	W/L (Kg/m)	D(mm)	B(mm)	Flang Thickness, T(mm)	Web Thickness, t(mm)	Root radius, r (mm)	Depth b/n the fillet,d(mm)	Area of section, A(cm ²)	Plastic Modulus (cm ³)	
											X-X	Y-Y
												
Grade C-20	W12-12X6 1/2 (356X406)	54	210.4	166.9	13.7	7.9	8.9	265.2	68.8	846	196	
Grade C-25	W14-14X6 3/4 (356X171)	57	358	172.2	13	8.1	10.2	311.6	72.6	1211	243	
Grade C-30	W10-10X8 (254X203)	58	252	202.8	13.4	8	12.7	199.8	73.8	765	280	
Grade C-35	W10-10X8 (254X203)	62.5	249.4	207	12.2	12.2	12.7	199.6	79.3	768	271	

		SAMPLE 2										
		Section Type	W/L (Kg/m)	D(mm)	B(mm)	Flang Thickness, T(mm)	Web Thickness, t(mm)	Root radius, r (mm)	Depth b/n the fillet,d(mm)	Area of section, A(cm ²)	Plastic Modulus (cm ³)	
											X-X	Y-Y
Grade C-20	W16-16X7 (406X178)	84.8	417.3	180.8	18.2	10.9	10.2	360.6	108	1724	309	
Grade C-25	W10-10X10 (254X254)	88.9	260.3	256.3	17.3	10.3	12.7	200.3	113	1224	575	
Grade C-30	W14-14X10 (356X254)	90.8	352.8	253.9	16.3	9.5	15.2	289.8	115	1668	534	
Grade C-35	W8-8X8 (203X203)	99.7	228.6	210.3	23.8	14.5	10.2	160.7	127	1150	536	

4.2 Checking of Steel Beam Cross Section

Steel beam cross section is checked for web subjected for bending, flange subjected to compression, and Section Modulus as per Euro Code.

Table 4.3: Check for Cross Section as per Euro Code

		SAMPLE 1														
		Section Type	W/L (Kg/m)	D(mm)	B(mm)	Flang Thickness, T(mm)	Web Thickness, t(mm)	Depth b/n the fillet,d(mm)	C (mm)	Check class of section for Web subject to bending			Check class of section for Flange subject to compression			
										d/tw	72ε	Section Class	C/tr	10ε	Section Class	
Grade C-20	W12-12X6 1/2 (356X406)	54	210.4	166.9	13.7	7.9	265.2	83.45	33.57	66.24	d/tw ≤ 72ε	Class 1 (Plastic)	6.0912	9.2	C/tr ≤ 10ε	Class 1 (Plastic)
Grade C-25	W14-14X6 3/4 (356X171)	57	358	172.2	13	8.1	311.6	86.1	38.47	66.24			6.6231	9.2		
Grade C-30	W10-10X8 (254X203)	58	252	202.8	13.4	8	199.8	101.4	24.98	66.24			7.5672	9.2		
Grade C-35	W10-10X8 (254X203)	62.5	249.4	207	12.2	12.2	199.6	199.6	16.36	66.24			16.361	9.2		

		SAMPLE 2														
		Section Type	W/L (Kg/m)	D(mm)	B(mm)	Flang Thickness, T(mm)	Web Thickness, t(mm)	Depth b/n the fillet,d(mm)	C (mm)	Check class of section for Web subject to bending			Check class of section for Flange subject to compression			
										d/tw	72ε	Section Class	C/tr	10ε	Section Class	
Grade C-20	W16-16X7 (406X178)	84.8	417.3	180.8	18.2	10.9	360.6	90.4	33.08	66.24	d/tw ≤ 72ε	Class 1 (Plastic)	4.967	9.2	C/tr ≤ 10ε	Class 1 (Plastic)
Grade C-25	W10-10X10 (254X254)	88.9	260.3	256.3	17.3	10.3	200.3	128.15	19.45	66.24			7.4075	9.2		
Grade C-30	W14-14X10 (356X254)	90.8	352.8	253.9	16.3	9.5	289.8	126.95	30.51	66.24			7.7883	9.2		
Grade C-35	W8-8X8 (203X203)	99.7	228.6	210.3	23.8	14.5	160.7	105.15	11.08	66.24			4.4181	9.2		

Table 4.4: Check for Cross Section Modulus as per Euro Code

SAMPLE 1							
Section Type	Plastic Modulus (mm ³)		Check Section Modulus				
	X-X	Y-Y	F _y (N/mm ²)	M _{pl} (N.mm)	M _{rd} (N.mm)		Status (M _{pl} > M _{rd})
					3 m Span length	4.5 m Span length	
W12-12X6 1/2 (356X406)	846,000.00	196,000.00	275	232,650,000.00	23,006,250.00	51,764,062.50	okay
W14-14X6 3/4 (356X171)	1,211,000.00	243,000.00		333,025,000.00	23,006,250.00	51,764,062.50	okay
W10-10X8 (254X203)	765,000.00	280,000.00		210,375,000.00	23,006,250.00	51,764,062.50	okay
W10-10X8 (254X203)	768,000.00	271,000.00		211,200,000.00	23,006,250.00	51,764,062.50	okay

SAMPLE 2							
Section Type	Plastic Modulus (mm ³)		Check Section Modulus				
	X-X	Y-Y	F _y (N/mm ²)	M _{pl} (N.mm)	M _{rd} (N.mm)		Status (M _{pl} > M _{rd})
					3 m Span length	4.5 m Span length	
W16-16X7 (406X178)	1,724,000.00	309,000.00	275	474,100,000.00	23,006,250.00	51,764,062.50	okay
W10-10X10 (254X254)	1,224,000.00	575,000.00		336,600,000.00	23,006,250.00	51,764,062.50	okay
W14-14X10 (356X254)	1,668,000.00	534,000.00		458,700,000.00	23,006,250.00	51,764,062.50	okay
W8-8X8 (203X203)	1,150,000.00	536,000.00		316,250,000.00	23,006,250.00	51,764,062.50	okay

4.3 Deflection of reinforced concrete beam due to fire and flexure

By using 200mmX240mm and 250mmx300mm cross sections the mid span deflection is analyzed for 3m and 4.5m simply supported beam span length for the combined effect of fire and flexure and it shown on Table 4.5.

Table 4.5: Deflection of Reinforced Concrete Beam due to fire and flexure

RC Beam Type	Cross Section	Span Length (mm)	Cubic Strength (N/mm ²)	Fire Resistance (Second)	Loading (N/mm ²)	Maximum Deflection (mm)	Location
RC-B1-C20	200mmX240mm	3000	20	7200	0.0718	145.3	Mid Span
RC-B1-C25			25			114.3	
RC-B1-C30			30			73.2	
RC-B1-C35			35			42.52	
RC-B2-C20		4500	20			452.9	
RC-B2-C25			25			435	
RC-B2-C30			30			409.8	
RC-B2-C35			35			239	
RC-B3-C20	250mmX300mm	3000	20	3.01			
RC-B3-C25			25	2.84			
RC-B3-C30			30	2.768			
RC-B3-C35			35	2.65			
RC-B4-C20		4500	20	64.3			
RC-B4-C25			25	60.1			
RC-B4-C30			30	44.18			
RC-B4-C35			35	37.2			

Figure 4.1 shows mid span deflection of RC-B1-C20 beam and it is 145.3 mm, when it compare to I section steel beam IS-B1-C20 by equivalent area converted on the basis of modular ratio it is increased by 129.7 mm.

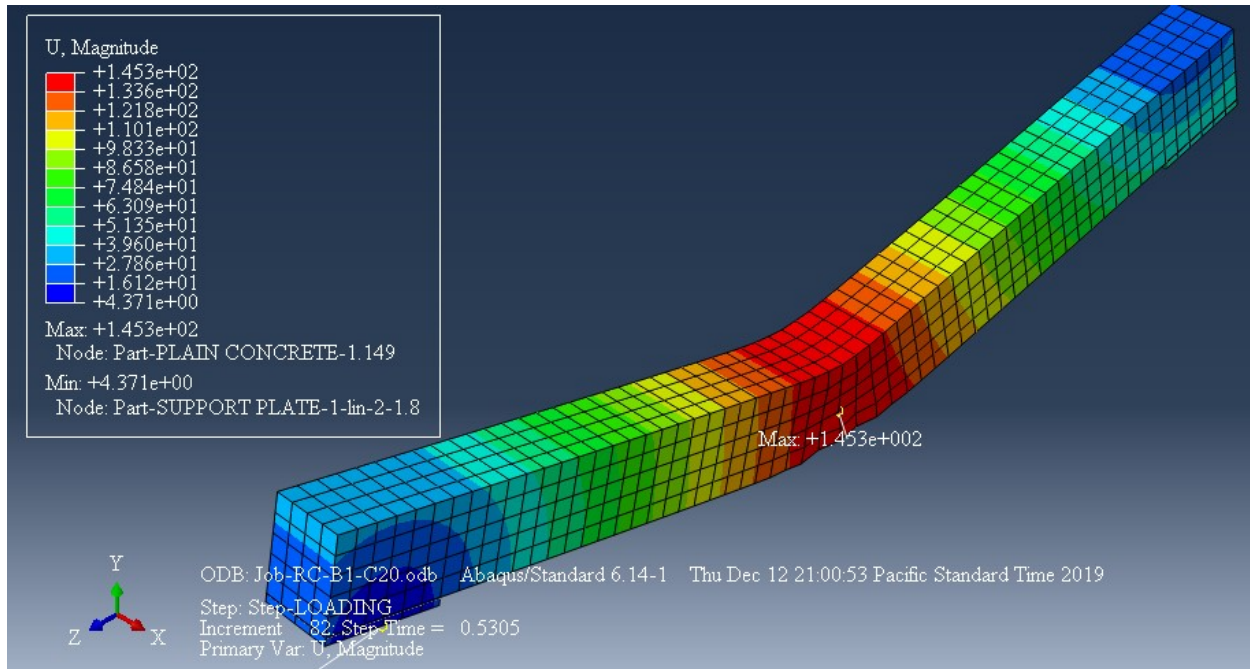


Figure 4.1: Mid span deflection of RC-B1-C20 beam(145.3 mm)

Figure 4.2 shows mid span deflection of RC-B1-C25 beam and it is 114.3 mm, when it compare to I section steel beam IS-B1-C25 by equivalent area converted on the basis of modular ratio it is increased by 108.44 mm.

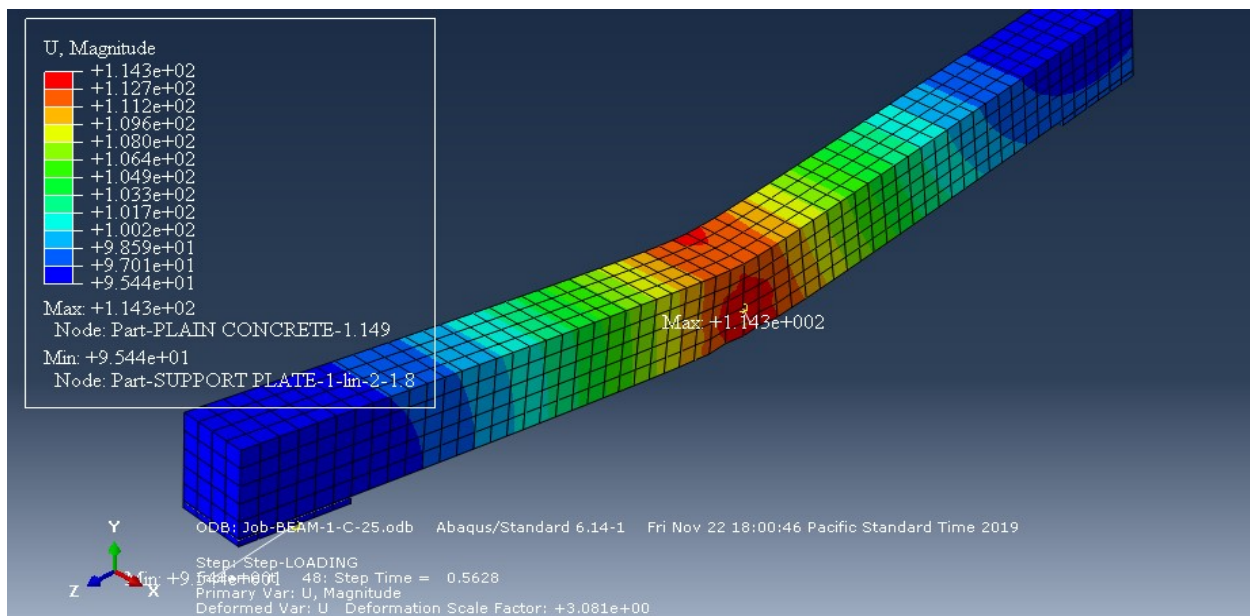


Figure 4.2: Mid span deflection of RC-B1-C25 beam(114.3 mm)

Figure 4.3 shows mid span deflection of RC-B1-C30 beam and it is 73.24 mm, when it compare to I section steel beam IS-B1-C30 by equivalent area converted on the basis of modular ratio it is increased by 60.8mm.

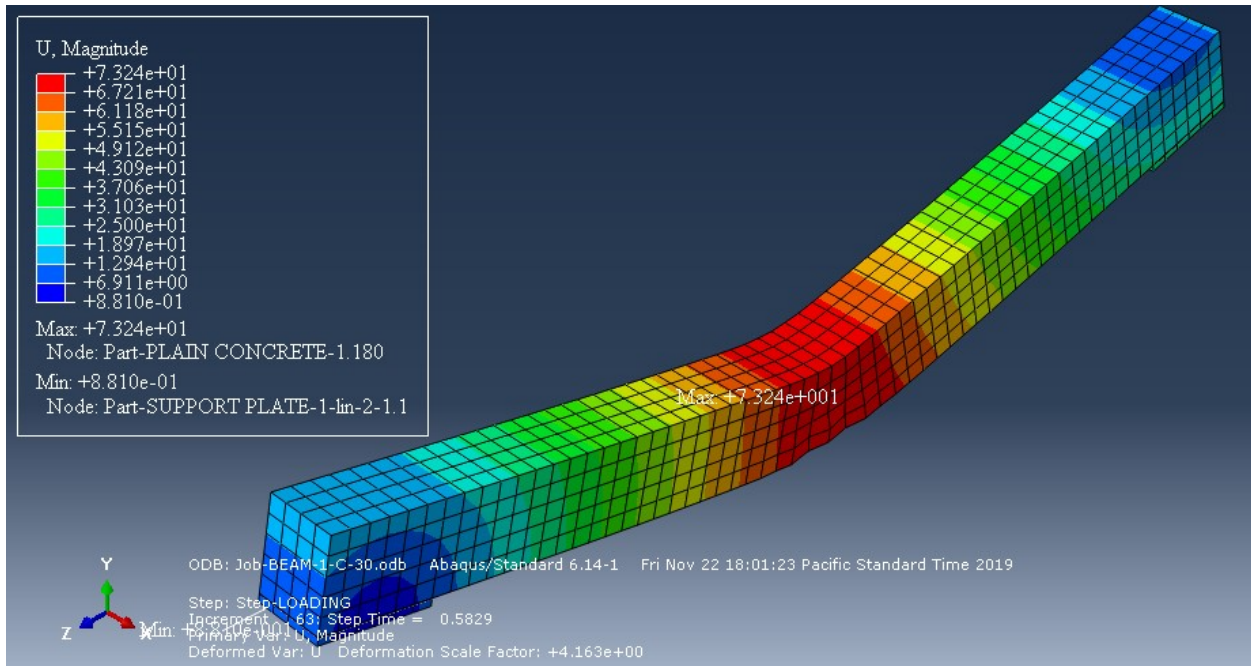


Figure 4.3: Mid span deflection of RC-B1-C30 beam(73.24 mm)

Figure 4.4 shows 42.52 mm mid span deflection of RC-B1-C35 beam, and in the case of reinforced concrete beam it is observed that with increasing of concrete strength bending resistance of the beam also increase and its mid span deflection decrease under fire.

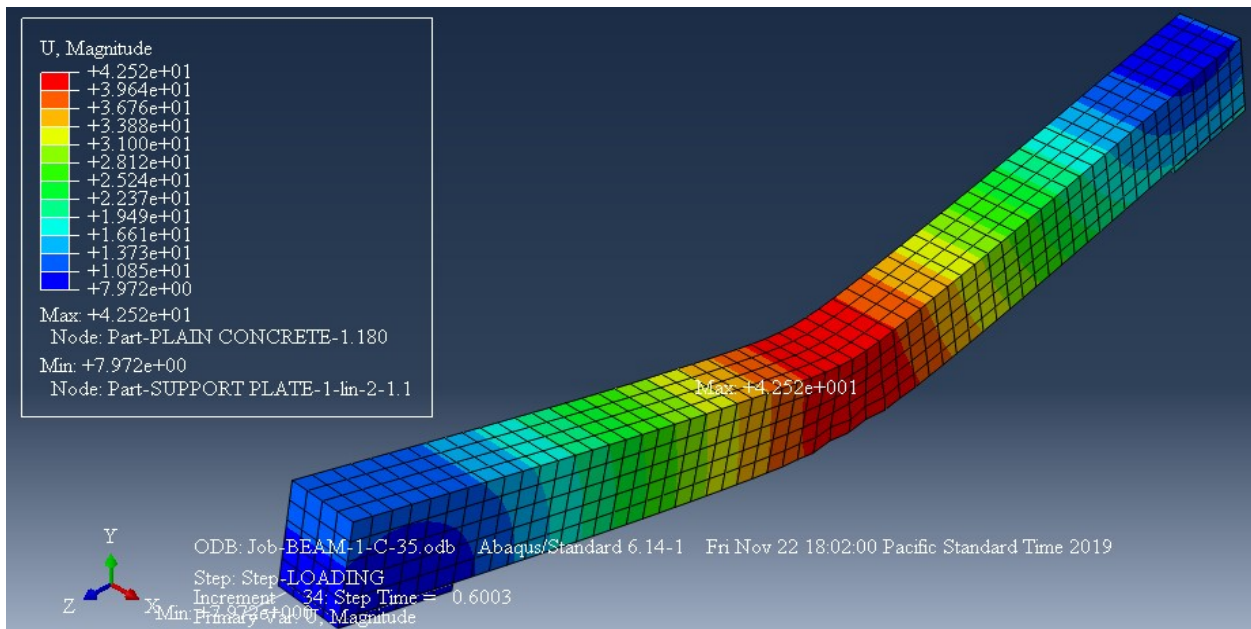


Figure 4.4: Mid span deflection of RC-B1-C35 beam (42.52 mm)

Figure 4.5 shows 452.9 mm mid span deflection of RC-B2-C20 beam, and it is observed that with increasing of beam span length bending resistance of the beam decreased and its mid span deflection increase under fire.

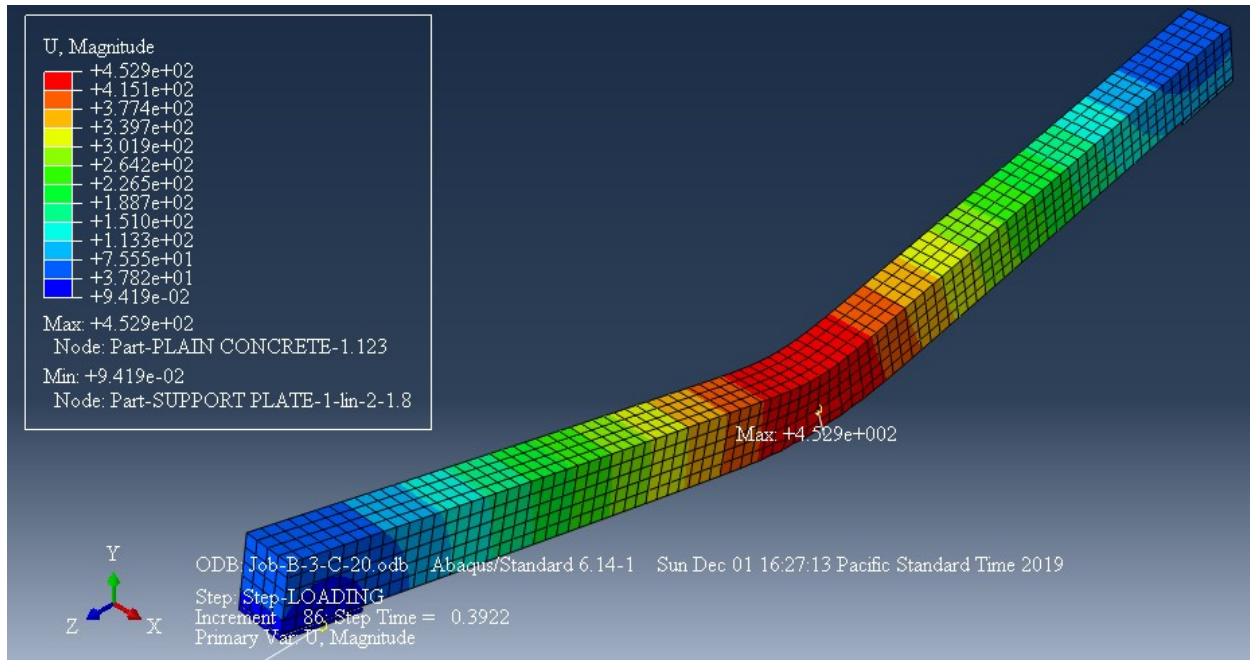


Figure 4.5: Mid span deflection of RC-B2-C20 beam(452.9 mm)

Figure 4.6 shows 435 mm mid span deflection of RC-B2-C25 beam, and it is observed that with increasing concrete strength bending resistance of the beam increased and its mid span deflection decreased under fire.

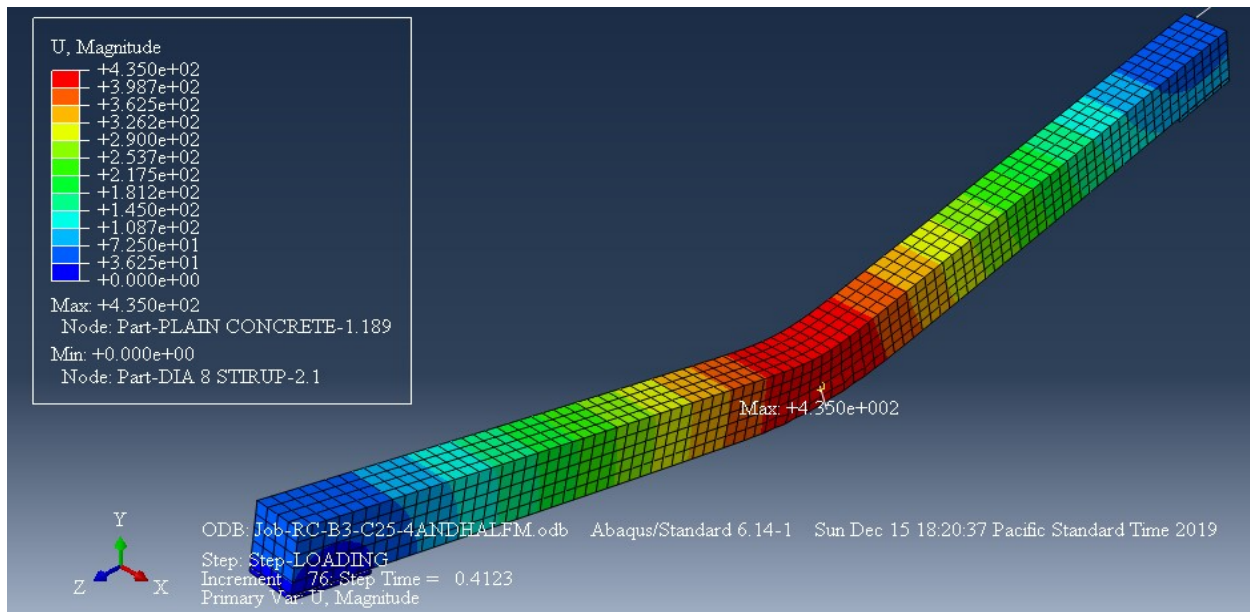


Figure 4.6: Mid span deflection of RC-B2-C25 beam(435 mm)

Figure 4.7 shows 409.8 mm mid span deflection of RC-B2-C30 beam, and it is observed that with increasing concrete strength bending resistance of the beam increased and its mid span deflection decreased under fire.

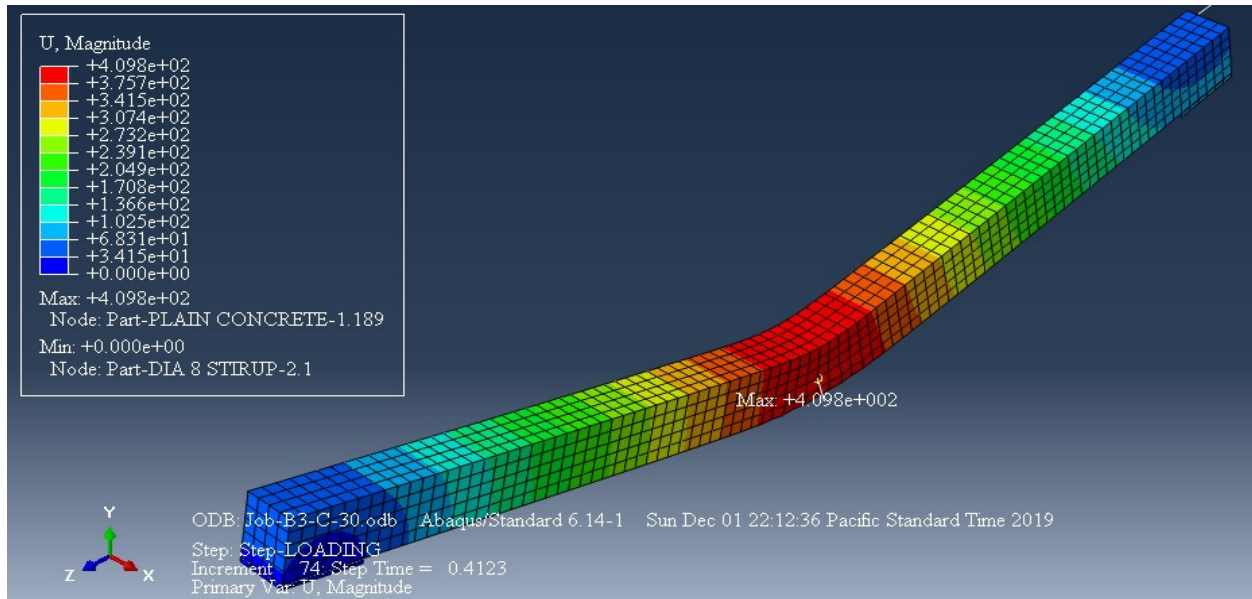


Figure 4.7: Mid span deflection of RC-B2-C30 beam(409.8 mm)

Figure 4.8 shows 239 mm mid span deflection of RC-B2-C35 beam, and it is observed that with increasing concrete strength bending resistance of the beam increased and its mid span deflection decreased under fire.

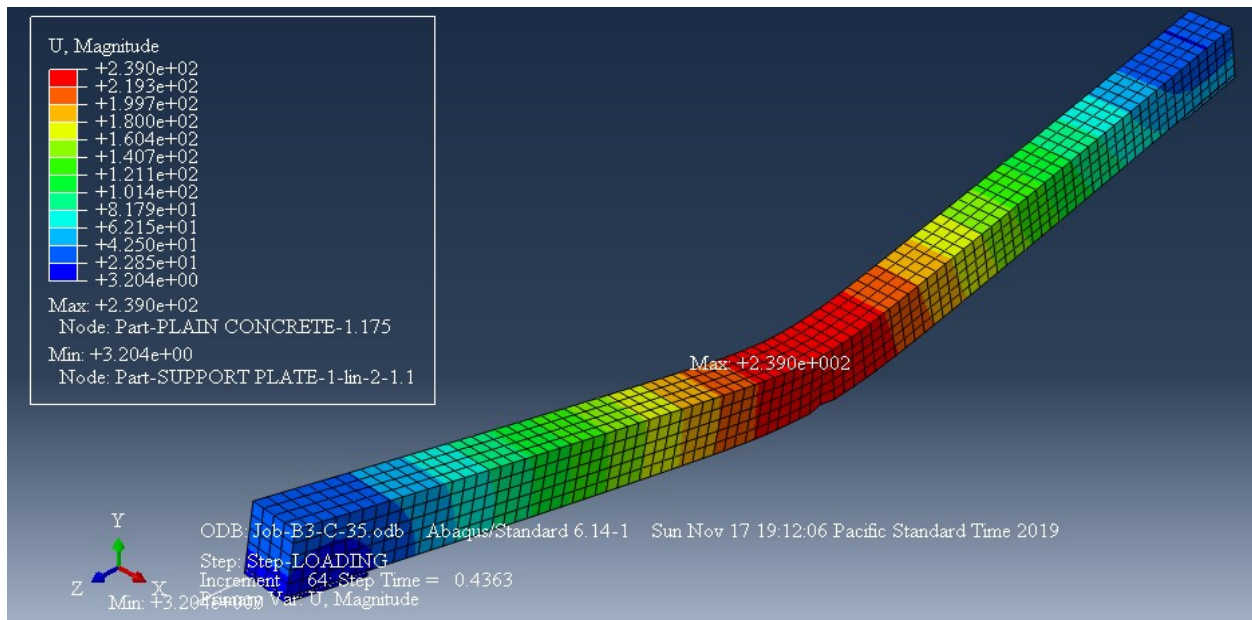


Figure 4.8: Mid span deflection of RC-B2-C35 beam(239 mm)

Figure 4.9 shows 3.01 mm mid span deflection of RC-B3-C20 beam, and it is observed that with increasing concrete strength bending resistance of the beam increased and its mid span deflection decreased under fire.

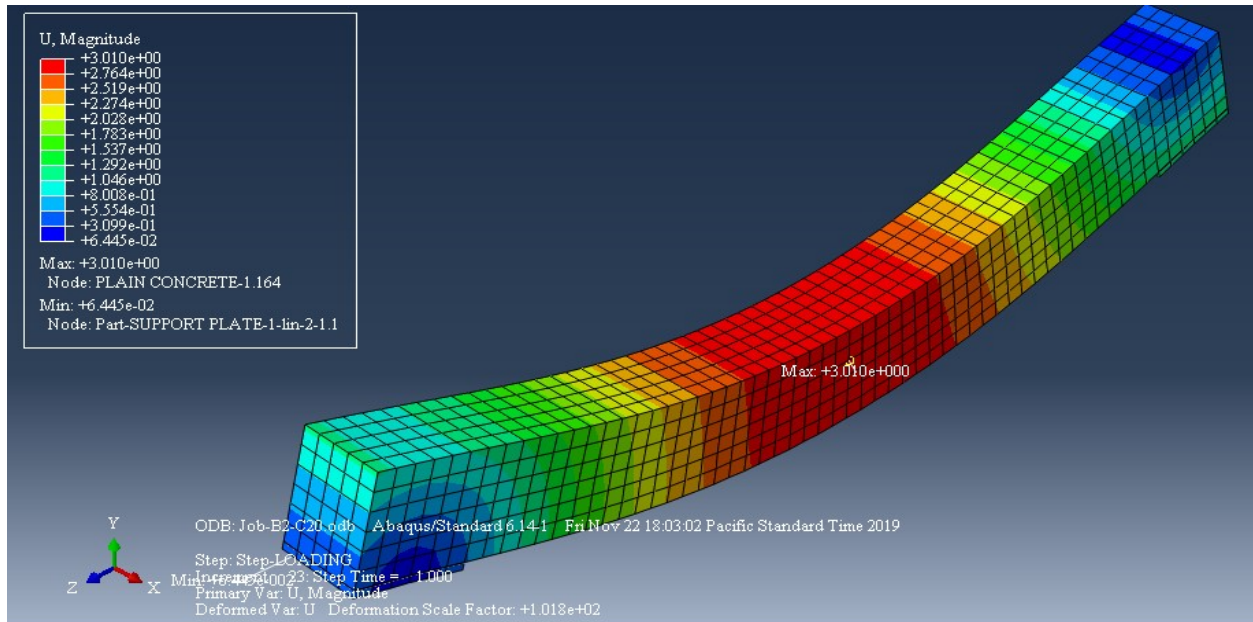


Figure 4.9: Mid span deflection of RC-B3-C20 beam(3.01 mm)

Figure 4.10 shows 2.841 mm mid span deflection of RC-B3-C25 beam, and it is observed that with increasing concrete strength bending resistance of the beam increased and its mid span deflection decreased under fire.

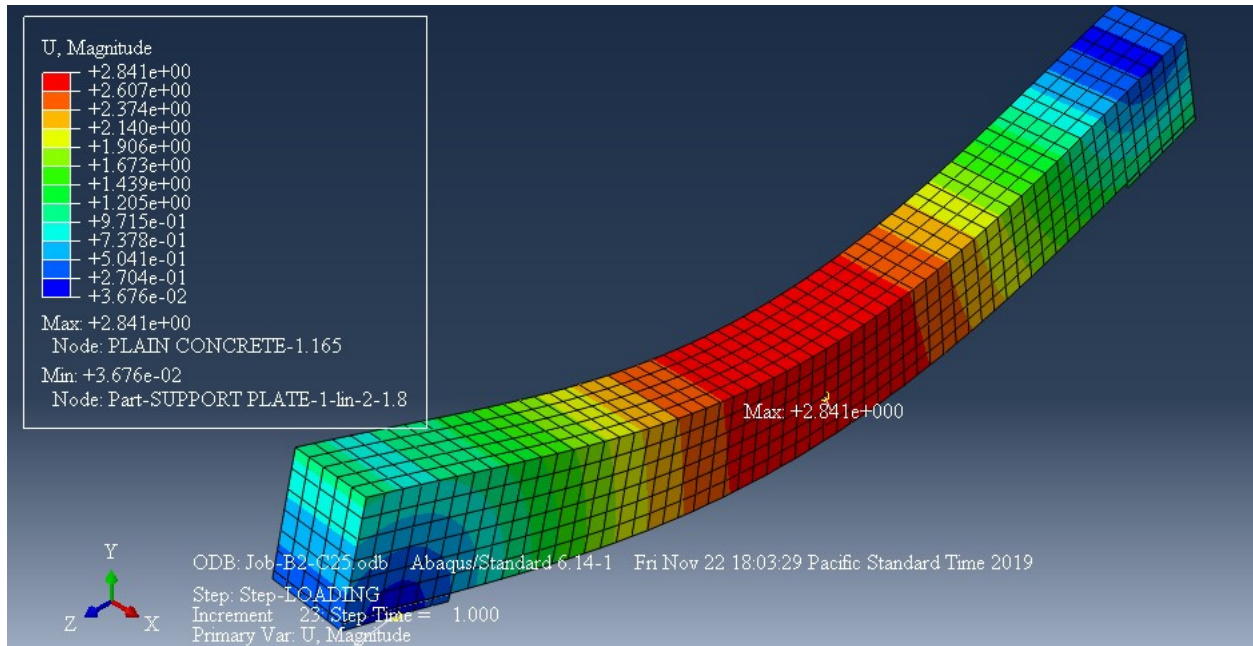


Figure 4.10: Mid span deflection of RC-B3-C25 beam (2.841 mm)

Figure 4.11 shows 2.768 mm mid span deflection of RC-B3-C30 beam, and it is observed that with increasing concrete strength bending resistance of the beam increased and its mid span deflection decreased under fire.

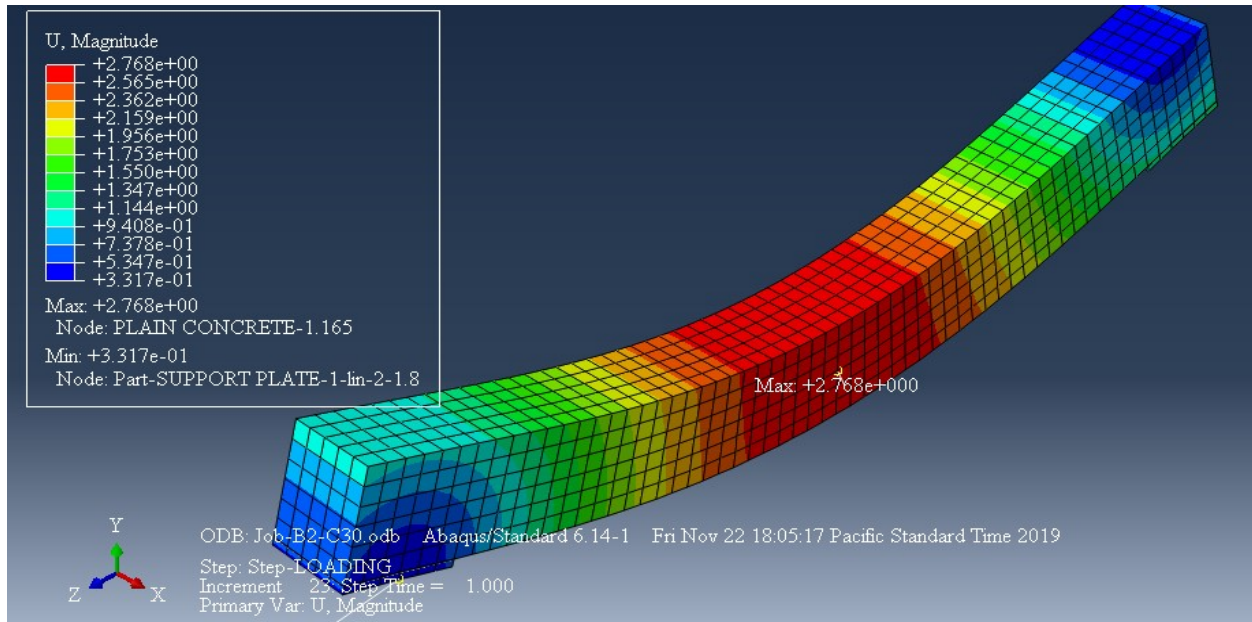


Figure 4.11: Mid span deflection of RC-B3-C30 beam (2.768 mm)

Figure 4.12 shows 2.65 mm mid span deflection of RC-B3-C35 beam, and it is observed that with increasing concrete strength bending resistance of the beam increased and its mid span deflection decreased under fire.

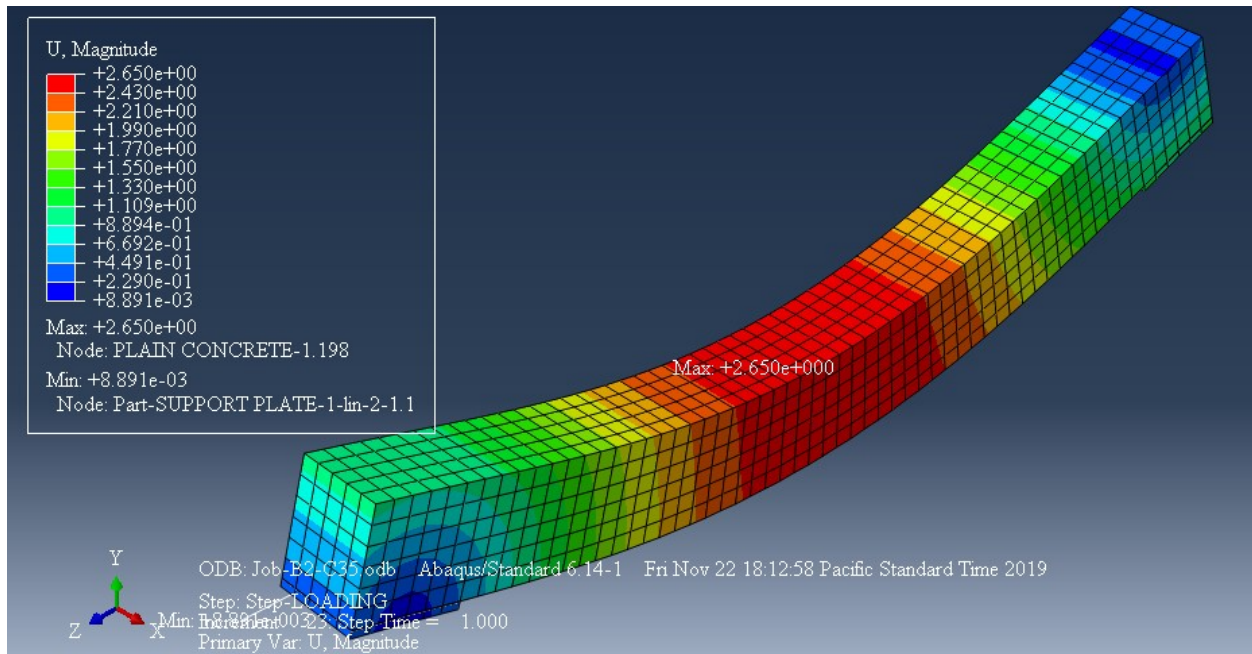


Figure 4.12: Mid span deflection of RC-B3-C35 beam (2.65 mm)

Figure 4.13 shows 64.31 mm mid span deflection of RC-B4-C20 beam, and it is observed that with increasing concrete strength bending resistance of the beam increased and its mid span deflection decreased under fire.

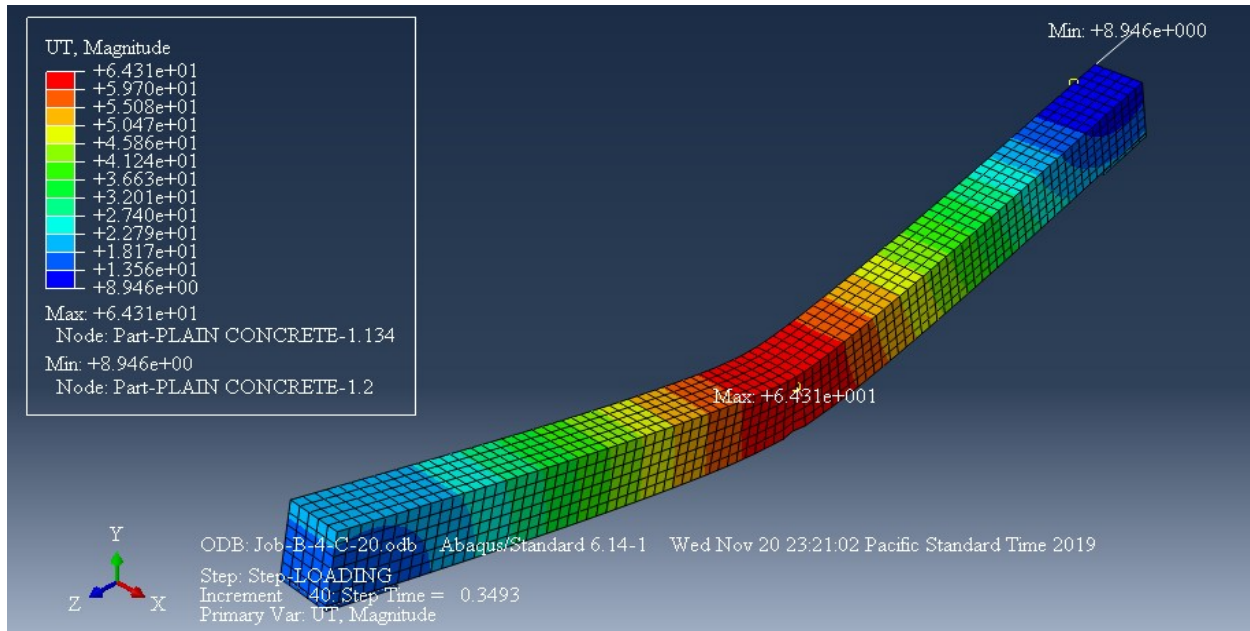


Figure 4.13: Mid span deflection of RC-B4-C20 beam (64.31 mm)

Figure 4.14 shows 63.03 mm mid span deflection of RC-B4-C25 beam, and it is observed that with increasing concrete strength bending resistance of the beam increased and its mid span deflection decreased under fire.

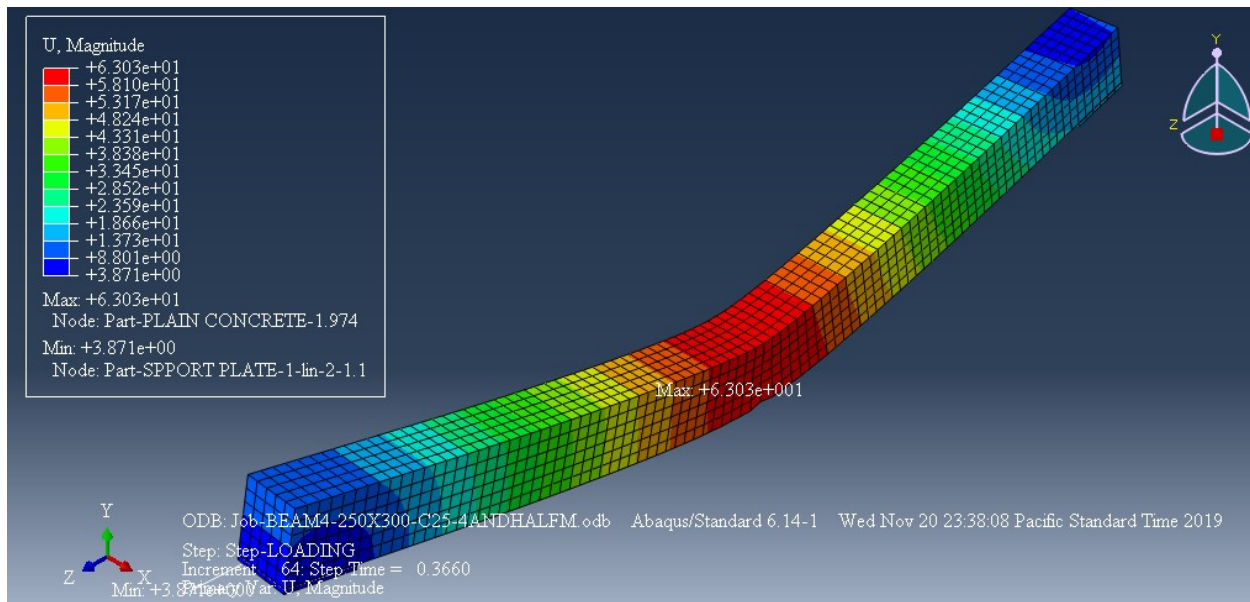


Figure 4.14: Mid span deflection of RC-B4-C25 beam (63.03 mm)

Figure 4.15 shows 44.18 mm mid span deflection of RC-B4-C30 beam, and it is observed that with increasing concrete strength bending resistance of the beam increased and its mid span deflection decreased under fire.

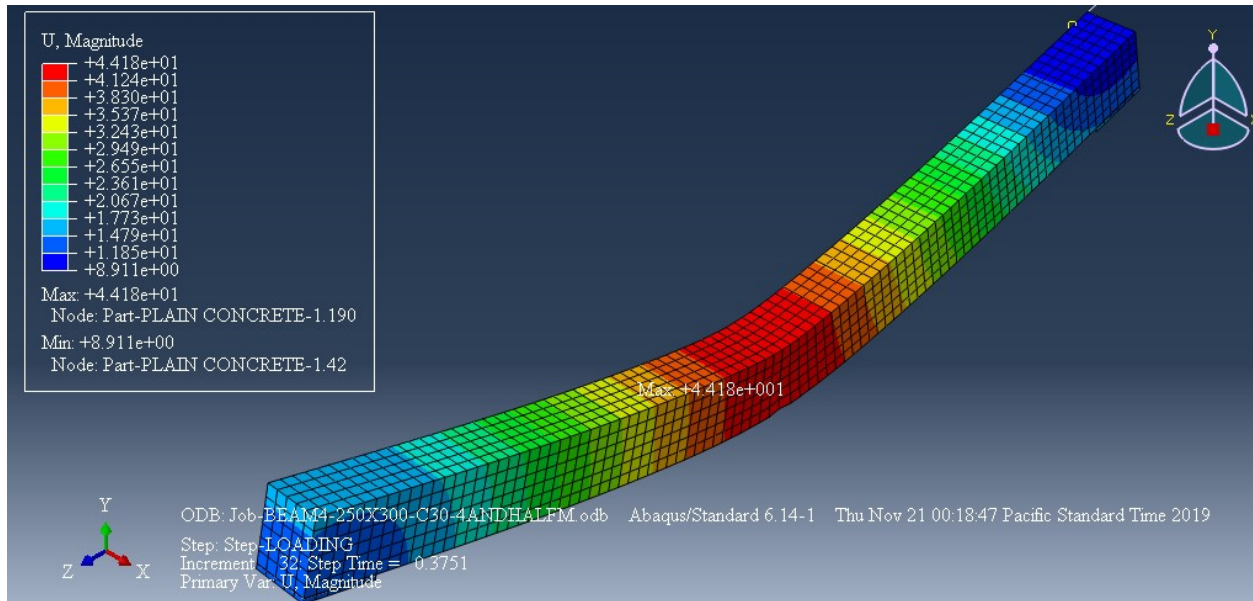


Figure 4.15: Mid span deflection of RC-B4-C30 beam (44.18 mm)

Figure 4.16 shows 37.2 mm mid span deflection of RC-B4-C35 beam, and it is observed that with increasing concrete strength bending resistance of the beam increased and its mid span deflection decreased under fire.

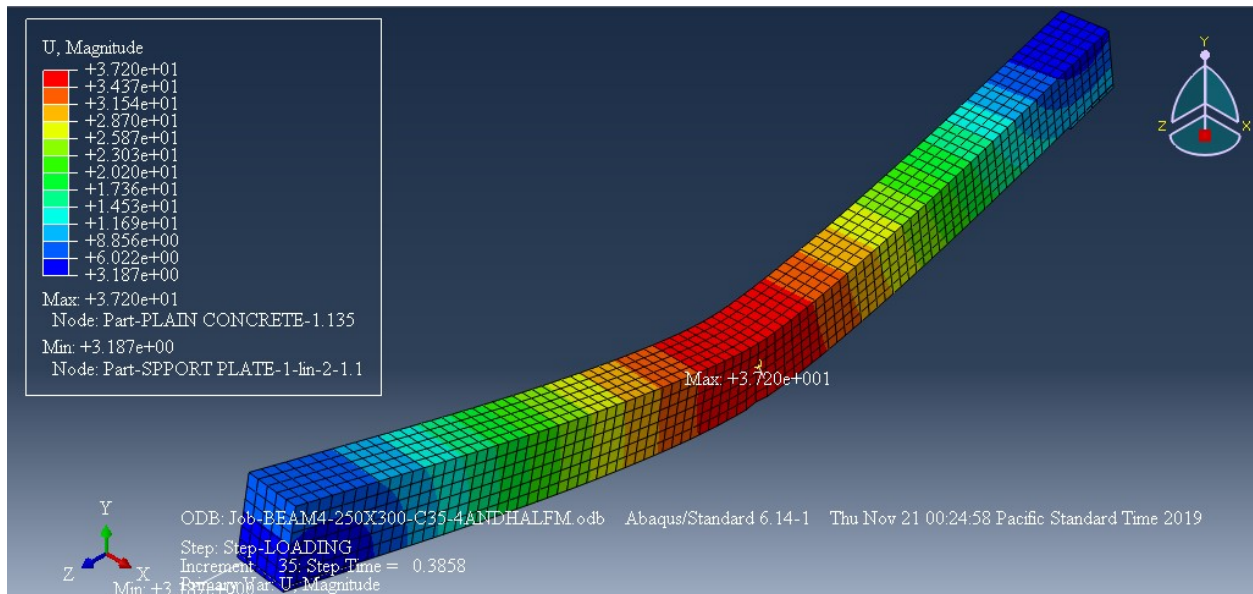


Figure 4.16: Mid span deflection of RC-B4-C35 beam (37.2 mm)

4.4 Deflection of I – Section Steel Beam due to fire and flexure

By changing reinforced concrete beam 200mmX240mm and 250mmx300mm cross sections by modular ratio to equivalent I section cross sectional area the mid span deflection is analyzed for 3m and 4.5m simply supported beam span length for the combined effect of fire and flexure. The deflection increase with increasing of beam cross section and it is shown on Table 4.6.

Table 4.6: Deformation of I – section steel beam due to fire and flexure

RC Beam Type	Modular Ratio	Steel Beam Type	By Modular Ratio Converted I section Steel Beam	Span Length (mm)	Fire Resistance (Second)	Loading (N/mm ²)	Maximum Deflection (mm)	Location									
RC-B1-C20	7.00	IS-B1-C20	W12-12X6 1/2 (356X406)	3000	7200	0.0718	15.6	Mid Span									
RC-B1-C25	6.77	IS-B1-C25	W14-14X6 3/4 (356X171)				5.86										
RC-B1-C30	6.56	IS-B1-C30	W10-10X8 (254X203)				12.4										
RC-B1-C35	6.18	IS-B1-C35	W14-14X8 (356X203)				13.32										
RC-B2-C20	7.00	IS-B2-C20	W12-12X6 1/2 (356X406)	4500			7200		0.0718	422	Mid Span						
RC-B2-C25	6.77	IS-B2-C25	W14-14X6 3/4 (356X171)							37.2							
RC-B2-C30	6.56	IS-B2-C30	W10-10X8 (254X203)							1625							
RC-B2-C35	6.18	IS-B2-C35	W14-14X8 (356X203)							2022							
RC-B3-C20	7.00	IS-B3-C20	W16-16X7 (406X178)	3000						7200		0.0718	3.2	Mid Span			
RC-B3-C25	6.77	IS-B3-C25	W10-10X10 (254X254)										9.46				
RC-B3-C30	6.56	IS-B3-C30	W24-24X7 (610X178)										6.27				
RC-B3-C35	6.18	IS-B3-C35	W8-8X8 (203X203)										11.6				
RC-B4-C20	7.00	IS-B4-C20	W16-16X7 (406X178)	4500									7200		0.0718	14.24	Mid Span
RC-B4-C25	6.77	IS-B4-C25	W10-10X10 (254X254)													390.5	
RC-B4-C30	6.56	IS-B4-C30	W24-24X7 (610X178)													2569	
RC-B4-C35	6.18	IS-B4-C35	W8-8X8 (203X203)													3634	

Figure 4.17 shows 15.6 mm mid span deflection of IS-B1-C20 beam, and it is observed that steel beam has limit of cross section or weight that has capacity to resist bending.

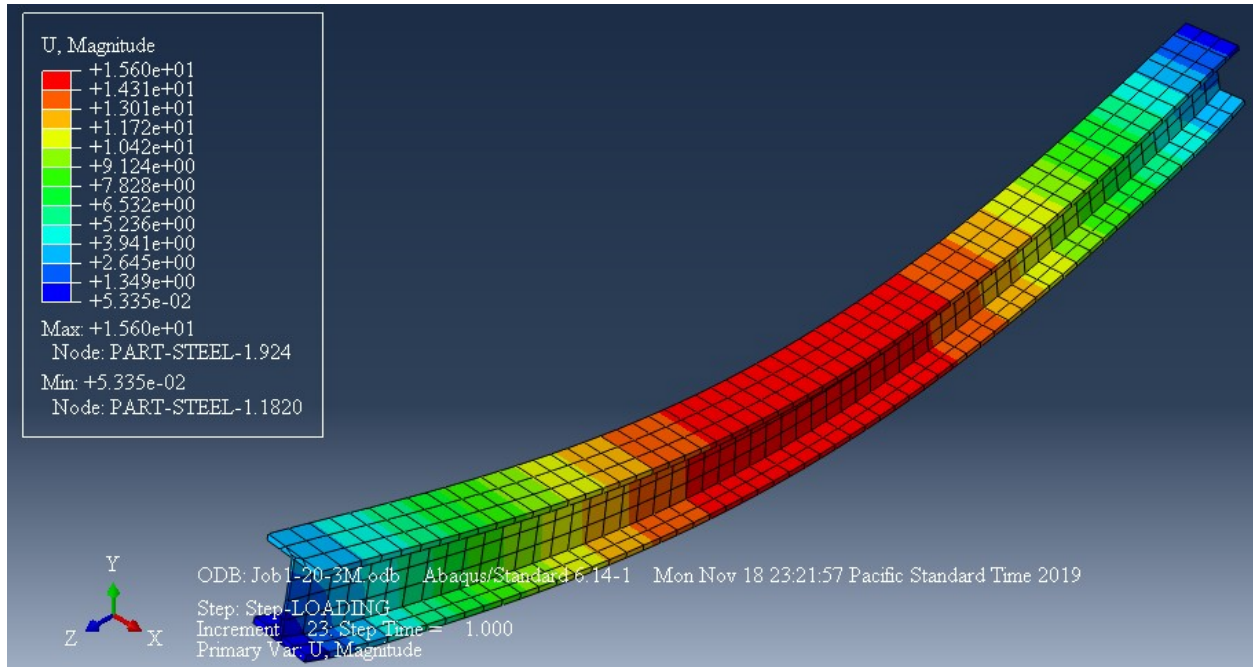


Figure 4.17: Mid span deflection of IS-B1-C20 beam (15.6 mm)

Figure 4.18 shows 5.855 mm mid span deflection of IS-B1-C25 beam, and it is observed that steel beam has limit of cross section or weight that has capacity to resist bending.

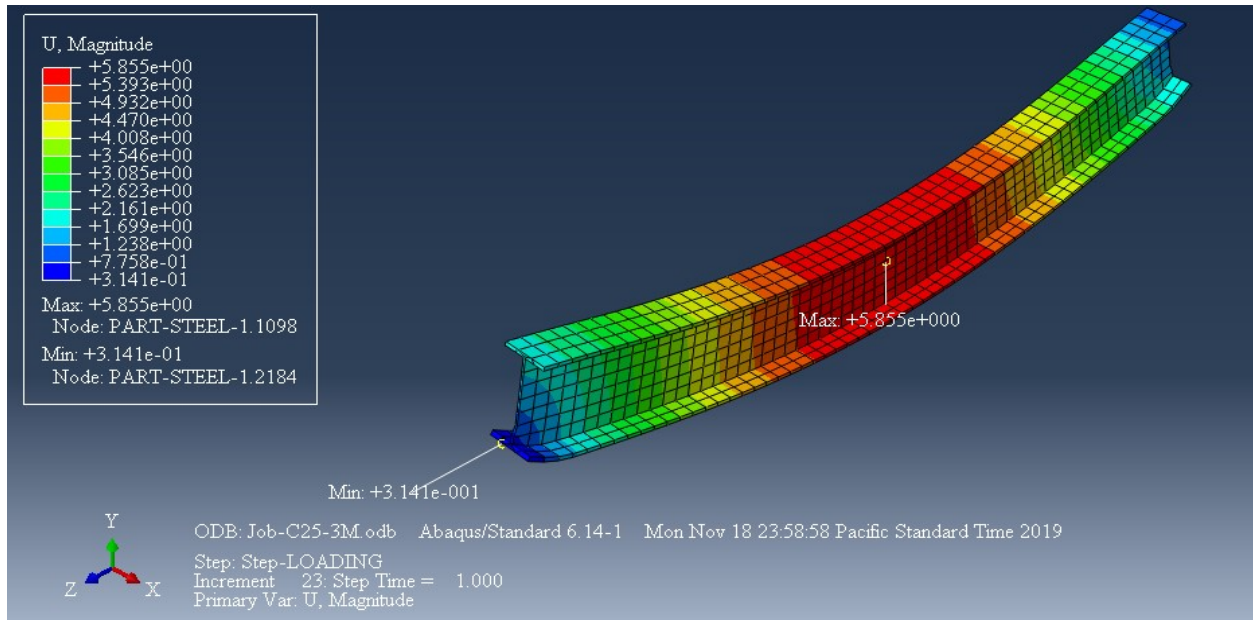


Figure 4.18: Mid span deflection of IS-B1-C25 beam (5.855 mm)

Figure 4.19 shows 12.41 mm mid span deflection of IS-B1-C30 beam, and it is observed that with increasing of beam cross section bending resistance of the beam is decreased under fire.

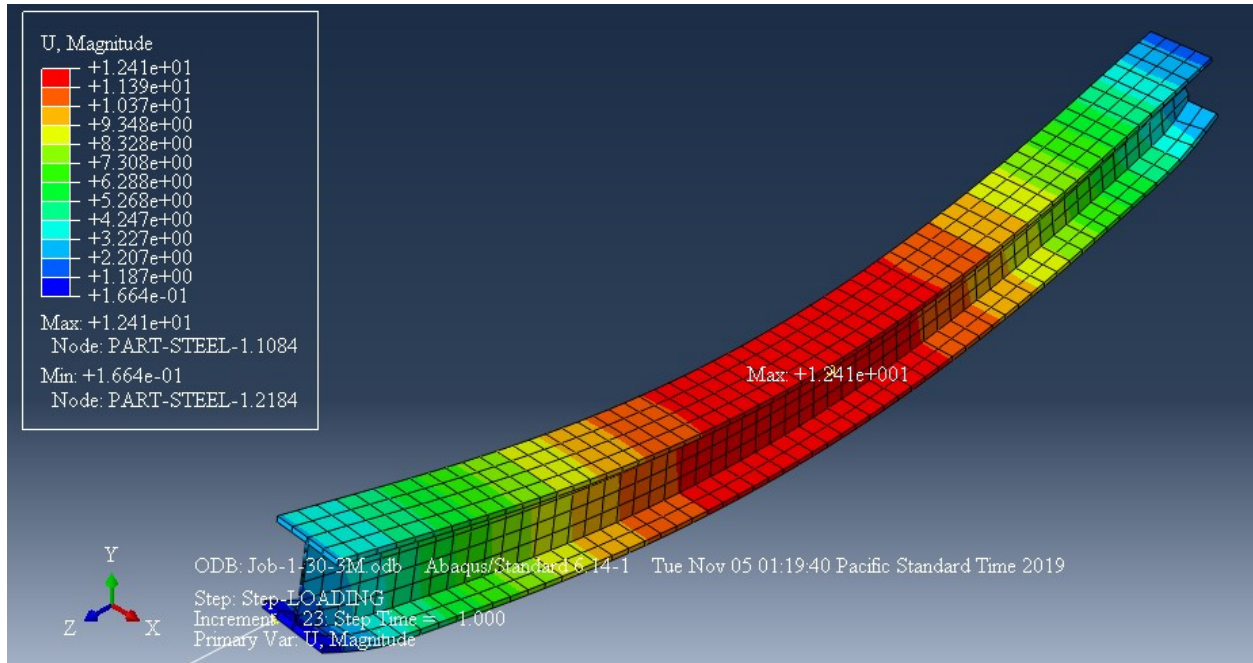


Figure 4.19: Mid span deflection of IS-B1-C30 beam (12.41 mm)

Figure 4.20 shows 13.32 mm mid span deflection of IS-B1-C35 beam, and it is observed that with increasing of beam cross section bending resistance of the beam is decreased under fire. And it also has limit of cross section or weight that has capacity to resist bending.

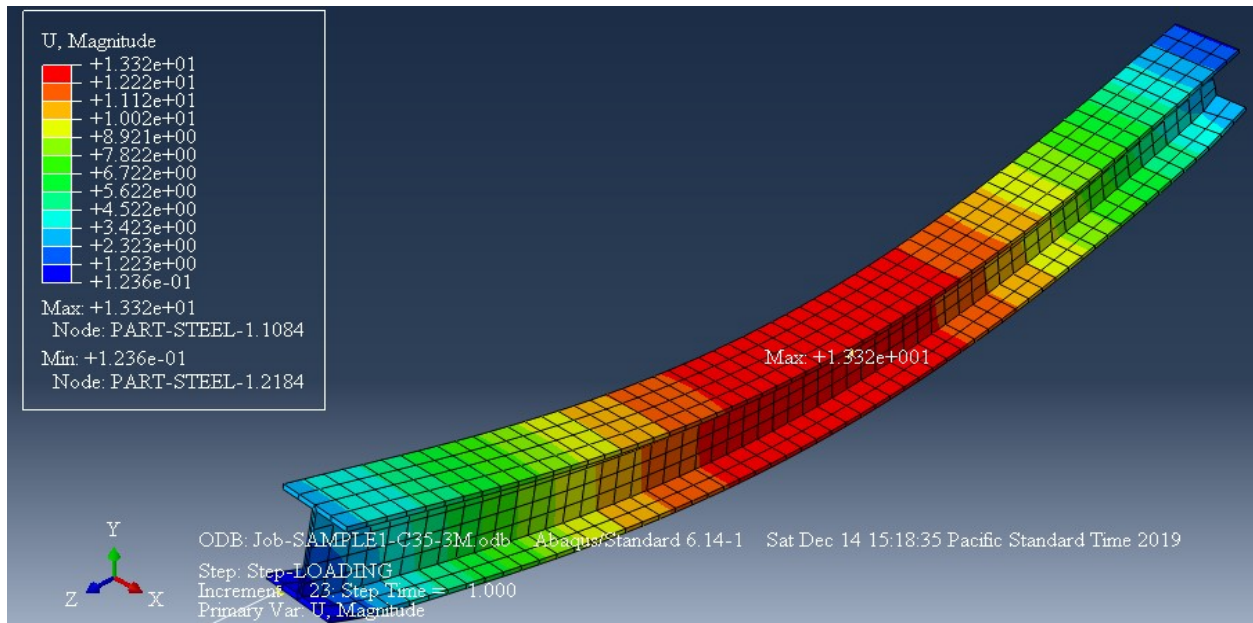


Figure 4.20: Mid span deflection of IS-B1-C35 beam (13.32 mm)

Figure 4.21 shows 422mm mid span deflection of IS-B2-C20 beam, and it is observed that with increasing of beam cross section bending resistance of the beam is decreased under fire. And it also has limit of cross section or weight that has capacity to resist bending.

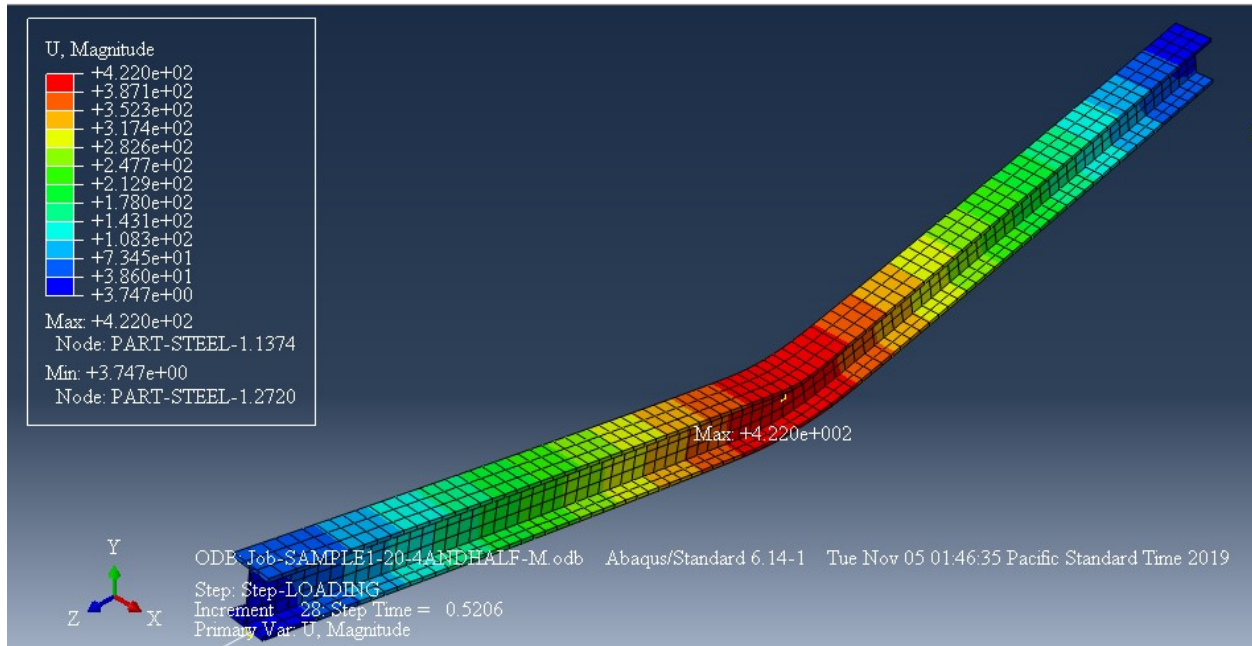


Figure 4.21: Mid span deflection of IS-B2-C20 beam (422 mm)

Figure 4.22 shows 37.21 mm mid span deflection of IS-B2-C25 beam, and it also has limit of cross section or weight that has increased capacity to resist bending under fire.

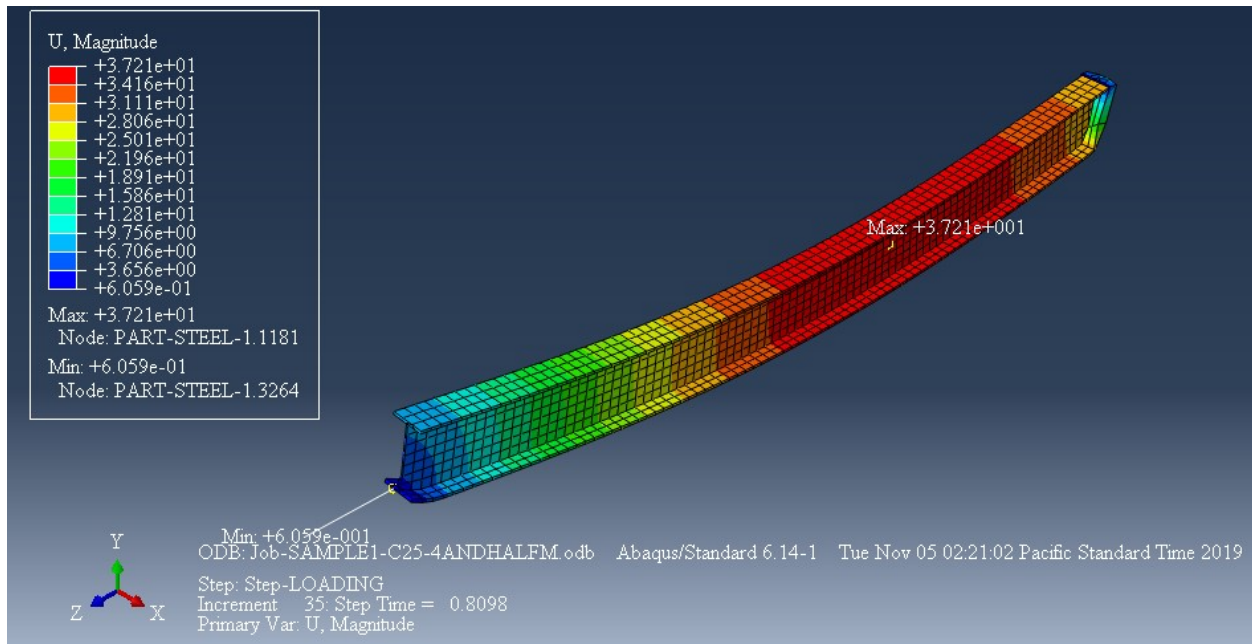


Figure 4.22: Mid span deflection of IS-B2-C25 beam (37.21 mm)

Figure 4.23 shows 1625mm mid span deflection of IS-B2-C30 beam, and it is observed that with increasing of beam cross section bending resistance of the beam is decreased under fire.

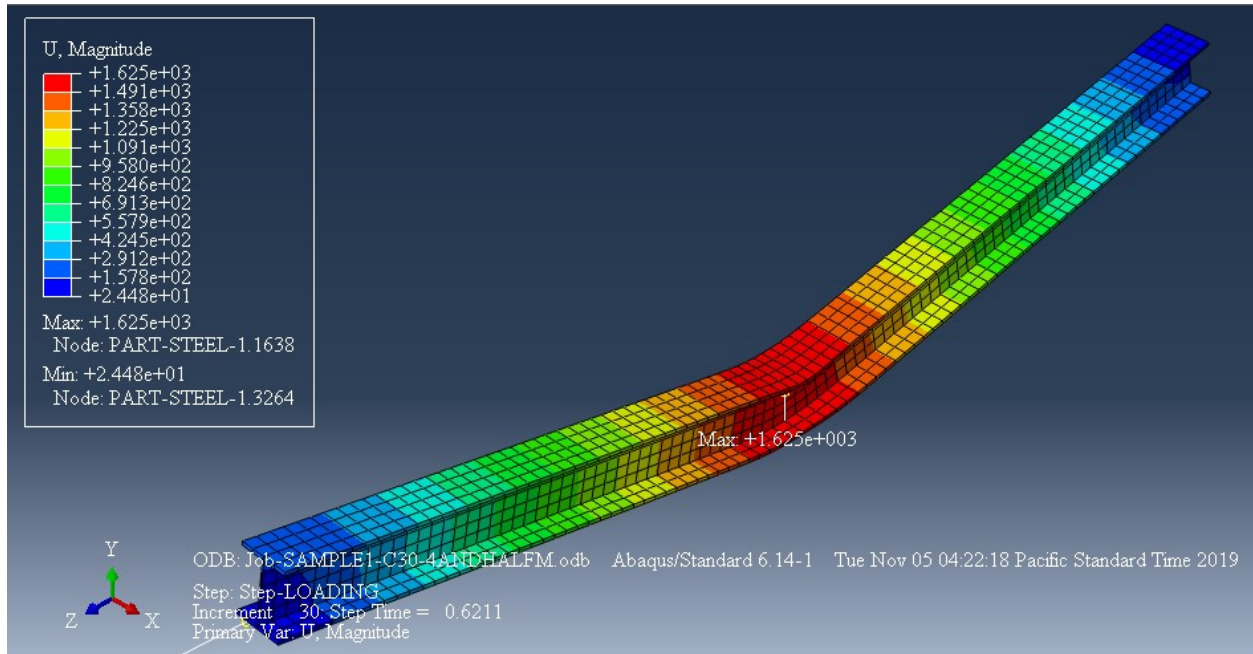


Figure 4.23: Mid span deflection of IS-B2-C30 beam (1625 mm)

Figure 4.24 shows 2022mm mid span deflection of IS-B2-C35 beam, and it is observed that with increasing of beam cross section bending resistance of the beam is decreased under fire.

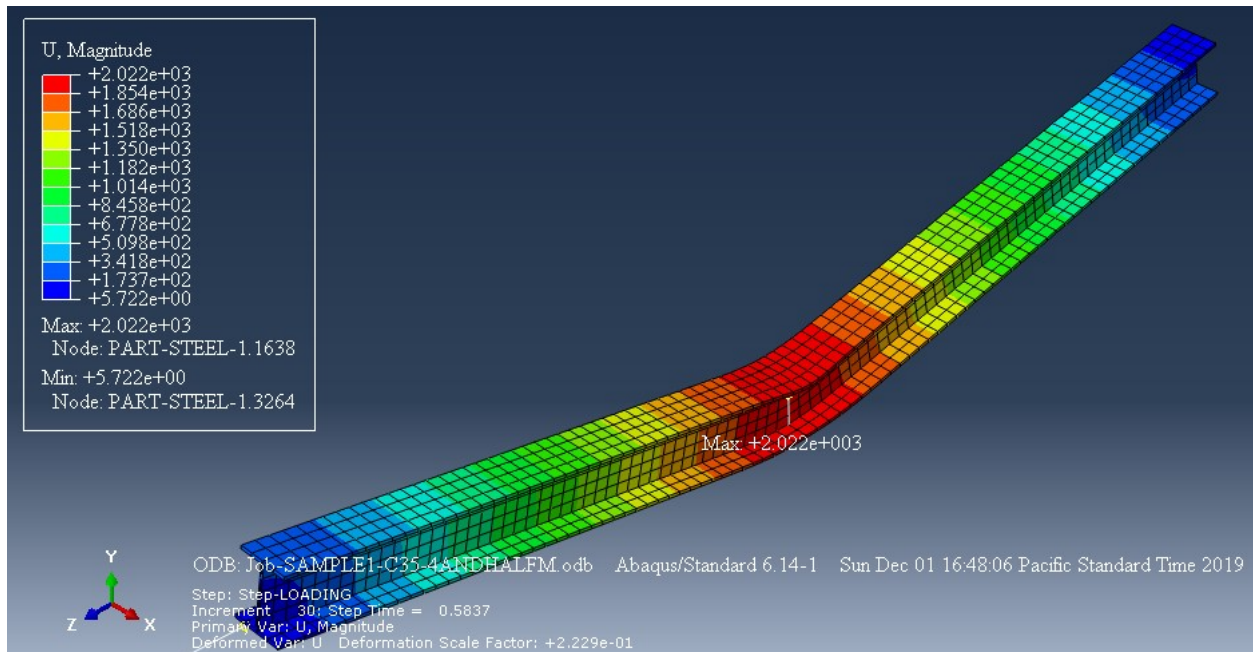


Figure 4.24: Mid span deflection of IS-B2-C35 beam (2022 mm)

Figure 4.25 shows mid span deflection of IS-B3-C20 beam and it is 3.204 mm, when it compare to RC beam RC-B3-C20 by equivalent area converted on the basis of modular ratio it is increased by 0.19 mm.

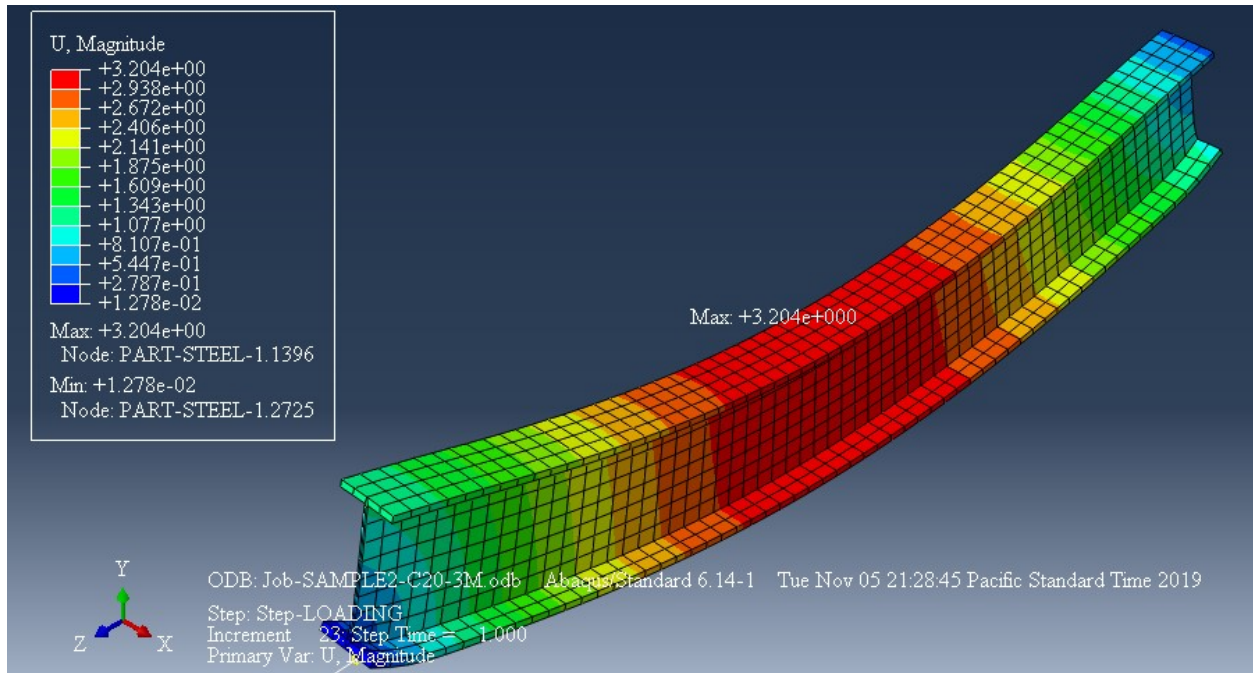


Figure 4.25: Mid span deflection of IS-B3-C20 beam (3.204 mm)

Figure 4.26 shows mid span deflection of IS-B3-C25 beam and it is 9.46 mm, when it compare to RC beam RC-B3-C25 by equivalent area converted on the basis of modular ratio it is increased by 6.62 mm.

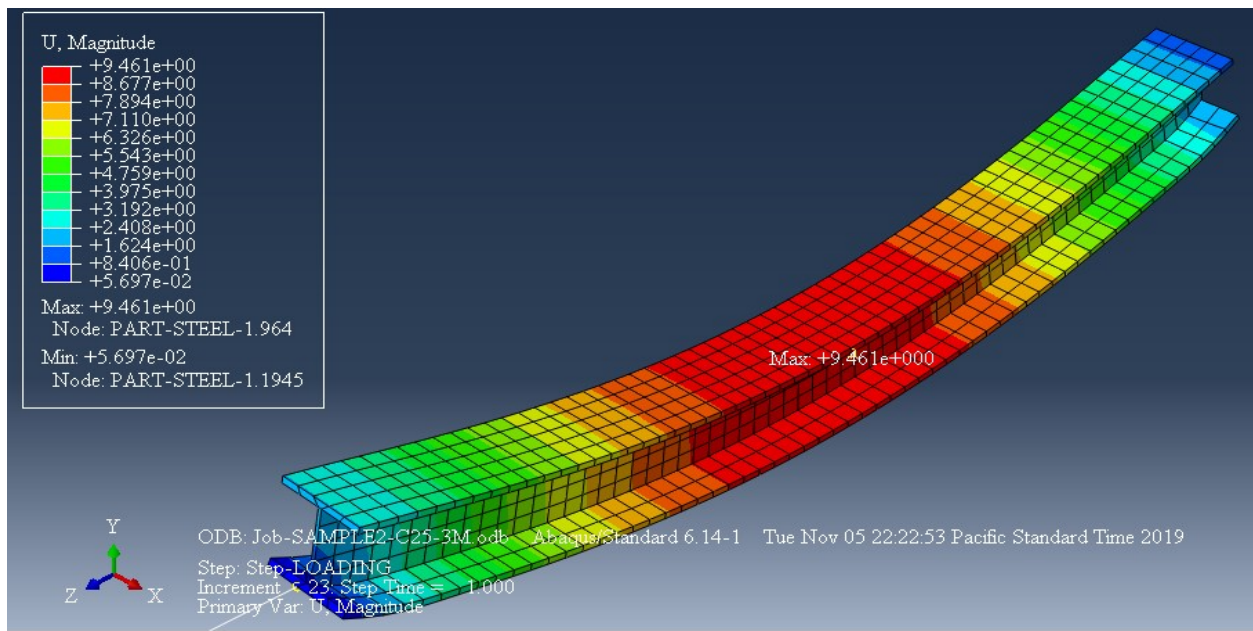


Figure 4.26: Mid span deflection of IS-B3-C25 beam (9.461 mm)

Figure 4.27 shows mid span deflection of IS-B3-C30 beam and it is 6.27 mm, when it compare to RC beam RC-B3-C30 by equivalent area converted on the basis of modular ratio it is increased by 3.502 mm.

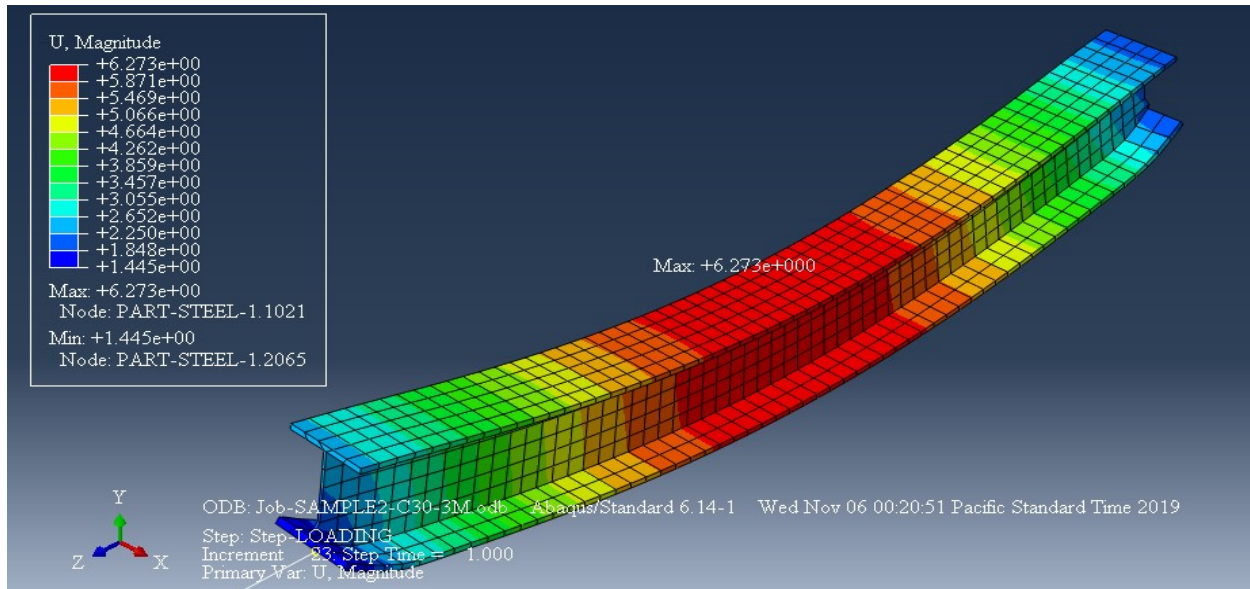


Figure 4.27: Mid span deflection of IS-B3-C30 beam (6.273 mm)

Figure 4.28 shows 11.64mm mid span deflection of IS-B3-C35 beam, and it is observed that with increasing of beam cross section bending resistance of the beam is decreased under fire. And it also has limit of cross section or weight that has capacity to resist bending.

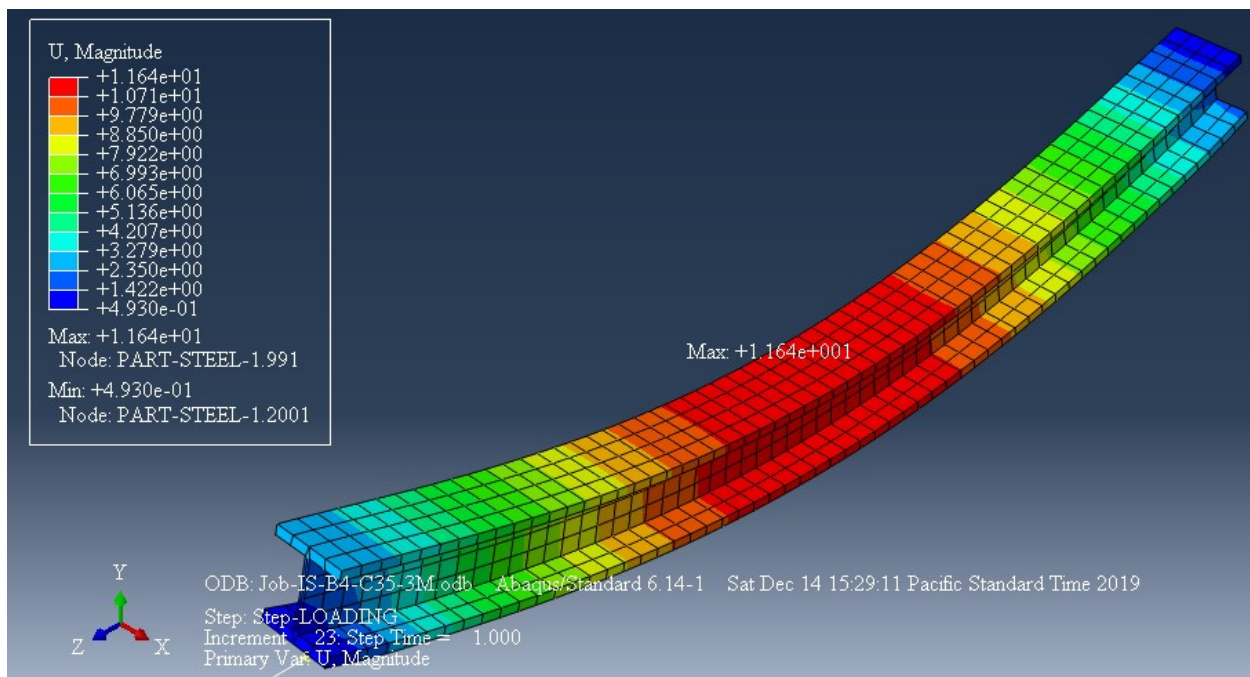


Figure 4.28: Mid span deflection of IS-B3-C35 beam(11.64 m)

Figure 4.29 shows 14.24 mm mid span deflection of IS-B4-C20 beam, and it is observed that with increasing of beam cross section bending resistance of the beam is decreased under fire. And it also has limit of cross section or weight that has capacity to resist bending.

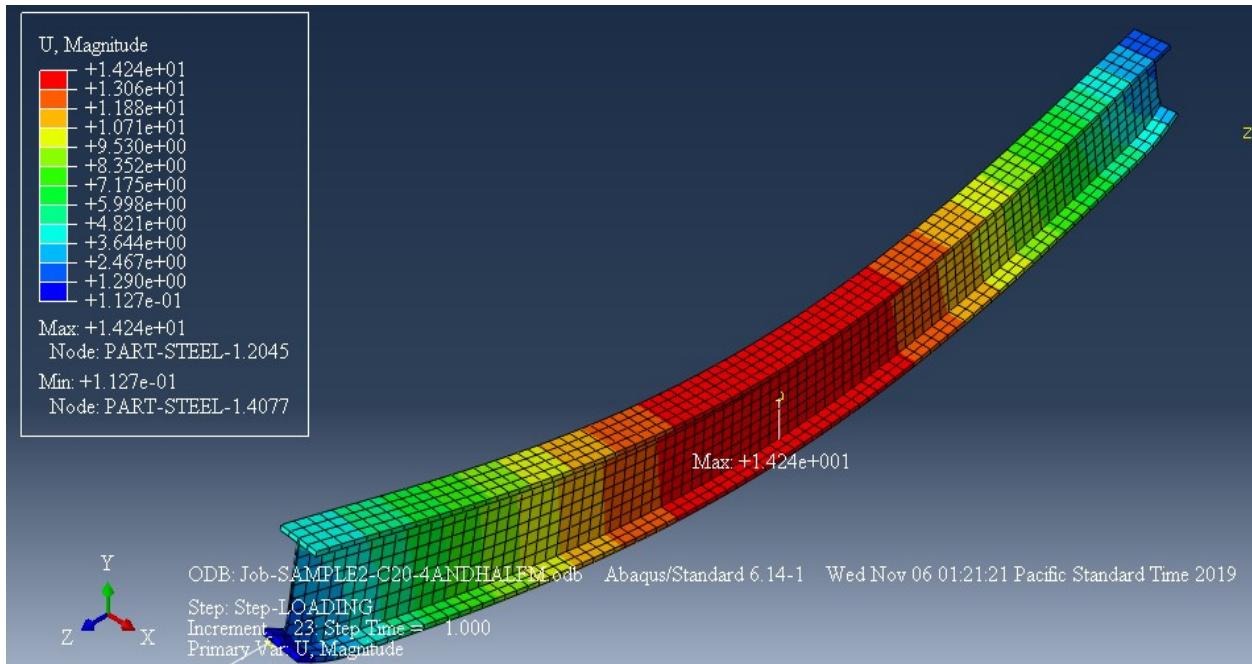


Figure 4.29: Mid span deflection of IS-B4-C20 beam (14.24 m)

Figure 4.30 shows 390.5 mm mid span deflection of IS-B4-C25 beam, and it is observed that with increasing of beam cross section bending resistance of the beam is decreased under fire.

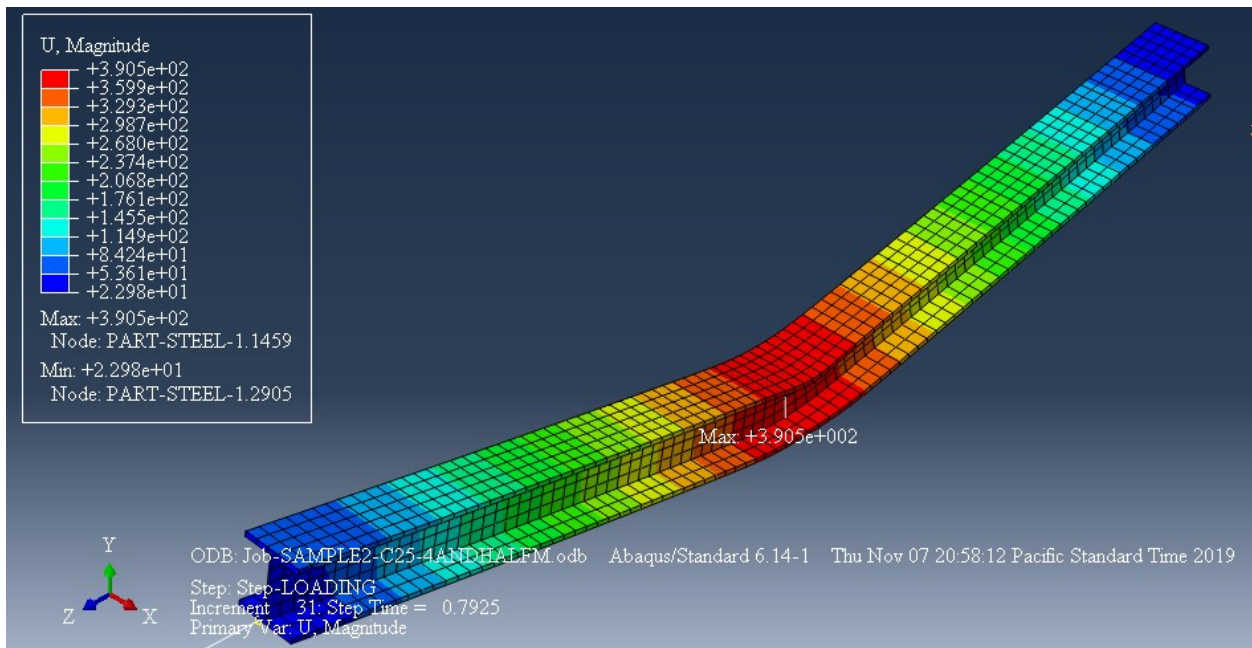


Figure 4.30: Mid span deflection of IS-B4-C25 beam (390.5 mm)

Figure 4.31 shows 2569 mm mid span deflection of IS-B4-C30 beam, and it is observed that with increasing of beam cross section bending resistance of the beam is decreased under fire.

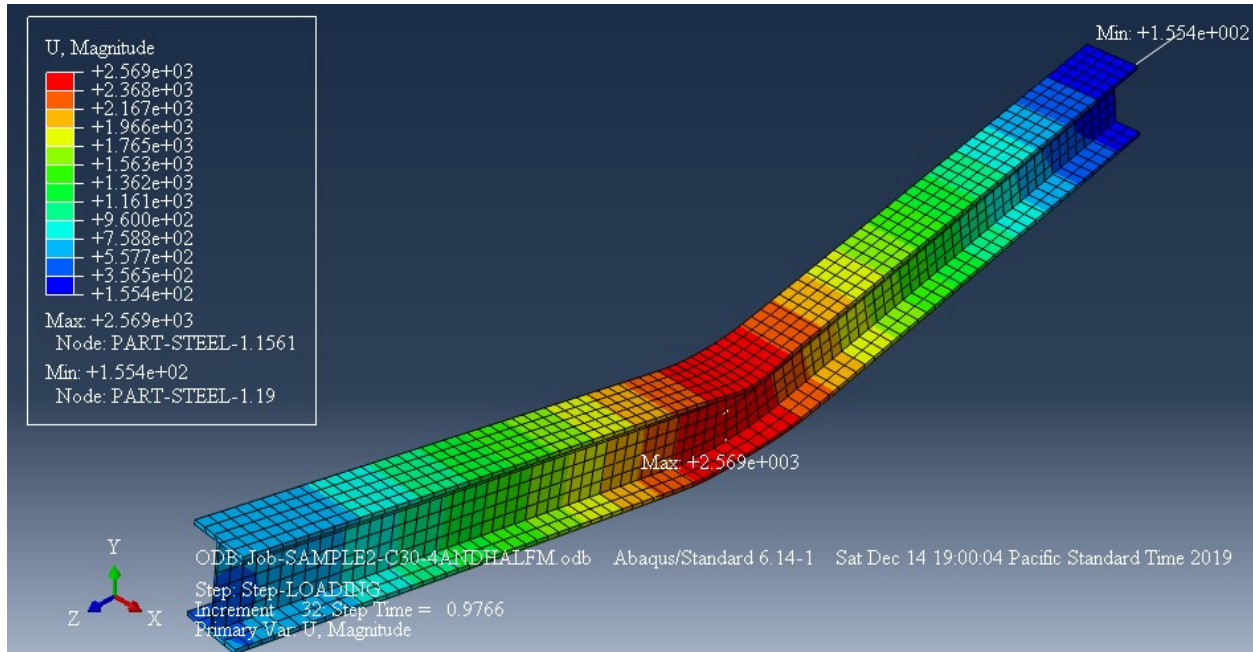


Figure 4.31: Mid span deflection of IS-B4-C30 beam (2569 mm)

Figure 4.32 shows 3634 mm mid span deflection of IS-B4-C35 beam, and it is observed that with increasing of beam cross section bending resistance of the beam is decreased under fire.

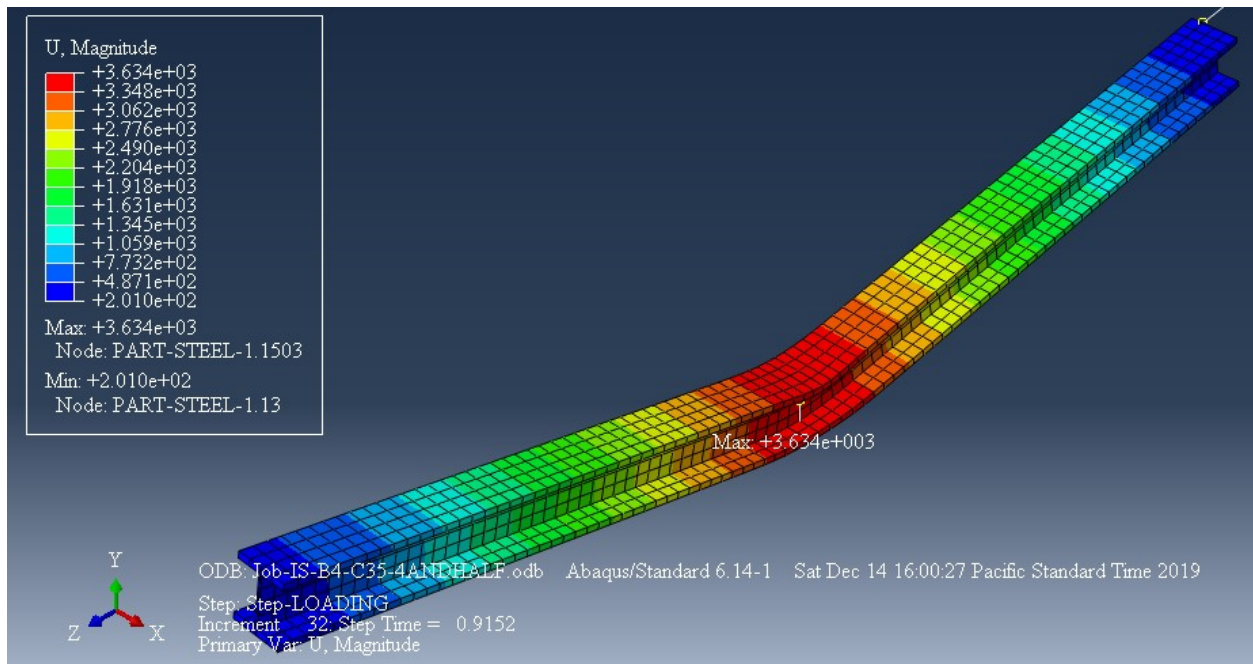


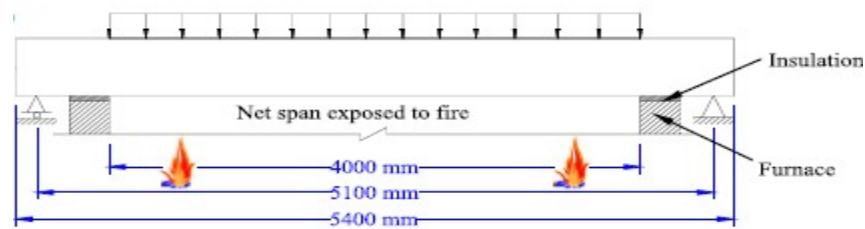
Figure 4.32: Mid span deflection of IS-B4-C35 beam (3634mm)

4.5 Validation of the Finite Element Model

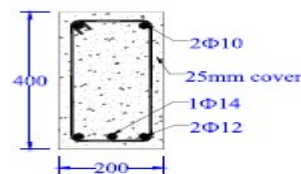
4.5.1 Validation of Reinforced Concrete Beam

RC beams tested under fire by Wu et al. [24] is selected and analyzed to illustrate the capability and accuracy of the present FE model. These tests were selected because their results have been reported in detail to facilitate FE simulations and detailed comparisons.

As part of a joint research project on the fire resistance of housing in China between the Fire Bureau of China and the Institute for Research in Construction of Canada, three RC beams were tested at Tianjin Fire Research Institute, China [24]. These beam specimens (Beam I, Beam II and Beam III) were designed to be identical. The dimensions and reinforcement details of these beams are shown in Fig. 4.33. The reinforcing steel had a yield stress and a tensile strength of 240 MPa and 380 MPa, respectively. The measured cube compressive strength of the concrete at 28 days was 24.2 MPa. The beams were 5.1 m in span with 4.0 m of the span exposed to fire (Fig. 4.33).

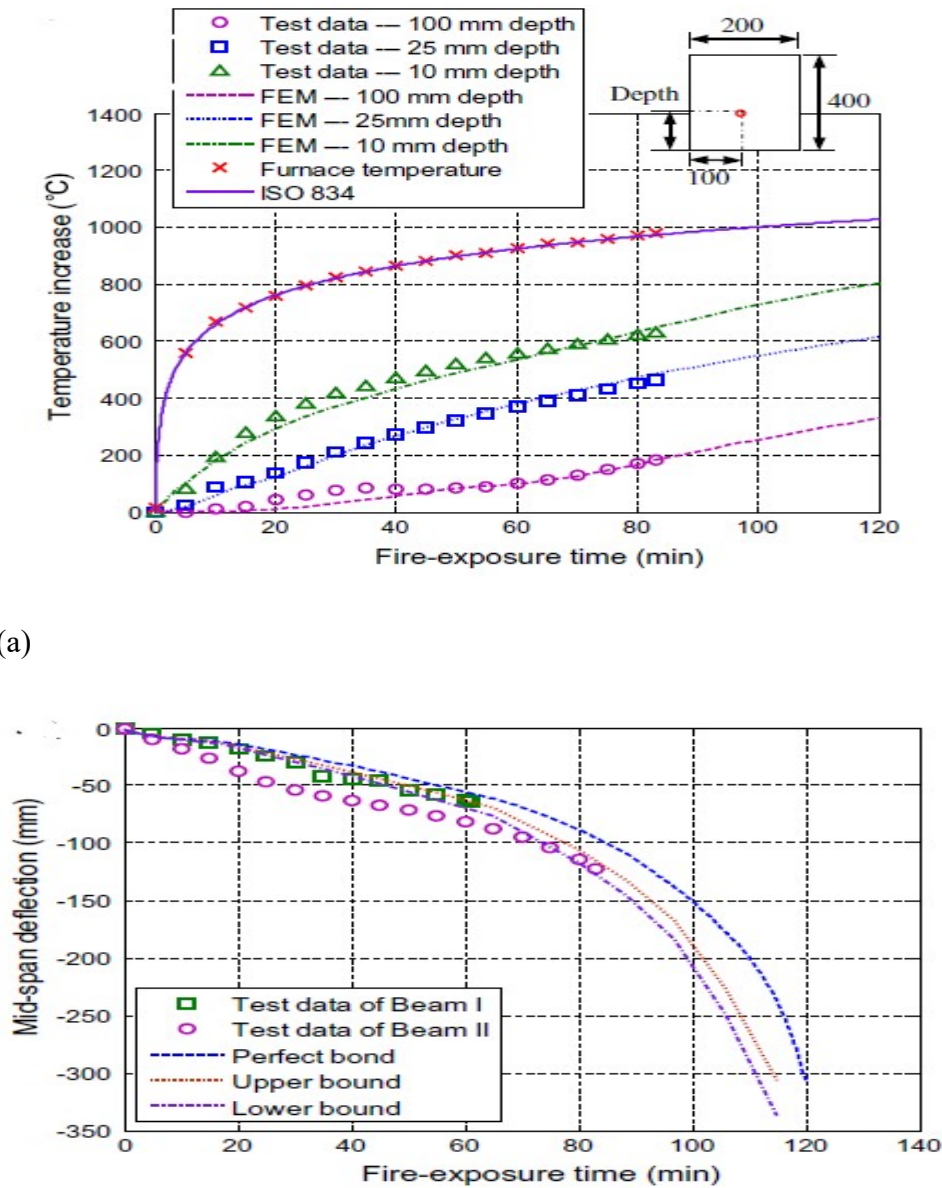


(a)



(b)

Figure 4.33: Details of specimens (200 mm x 400 mm x 5400 mm): (a) elevation and (b) cross-section.



(a)

(b)

Figure 4.34: Comparisons of the reinforced concrete beams tested by Wu et al. [24]: (a) predicted and measured temperatures at various locations, (b) predicted and measured mid-span deflections of Beams I and II

During the heat transfer analysis, the beam was subjected to the standard fire from its bottom and two sides. Fig.4.34. a compares the predicted temperature increases at various locations in the beam with the experimental results, showing very close agreement in general. The temperature at 100 mm from the bottom face is somewhat underestimated within the first 40 min of fire exposure, which may be attributed to the migration of moisture toward the inner part of the beam. However, the mechanical properties of concrete and steel remain almost unchanged during this stage as the temperature is still relatively low (around 100 °C), this underestimation of temperature has little effect on the predicted fire performance of the RC beam.

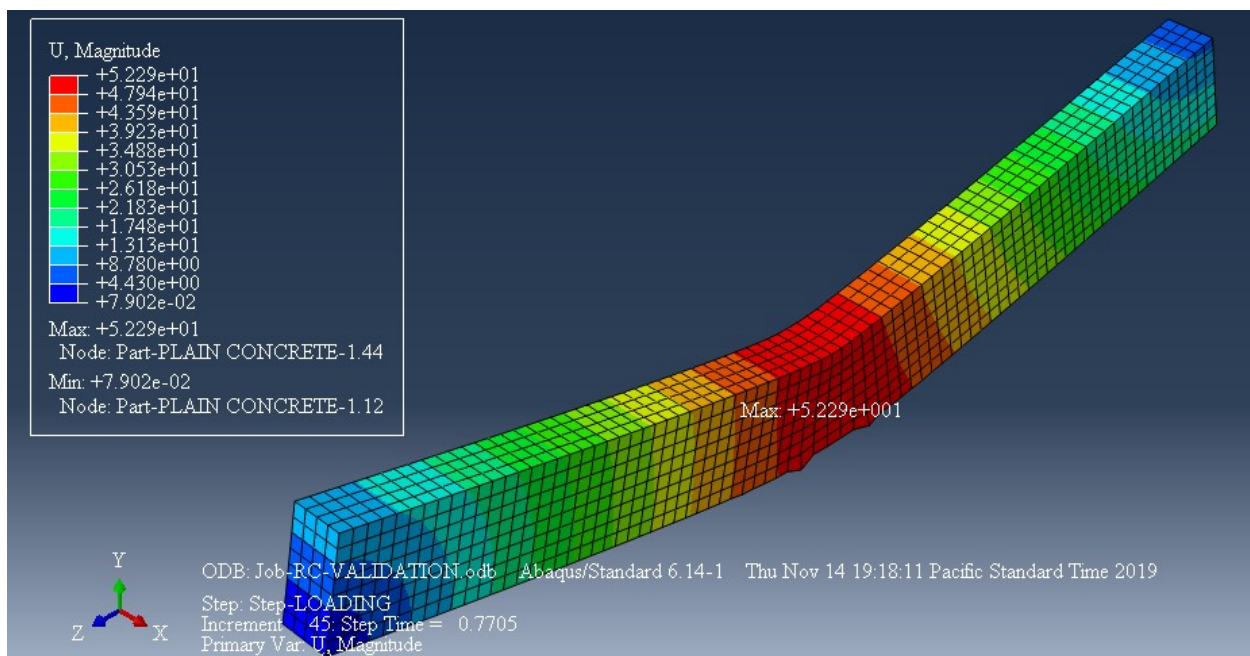


Figure 4.35: Validation of reinforced concrete beam result using ABAQUS 6.14-1

As shown on figure 4.35, the result gained from the test for mid span deflection is 58 mm and result using ABAQUS 6.14-1 is 52.3 mm.

4.5.2 Validation of I Section Steel Beam

The test results of fire resistance test of unprotected steel beams, compared with simple and advanced calculation models given in EN 1993-1-2. The comparison shows differences between temperatures recorded during tests, temperatures calculated in accordance with EN 1993-1-2 [25].

Tests were performed on two identical HEB 300 hot rolled steel beams made of carbon steel of grade S355, reinforced by 8 welded stiffeners, in accordance with EN 1365-3 [26]. The real elastic limit has been determined by tensile tests at an average value of 448 MPa. The stiffeners were provided at the supports and at the load application points on both sides of the web. Aerated concrete blocks were placed on the upper flange of the beam, as required in EN 1365-3 [26] in order to simulate the floor and provide three-sided heating. Total length of each beam was $L_{spec} = 4400$ mm, with span between supports $L_{sup} = 4200$ mm and length subjected to heating $L_{exp} = 4000$ mm, see Fig. 4.30. The load was applied with two hydraulic jacks, spaced 140 cm, each applying force $P = 100$ kN. No fire protection material was used to insulate the beams from the heating.

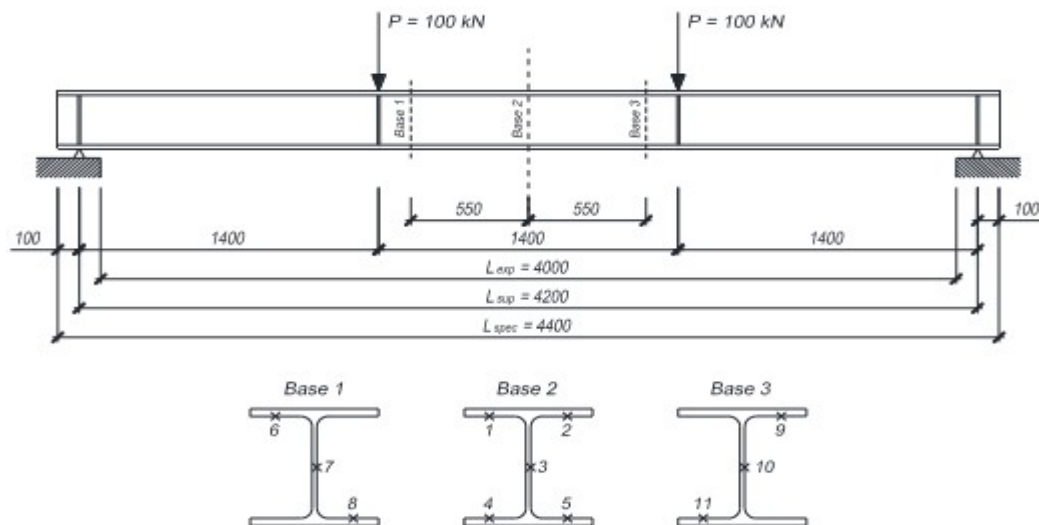


Figure 4.36: Test specimen design and thermocouples locations.

The temperature of steel in tests was measured with 11 K-type thermocouples mounted on the web and both flanges see Fig.4.37. Furnace temperature was measured with 8 plate thermometers, in accordance with EN 1363-1 [27]. Furnace pressure was set in such a way, as to achieve 20 Pa on the bottom of the test specimen, as required in EN 1363-1 [27]. Average steel temperature was calculated as the arithmetic mean temperature of the lower flange, the web and the upper flange.

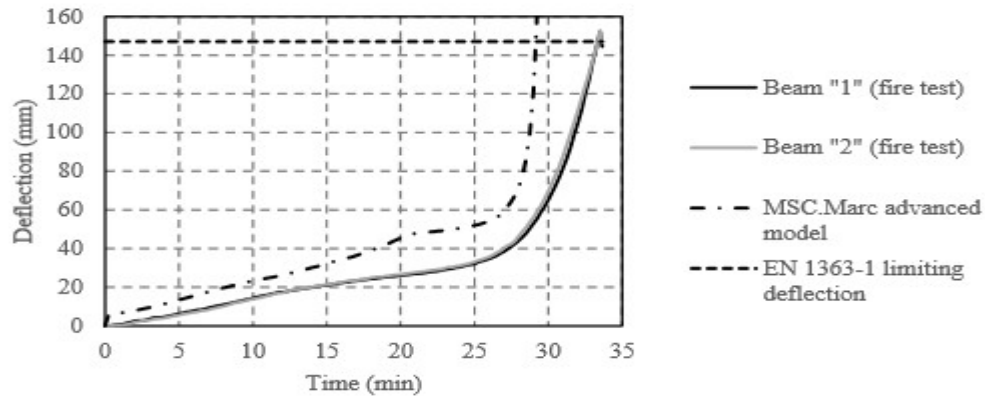


Figure 4.37: View of the Beam at the end of test.

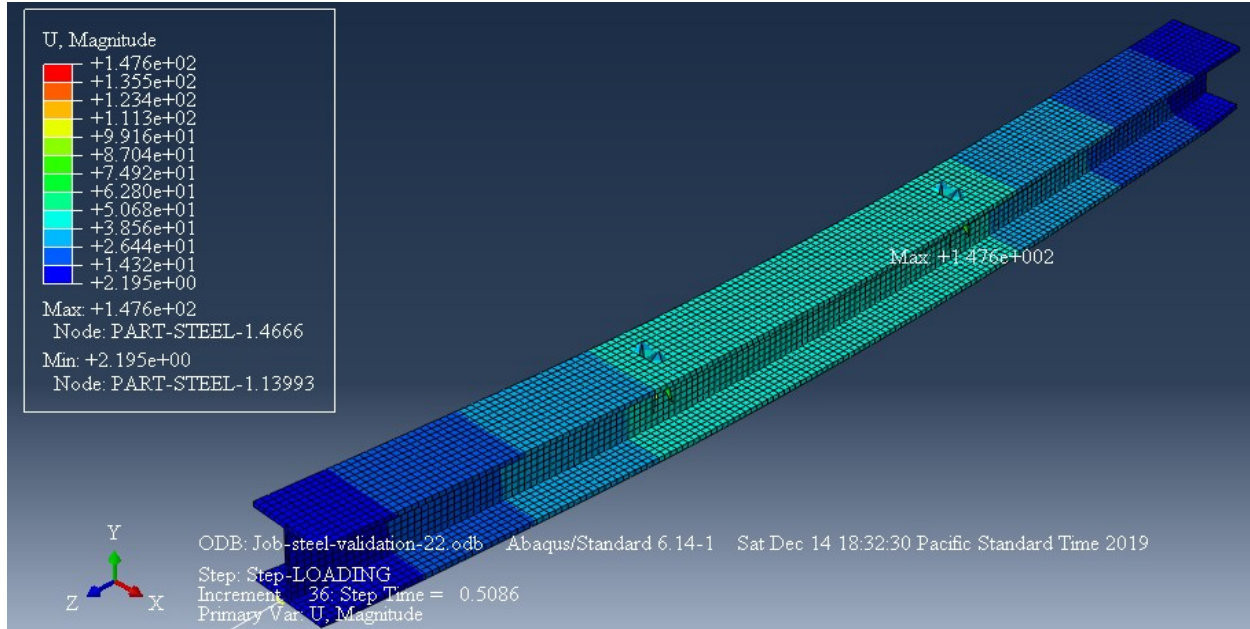


Figure 4.38: Validation result of I section steel beam using ABAQUS 6.14-2

As shown on figure 4.32, the result gained from the test for mid span deflection is 145 mm and result using ABAQUS 6.14-1 is 147.6 mm.

CHAPTER FIVE

CONCLUSIONS AND RECOMMENDATIONS

5.1 Conclusions

By using ABAQUS 6.14-2 software were analyzed for flexural and for fire resistance based on Euro code. The following conclusions are drawn from the present study:

- Bending resistance of reinforced concrete beam is higher than I section steel beam. As example mid span deflection of I section steel beam of IS-B4-C35 is greater than reinforced concrete beam of RC-B4-C35 by 209.4 mm.
- Bending resistance of both reinforced concrete and steel beam were highly affected by fire exposure.
- The Bending resistance decrease directly with the increase of length for the same cross section for reinforced concrete beam. And when we increase the size of the cross section with the same length the Bending resistance increases.
- The Bending resistance decrease directly with the increase of length for the same cross section for I section steel beam. And also when we increase the size of the cross section with the same length the Bending resistance decrease.
- Bending resistance of steel beam decrease with increasing weight of steel beam.

5.2 Recommendations

- The use of reinforced concrete members in the future should have to increase in Ethiopia for better bending and fire resistance.
- Steel has a very good bending resistance than concrete, but it is too poor at fire resistance. So, using protecting methods should have to be considered.
- Fire is one of the serious potential risks to most buildings and structures. Progress in the field of theoretical prediction of fire resistance has been rapid in recent years in most of countries. But in Ethiopia there is nothing done at this field of study so it should have to be a progress from now on as the construction industry is rapidly growing.

- EBCS has limitation on fire design methods, but fire analysis is most important analysis like strength and stability analysis. Everyone who is concerned with building codes should have to consider fire design part as one part of the document.
- Those Fire analysis methods mentioned in this research are important if we use them in our designs. The government should have to enforce to make the fire design code and implemented by contractors and designers or consultants
- In this research the fire analysis is mainly based on Euro-code for the future study it is useful to consider other codes.
- On the future it have to be carried out further investigation by varying concrete cover thickness of reinforced concrete beam to now its resistance for fire.
- On the future it is good to carry out analysis for class-2 and class-3 I section steel beam.

REFERENCE

- [1] Kodur, V., Asce, F., Dwaikat, M., & Fike, R. (2010). High-Temperature Properties of Steel for Fire Resistance Modeling of Structures. 2010; 423–434.
- [2] Wight K.J., Macgregor G.J., Reinforced Concrete Mechanics And Design. 6th edition. 2012.
- [3] Salmon, G., Johnson, E., Malhas, A., Steel structures design and behaviors, 5th edition. 2009.
- [4] Bansal R. Strength of Materials. 4th ed. NEW DELHI: LAXMI PUBLICATIONS(P) LTD; 2009.
- [5] Kodur V, Asce F, Dwaikat M, Fike R. High-Temperature Properties of Steel for Fire Resistance Modeling of Structures. 2010;22(May):423–34.
- [6] Huang ZH. Modelling the bond between concrete and reinforcing steel in a fire. EngStruct 2010;32(11):3660–9.
- [7] Buchanan, A.H., Structural Design for Fire Safety, John Wiley & Sons, Ltd. Chichester. 2001
- [8] Inwood, M. (1999). “Review of NZS 3101 for high strength concrete and lightweight concrete exposed to fire.” Fire Engineering Research Report 99/10. University of Canterbury, New Zealand.
- [9] Buchanan, A.H., Structural Design for Fire Safety, John Wiley & Sons, Ltd. Chichester. 2001.
- [10] Malhotra, H.L. (1984). “Spalling of concrete in fires.” CIRIA Technical Note No. 118. Construction Industry Research and information Association, London, UK.
- [11] Phan, L.T. (1996). “ Fire performance of high-strength concrete: a report of the state of the art”. NISTIR 5934. National Institute of Standards and Technology.
- [12] Buchanan, A.H., Structural Design for Fire Safety, John Wiley & Sons, Ltd. Chichester. 2001

- [13] Swinden Technology Centre British Steel plc. The behavior of multi-storey steel framed buildings in fire. Technical report, European Joint Research Program Report... British Steel plc (now CORUS), 1999.
- [14] S.C.I. Investigation of Broadgate Phase 8 Fire. Structural fire engineering. Steel Construction Institute, Ascot, Berkshire, 1991.
- [15] Gao WY, Dai J, Teng JG, Chen GM. Finite element modeling of reinforced concrete beams exposed to fire. *EngStruct.* Elsevier Ltd; 2013;52:488–501.
- [16] Taranath, B. S. Reinforced concrete design of tall buildings. Las Vegas, Nevada: CRC Press, 2000; 8.
- [17] IIT: Working stress method. Kharagpur, Indian: Indian Institution of Technology; 2019; 3.
- [18] Getting started with ABAQUS. United States of America; Simulia corp, 2008.
- [19] BS 476, Fire tests on building materials and structures, Part 21 Methods for determination of the fire resistance of load bearing elements of construction, British Standard Institute
- [20] Usmani, A.S, Chung, Y.C., Torero, J.L. “How did the WTC towers collapse: a new theory.” p. 513
- [21] ENV 1993-1-2:1995, Design of steel structures, Part 1-2: Structural fire design, British Standard Institute, 1995.
- [22] ENV 1992-1-2:1993, Design of concrete structures, Part 1-2: Structural fire design, British Standard Institute, 1993
- [23] British Standards Institution. The structural use of steelwork in buildings: fire resistant design. BS 5980. Part 8: 1990.
- [24] Wu HJ, Lie TT, Hu JY. Fire resistance of beam-slab specimens – experimental studies. Internal Report No. 641, Institute for Research in Construction, National Research Council Canada, Canada; 1993.

[25] Łukomsk M, Turkowski P, Roszkowski P, Papis B. Fire Resistance of Unprotected Steel Beams – Comparison between Fire Tests and Calculation Models. *ProcediaEng* [Internet]. 2017;172:665–72. Available from: <http://dx.doi.org/10.1016/j.proeng.2017.02.078>

[26] EN 1365-3:1999. Fire resistance tests for loadbearing elements – Part 3: Beams. European Committee for Standardization, Brussels, Belgium, December 1999.

[27] EN 1363-1:2012. Fire resistance tests. General requirements. European Committee for Standardization, Brussels, Belgium, July 2012.

Comparative Study on Steel and Reinforced Concrete Beam on the Basis of Modular Ratio for Flexural Capacity and Fire Resistance Using Finite Element Analysis

Appendix A: Design calculations

A-1 Reinforced Concrete Beam Design

				length (m)	Pd (KN/m)	Md (KNm)	b(mm)	D (mm)	D'(mm)			
Beam - 1 200 mm x 240 mm				3	20.45	23.00625	200	197	43			
Concrete Cubic Strength (Mpa)	Fck (Mpa)	Fcd (Mpa)	Fyd (Mpa)	m	C1	C2 (Mpa)	Steel Ratio, ρ_{max}	Steel Ratio, ρ		Ast (mm ²)	Use Dia	20
20	20.00	11.33	260.87	28.77	0.09	3,002.34	0.02	0.01	If $\rho < \rho_{max}$ Singel Reinforcement	529.60	2.00	
25	25.00	14.17	260.87	23.02	0.11	2,401.87	0.02	0.01	If $\rho > \rho_{max}$ Double Reinforcement	507.97	2.00	
30	30.00	17.00	260.87	19.18	0.13	2,001.56	0.03	0.01		495.48	2.00	
35	35.00	19.83	260.87	16.44	0.15	1,715.62	0.03	0.01		487.31	2.00	

				length (m)	Vrd=Vld (KN)	Md (KNm)	b(mm)	D (mm)	D'(mm)	Fctd(Mpa)			
Beam - 1 200 mm x 240 mm				3	30.675	34.509375	200	197	43	1.03			
Concrete Cubic Strength (Mpa)	Fck	Fcd	Fyd	ρ	K1	K2	Vc(KN)	Vrd(KN)	Vsd(KN)		Smax	Use Smax	provide
20	20.00	11.33	260.87	0.01	1.29	1.40	18.32	111.63	30.68	Vsd<2/3 Vrd	98.50	100.00	Ø8c/c100mm
25	25.00	14.17	260.87	0.01	1.29	1.40	18.32	139.54					
30	30.00	17.00	260.87	0.01	1.29	1.40	18.32	167.45					
35	35.00	19.83	260.87	0.01	1.29	1.40	18.32	195.36					

				length (m)	Pd (KN/m)	Md (KNm)	b(mm)	D (mm)	D'(mm)			
Beam - 2 250 mm x 300 mm				3	20.45	23.00625	250	257	43			
Concrete Cubic Strength (Mpa)	Fck (Mpa)	Fcd (Mpa)	Fyd (Mpa)	m	C1	C2 (Mpa)	Steel Ratio, ρ_{max}	Steel Ratio, ρ		Ast (mm ²)	Use Dia	20
20	20.00	11.33	260.87	28.77	0.09	3,002.34	0.02	0.01	If $\rho < \rho_{max}$ Singel Reinforcement	367.32	2.00	
25	25.00	14.17	260.87	23.02	0.11	2,401.87	0.02	0.01	If $\rho > \rho_{max}$ Double Reinforcement	361.93	2.00	
30	30.00	17.00	260.87	19.18	0.13	2,001.56	0.03	0.01		358.50	2.00	
35	35.00	19.83	260.87	16.44	0.15	1,715.62	0.03	0.01		356.14	2.00	

				length (m)	Vrd=Vld (KN)	Md (KNm)	b(mm)	D (mm)	D'(mm)	Fctd(Mpa)			
Beam - 2 250 mm x 300 mm				3	30.675	34.509375	250	257	43	1.03			
Concrete Cubic Strength (Mpa)	Fck	Fcd	Fyd	ρ	K1	K2	Vc(KN)	Vrd(KN)	Vsd(KN)		Smax	Use Smax	provide
20	20.00	11.33	260.87	0.00	1.18	1.40	27.29	182.04	30.68	Vsd<2/3 Vrd	128.50	130.00	Ø8c/c130mm
25	25.00	14.17	260.87	0.00	1.18	1.40	27.29	227.55					
30	30.00	17.00	260.87	0.00	1.18	1.40	27.29	273.06					
35	35.00	19.83	260.87	0.00	1.18	1.40	27.29	318.57					

Comparative Study on Steel and Reinforced Concrete Beam on the Basis of Modular Ratio for Flexural Capacity and Fire Resistance Using Finite Element Analysis

				length (m)	Pd (KN/m)	Md (KNm)	b(mm)	D (mm)	D'(mm)	Xmax
Beam - 3 200 mm x 240 mm				4.5	20.45	51.764063	200	197	43	88.256
Concrete Cubic Strength (Mpa)	Fck (Mpa)	Fcd (Mpa)	Fyd (Mpa)	m	C1	C2 (Mpa)	μ max	μ req		M1 (Nmm)
20	20.00	11.33	260.87	28.77	0.09	3,002.34	0.29	0.59	If μ req < μ max Single Reinforcement	25,862,317.60
25	25.00	14.17	260.87	23.02	0.11	2,401.87	0.29	0.47	If μ req > μ max Double Reinforcement	32,327,897.00
30	30.00	17.00	260.87	19.18	0.13	2,001.56	0.29	0.39		38,793,476.40
35	35.00	19.83	260.87	16.44	0.15	1,715.62	0.29	0.34		45,259,055.80

As 1 (mm2)	M2 (Nmm)	As 2 (mm2)	As Total=As1+As2 (mm2)	Use Dia 20	As'=As2	Use Dia 12
589.97	25,901,744.90	644.74	1,234.71	4.00	644.74	6.00
737.46	19,436,165.50	483.80	1,221.26	4.00	483.80	5.00
884.95	12,970,586.10	322.86	1,207.81	4.00	322.86	3.00
1,032.44	6,505,006.70	161.92	1,194.37	4.00	161.92	2.00

				length (m)	Vrd=Vld (KN)	Md (KNm)	b(mm)	D (mm)	D'(mm)	Fctd(Mpa)			
Beam - 3 200 mm x 240 mm				4.5	46.0125	116.46914	200	197	43	1.03			
Concrete Cubic Strength (Mpa)	Fck	Fcd	Fyd	ρ	K1	K2	Vc(KN)	Vrd(KN)	Vsd(KN)	Smax	Use Smax	provide	
20	20.00	11.33	260.87	0.03	2.59	1.40	36.92	111.63	46.01	Vsd<2/3 Vrd	98.50	100.00	Ø8c/c100mm
25	25.00	14.17	260.87	0.03	2.59	1.40	36.92	139.54					
30	30.00	17.00	260.87	0.03	2.59	1.40	36.92	167.45					
35	35.00	19.83	260.87	0.03	2.59	1.40	36.92	195.36					

				length (m)	Pd (KN/m)	Md (KNm)	b(mm)	D (mm)	D'(mm)		
Beam - 4 250 mm x 300 mm				4.5	20.45	51.764063	250	257	43		
Concrete Cubic Strength (Mpa)	Fck (Mpa)	Fcd (Mpa)	Fyd (Mpa)	m	C1	C2 (Mpa)	Steel Ratio, ρ	Steel Ratio, ρ		Ast (mm2)	Use Dia 20
20	20.00	11.33	260.87	28.77	0.09	3,002.34	0.02	0.01	If ρ < ρ max Singel Reinforcement	925.54	3.00
25	25.00	14.17	260.87	23.02	0.11	2,401.87	0.02	0.01	If ρ > ρ max Double Reinforcement	884.11	3.00
30	30.00	17.00	260.87	19.18	0.13	2,001.56	0.03	0.01		860.53	3.00
35	35.00	19.83	260.87	16.44	0.15	1,715.62	0.03	0.01		845.22	3.00

				length (m)	Vrd=Vld (KN)	Md (KNm)	b(mm)	D (mm)	D'(mm)	Fctd(Mpa)			
Beam - 4 250 mm x 300 mm				4.5	46.0125	116.46914	250	257	43	1.03			
Concrete Cubic Strength (Mpa)	Fck	Fcd	Fyd	ρ	K1	K2	Vc(KN)	Vrd(KN)	Vsd(KN)	Smax	Use Smax	provide	
20	20.00	11.33	260.87	0.01	1.73	1.40	40.23	182.04	46.01	Vsd<2/3 Vrd	128.50	130.00	Ø8c/c130mm
25	25.00	14.17	260.87	0.01	1.73	1.40	40.23	227.55					
30	30.00	17.00	260.87	0.01	1.73	1.40	40.23	273.06					
35	35.00	19.83	260.87	0.01	1.73	1.40	40.23	318.57					

A-2 Loading Calculation

Live load as per EBCs,

C-3, from 3 KN/m² - 5 KN/m²

3 KN/m² is selected

Live load-

$$=3 \text{ KN/m}^2 \times (2/2 + 2/2) \text{ m}$$

$$= 6\text{KN/m}$$

Dead load-

150 mm thick slab is assumed

$$=2 \times 0.15 \times 24 = 7.2 \text{ KN/m} \quad \text{where, self-weight of concrete is } 24 \text{ KN/m}^3$$

Beam weight

$$=0.24 \times 0.2 \times 24 = 1.152 \text{ KN/m}$$

Factored uniformly distributed load as per EBCs,

$$P_d = (6 \times 1.6)\text{KN/m} + (8.352 \times 1.3) \text{ KN/m} = 20.45 \text{ KN/m} = 0.0718 \text{ N/mm}^2$$

Appendix B: Input Material Properties

B-1: Input Material Properties for Concrete as per Euro Code 1992-1-2:2004

1. Values for the main parameters of the stress-strain relationships of normalweight concrete with siliceous concrete at elevated temperatures

For C-20

Concrete temp, θ	fck	fc, θ	$\epsilon_{c1,\theta}$	$\epsilon_{cu1,\theta}$
[°C]	N/mm ²	N/mm ²	[-]	[-]
20	16	16	0.0025	0.02
100	16	16	0.004	0.0225
200	16	15.2	0.0055	0.025
300	16	13.6	0.007	0.0275
400	16	12	0.01	0.03
500	16	9.6	0.015	0.0325
600	16	7.2	0.025	0.035
700	16	4.8	0.025	0.0375
800	16	2.4	0.025	0.04

For C-25

Concrete temp, θ	fck	fc, θ	$\epsilon_{c1,\theta}$	$\epsilon_{cu1,\theta}$
[°C]	N/mm ²	N/mm ²	[-]	[-]
20	20	20	0.0025	0.02
100	20	20	0.004	0.0225
200	20	19	0.0055	0.025
300	20	17	0.007	0.0275
400	20	15	0.01	0.03
500	20	12	0.015	0.0325
600	20	9	0.025	0.035
700	20	6	0.025	0.0375
800	20	3	0.025	0.04

Comparative Study on Steel and Reinforced Concrete Beam on the Basis of Modular Ratio for Flexural Capacity and Fire Resistance Using Finite Element Analysis

For C-30

Concrete temp. θ	fck	fc, θ	$\epsilon_{c1,\theta}$	$\epsilon_{cu1,\theta}$
[°C]	N/mm ²	N/mm ²	[-]	[-]
20	24	24	0.0025	0.02
100	24	24	0.004	0.0225
200	24	22.8	0.0055	0.025
300	24	20.4	0.007	0.0275
400	24	18	0.01	0.03
500	24	14.4	0.015	0.0325
600	24	10.8	0.025	0.035
700	24	7.2	0.025	0.0375
800	24	3.6	0.025	0.04

For C-35

Concrete temp. θ	fck	fc, θ	$\epsilon_{c1,\theta}$	$\epsilon_{cu1,\theta}$
[°C]	N/mm ²	N/mm ²	[-]	[-]
20	28	28	0.0025	0.02
100	28	28	0.004	0.0225
200	28	26.6	0.0055	0.025
300	28	23.8	0.007	0.0275
400	28	21	0.01	0.03
500	28	16.8	0.015	0.0325
600	28	12.6	0.025	0.035
700	28	8.4	0.025	0.0375
800	28	4.2	0.025	0.04

2. Values for the tensile strength with normal weight siliceous concrete at elevated temperatures

For C-20

Concrete temp. θ	f _{ctk}	f _{ctk,θ}
[°C]	N/mm ²	N/mm ²
20	1.5	1.5
100	1.5	1.5
200	1.5	1.2
300	1.5	0.9
400	1.5	0.6
500	1.5	0.3
600	1.5	0
700	1.5	0
800	1.5	0

For C-25

Concrete temp. θ	f _{ctk}	f _{ctk,θ}
[°C]	N/mm ²	N/mm ²
20	1.8	1.8
100	1.8	1.8
200	1.8	1.44
300	1.8	1.08
400	1.8	0.72
500	1.8	0.36
600	1.8	0
700	1.8	0
800	1.8	0

For C-30

Concrete temp. θ	f _{tk}	f _{tk,θ}
[°C]	N/mm ²	N/mm ²
20	2	2
100	2	2
200	2	1.6
300	2	1.2
400	2	0.8
500	2	0.4
600	2	0
700	2	0
800	2	0

For C-35

Concrete temp. θ	f _{tk}	f _{tk,θ}
[°C]	N/mm ²	N/mm ²
20	2.2	2.2
100	2.2	2.2
200	2.2	1.76
300	2.2	1.32
400	2.2	0.88
500	2.2	0.44
600	2.2	0
700	2.2	0
800	2.2	0

3. Stress-strain relationship of hot rolled worked reinforcing steel at elevated temperatures as per

For - S-300

Steel Temperature θ	f_{ys}	$f_{sy,\theta}$	E_s	$E_{s,\theta}$
[°C]	N/mm ²	N/mm ²	N/mm ²	N/mm ²
1	2	3	4	5
20	300.00	300.00	200,000.00	200,000.00
100	300.00	300.00	200,000.00	200,000.00
200	300.00	300.00	200,000.00	180,000.00
300	300.00	300.00	200,000.00	160,000.00
400	300.00	300.00	200,000.00	140,000.00
500	300.00	234.00	200,000.00	120,000.00
600	300.00	141.00	200,000.00	62,000.00
700	300.00	69.00	200,000.00	26,000.00
800	300.00	33.00	200,000.00	18,000.00

4. Specific heat with normal weight siliceous concrete at elevated temperatures as per EN 1992-1-2:2004

Concrete temp. θ	$c_p(\theta)$
[°C]	J/kg K
20	900
100	900
200	1000
300	1100
400	1200
500	1100
600	1100
700	1100
800	1100

5. Density of concrete at elevated temperatures

Concrete temp.θ	$\rho(\theta)$
[°C]	kg/m ³
20	2300
100	2300
200	2254
300	2219.5
400	2185
500	2164.875
600	2144.75
700	2124.625
800	2104.5

6. Thermal conductivity of concrete at elevated temperatures

Concrete temp.θ	λ_c	
[°C]	W/mK	
	lower	upper
20	1.332572	1.996732
100	1.2183	1.9970124
200	1.0652	1.997388
300	0.9007	1.9977915
400	0.7248	1.998223
500	0.5375	1.9986823
600	0.3388	1.9991695
700	0.1287	1.9996845
800	0	2.0002274

7. Modulus of Elasticity with normal weight siliceous concrete at elevated temperatures

For C-20

Concrete temp. θ	E(θ)
[°C]	N/mm ²
20	30000
100	30000
200	27272.7273
300	21818.1818
400	16363.6364
500	10909.0909
600	5454.54545
700	0
800	0

For C-25

Concrete temp. θ	E(θ)
[°C]	N/mm ²
20	31000
100	31000
200	28181.81818
300	22545.45455
400	16909.09091
500	11272.72727
600	5636.363636
700	0
800	0

For C-30

Concrete temp. θ	E(θ)
[°C]	N/mm ²
20	32000
100	32000
200	29090.9
300	23272.7
400	17454.5
500	11636.4
600	5818.18
700	0
800	0

For C-35

Concrete temp. θ	E(θ)
[°C]	N/mm ²
20	34000
100	34000
200	30909.1
300	24727.3
400	18545.5
500	12363.6
600	6181.82
700	0
800	0

A-II Input Material Properties for I section Steel as per Euro Code 1993-1-2

1. stress-strain relationship of carbon steel at elevated temperature

steel temp. θ	f_y	$f_{y,\theta}$	E_a	$E_{a,\theta}$
[°C]	N/mm ²	N/mm ²	N/mm ²	N/mm ²
20	275	275	210000	210000
100	275	275	210000	210000
200	275	275	210000	189000
300	275	275	210000	168000
400	275	275	210000	147000
500	275	214.5	210000	126000
600	275	129.25	210000	65100
700	275	63.25	210000	27300
800	275	30.25	210000	18900

2. Specific heat steel at elevated temperature

steel temp. θ	C_a
[°C]	J/kg K
20	439.80176
100	487.62
200	529.76
300	564.74
400	605.88
500	666.5
600	760.21739
700	1008.1579
800	803.26087

3. Thermal conductivity steel at elevated temperature

steel temp. θ	λ_a
[°C]	W/mK
20	53.334
100	50.67
200	47.34
300	44.01
400	40.68
500	37.35
600	34.02
700	30.69
800	27.3